

โครงข่ายประสาทเทียมเพื่อใช้คาดการณ์อัตราการเคลื่อนย้ายของหัวเจาะ
สำหรับการเจาะหลุมในอ่าวไทย



นาย พลเลิศ สุทธิเกียรติ

ศูนย์วิทยทรัพยากร
จุฬาลงกรณ์มหาวิทยาลัย

วิทยานิพนธ์นี้เป็นส่วนหนึ่งของการศึกษาตามหลักสูตรปริญญาวิศวกรรมศาสตรมหาบัณฑิต

สาขาวิชาวิศวกรรมปิโตรเลียม ภาควิชาวิศวกรรมเหมืองแร่และปิโตรเลียม

คณะวิศวกรรมศาสตร์ จุฬาลงกรณ์มหาวิทยาลัย

ปีการศึกษา 2553

ลิขสิทธิ์ของจุฬาลงกรณ์มหาวิทยาลัย

AN ARTIFICIAL NEURAL NETWORK TO PREDICT BIT WALK RATE
FOR DRILLING IN THE GULF OF THAILAND



Mr. Phornlerd Sudhikiat

ศูนย์วิทยทรัพยากร

A Thesis Submitted in Partial Fulfillment of the Requirements
for the Degree of Master of Engineering Program in Petroleum Engineering
Department of Mining and Petroleum Engineering

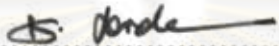
Faculty of Engineering
Chulalongkorn University

Academic Year 2010

Copyright of Chulalongkorn University

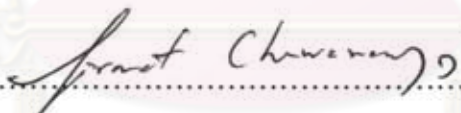
Thesis Title AN ARTIFICIAL NEURAL NETWORK TO PREDICT BIT
WALK RATE FOR DRILLING IN THE GULF OF
THAILAND
By Mr. Phornlerd Sudhikiat
Field of Study Petroleum Engineering
Thesis Advisor Assistant Professor Jirawat Chewaroungroj, Ph.D.

Accepted by the Faculty of Engineering, Chulalongkorn University in
Partial Fulfillment of the Requirements for the Master's Degree



..... Dean of the Faculty of Engineering
(Associate Professor Boonsom Lerdhirunwong, Dr. Ing.)

THESIS COMMITTEE


..... Chairman
(Associate Professor Sarithdej Pathanasethpong)


..... Thesis Advisor
(Assistant Professor Jirawat Chewaroungroj, Ph.D.)


..... Examiner
(Assistant Professor Suwat Athichanagorn, Ph.D.)


..... External Examiner
(Thotsaphon Chaianansutcharit, Ph.D.)

พรเลิศ สุทธิเกียรติ : โครงข่ายประสาทเทียมเพื่อใช้คาดการณ์อัตราการเคลื่อนที่ของหัวเจาะสำหรับการเจาะหลุมในอ่าวไทย. (AN ARTIFICIAL NEURAL NETWORK TO PREDICT BIT WALK RATE FOR DRILLING IN THE GULF OF THAILAND)
 อ. ที่ปรึกษาวิทยานิพนธ์หลัก: ผศ. ดร. จิรวัดน์ ชีวรุ่งโรจน์, 106 หน้า.

การขุดเจาะปิโตรเลียมจำเป็นต้องมีการควบคุมความเอียงและทิศทางของหัวเจาะเพื่อให้มั่นใจว่าการขุดเจาะนั้นไปถึงเป้าหมายแหล่งกักเก็บในระยะที่ยอมรับได้ การขุดเจาะทั่วไปนั้นใช้ Adjustable Gauge Stabilizer (AGS) เพื่อควบคุมความเอียงและใช้ steerable motor ในการควบคุมทิศทาง แหล่งกักเก็บที่อยู่ในบริเวณส่วนลึกของหลุมในอ่าวไทยนั้นมีความสูงมากกว่าปกติจนทำให้ส่วนประกอบของมอเตอร์ซึ่งเป็นยางนั้นไม่สามารถทำงานได้อย่างมีประสิทธิภาพได้ ดังนั้น AGS จึงเป็นเพียงเครื่องมือเดียวที่ใช้ควบคุมการขุดเจาะในที่นี้เพื่อควบคุมความเอียงโดยไม่มีเครื่องมือควบคุมทิศทางติดตั้งอยู่ วิทยานิพนธ์ฉบับนี้จึงพยายามที่จะบ่งชี้และสร้างตัวแบบเพื่อทำนายพฤติกรรมของการเคลื่อนที่ของหัวเจาะโดยใช้ค่าพารามิเตอร์ที่ควบคุมได้เป็นปัจจัยนำเข้าสู่โครงข่ายประสาทเทียม การสร้างตัวแบบกระทำโดยการป้อนข้อมูลจริงที่ได้จากการขุดเจาะในบริเวณอ่าวไทยเพื่อสร้างเครื่องมือทำนายสภาพการเปลี่ยนทิศทางของหัวเจาะหรือที่เรียกในวิทยานิพนธ์ฉบับนี้ว่า อัตราการเคลื่อนที่

การศึกษาถูกแบ่งออกเป็นสองแง่มุมโดยการทำนายทิศทางและปริมาณการเคลื่อนที่ของหัวเจาะ จากผลการทดลองพบว่าโครงข่ายประสาทเทียมมีความสามารถในการทำนายอัตราการเคลื่อนที่ในเชิงปริมาณและยังสามารถใช้ในการบ่งชี้และยืนยันถึงตัวแปรต่างๆที่ส่งผลต่ออัตราการเคลื่อนที่ของหัวเจาะซึ่งเกี่ยวข้องกับ การวางแบบของหลุม ตัวแปรที่ใช้ควบคุมการขุดเจาะ และ ชั้นหินในแหล่งกักเก็บ ตัวแบบที่ใช้คาดการณ์อัตราการเคลื่อนที่ซึ่งมีการปรับแต่งที่ดีที่สุดและทำให้คาดการณ์ได้ดีที่สุด เมื่อทดลองกับข้อมูลชุดทดสอบ ให้ค่าสัดส่วนของความถูกต้องเป็นที่น่าพอใจ

ภาควิชาวิศวกรรมเหมืองแร่และปิโตรเลียม..
 สาขาวิชา ..วิศวกรรมปิโตรเลียม.....
 ปีการศึกษา 2553.....

ลายมือชื่อนิสิต *Thorlud Sathikhat*
 ลายมือชื่อ อ.ที่ปรึกษาวิทยานิพนธ์หลัก *จิรวัดน์ ชีวรุ่งโรจน์*

517 16116 21 : MAJOR PETROLEUM ENGINEERING

KEYWORDS : BIT WALK / ARTIFICIAL NEURAL NETWORK / DRILLING IN THE GULF OF THAILAND/ DRILLING PARAMETERS / FORMATION CHARACTERISTICS

PHORNLERD SUDHIKIAT: AN ARTIFICIAL NEURAL NETWORK TO PREDICT BIT WALK RATE FOR DRILLING IN THE GULF OF THAILAND. THESIS ADVISOR : ASSISTANT PROFESSOR JIRAWAT CHEWAROUNGROAJ, Ph.D., 106 pp.

Petroleum well drilling requires inclination and direction control of the bit to assure that the reservoir target is met within an acceptable range. General drilling operation uses Adjustable Gauge Stabilizer (AGS) to control inclination while using steerable motor to control direction. The reservoir located at the deep section of the well in the Gulf of Thailand exceptionally contains high temperature where rubber part of the directional control tool is not able to effectively handle. As a result, AGS is solely used in the operation to control inclination without a directional control tool in place. This paper is then attempting to address and model the bit directional behavior with the available controllable parameters by using an Artificial Neural Network (ANN). The modeling is carried out by using the field data from the Gulf of Thailand and inputting into the ANN to create a bit directional deviation, referred in this paper as bit walk, predictive tool.

The study is divided into two perspectives of predicting bit walk direction and quantity. The result shows that the ANN can be effectively used to predict bit walk quantity as well as identifying and confirming affecting parameters which are related to well configuration, drilling parameters and formation. The walk rate prediction model with the best configuration making best prediction when testing with the testing dataset yield a result of satisfied hit fraction (correct prediction).

Department : Mining and Petroleum Engineering

Field of Study : Petroleum Engineering

Academic Year : 2010

Student's Signature *Phornlert Sudhikiat*

Advisor's Signature *Jirawat Chewarongroj*

ACKNOWLEDGEMENTS

I would like to express my gratefulness to Dr. Jirawat Chewaroungroj for his expertise in drilling operation and guidance throughout the development of this thesis, and also Dr. Suwat Athichanagorn for his guidance regarding the Artificial Neural Network.

I also would like to extend my thanks to PTTEP Co.Ltd. drilling department for providing such valuable information to develop and study the bit walk model. And also a special thanks to the Engineering Computer Center of Faculty of Engineering, Chulalongkorn University in providing the MATLAB software for facilitating this study.

Lastly, I would like to express my thankful to my family and friends for their sympathy, encouragement and continuing support throughout the course of my studies and this research.



ศูนย์วิทยทรัพยากร
จุฬาลงกรณ์มหาวิทยาลัย

CONTENTS

	Page
Abstract (Thai).....	iv
Abstract (English).....	v
Acknowledgements.....	vi
Contents.....	vii
List of Tables.....	x
List of Figures.....	xii
Chapter	
I. Introduction.....	1
II. Literature Review.....	3
III. Theories and Concepts.....	6
3.1 Bit directional tendency (Bit walk).....	6
3.2 Factors affecting bit walk.....	8
3.2.1 Bit Model.....	8
3.2.2 Bottom Hole Assembly (BHA).....	13
3.2.3 Well geometry.....	13
3.2.4 Drilling operating parameters.....	14
3.2.5 Formation characteristics.....	15
3.2.5.1 Formation anisotropy.....	15
3.2.5.2 Formation hardness.....	19

CONTENTS (continued)

Chapter	Page
3.3 Artificial Neural Network.....	19
IV. Bit walk prediction model development.....	24
4.1 Model Parameters and Conditions.....	24
4.1.1 Bit type.....	25
4.1.2 BHA configuration.....	25
4.1.3 Drilling parameters.....	26
4.1.4 Wellbore inclination.....	26
4.1.5 Formation.....	26
4.2 Data compilation and formatting.....	27
4.3 Bit walk prediction model development.....	30
4.3.1 Case 1 – Bit walk direction.....	30
4.3.1.1 Bit walk direction data analysis.....	30
4.3.1.2 Results and Discussion.....	31
4.3.2 Case 2 – Bit walk quantity (rate).....	32
4.3.2.1 Case 2.1 – Bit walk quantity in absolute amount.....	42
4.3.2.1.1 Data preprocessing.....	43
4.3.2.1.2 Model training	51
4.3.2.1.3 Model testing results and discussion.....	66
4.3.2.2 Case 2.2 – Bit walk quantity in range.....	70
4.3.2.2.1 Data preprocessing.....	71
4.3.2.2.2 Model training	72
4.3.2.2.3 Model testing results and discussion.....	76

CONTENTS (continued)

Chapter	Page
V. Conclusions and Recommendations.....	85
5.1 Conclusions.....	85
5.2 Recommendations.....	86
References.....	88
Appendices.....	91
Vitae.....	106



ศูนย์วิทยทรัพยากร
จุฬาลงกรณ์มหาวิทยาลัย

LIST OF TABLES

Table	Page
3.1 Bit Configuration.....	9
3.2 Bit steerability and walk angle from varying bit models and configurations.....	12
4.1 IADC classification of the PDC bit.....	25
4.2 BHA components.....	25
4.3 Measured parameters from Drilling Parameters Ascii and Definitive Survey..	29
4.4 Comparison of left and right bit walk dataset.....	31
4.5 Walk rate parameters (sampled dataset).....	33
4.6 Walk rate parameters and their ranges.....	33
4.7 Walk rate parameters and their ranges (after screening).....	37
4.8 Examples of dataset used in the model learning process (Case 2.1).....	43
4.9 Summary of statistical representation of training, validating and testing set....	50
4.10 Model configuration – Case 2.1.....	51
4.11 Error fraction (Training sets).....	60
4.12 Error fraction (Validating sets).....	60
4.13 Details dataset (Model number 3 – Training sets).....	62
4.14 Details dataset (Model number 3 – Validating sets).....	65
4.15 Error fraction (Testing sets).....	68

LIST OF TABLES (continued)

Table	Page
4.16 Model output in group.....	71
4.17 Output node representation.....	71
4.18 Model configuration – Case 2.2.....	72
4.19 Result from ANN model prediction (Case 2.2).....	77
4.20 Result from ANN model prediction (after transforming to binary).....	77
4.21 Example of the comparison between the predicted and actual walk range.....	78
4.22 Hit fraction – Case 2.2.....	78
4.23 Change in walk according to each parameter.....	80



 ศูนย์วิทยทรัพยากร
 จุฬาลงกรณ์มหาวิทยาลัย

LIST OF FIGURES

Figure	Page
3.1 Inclination and direction angle.....	6
3.2 Drilling section.....	7
3.3 Bit used in the drilling operation.....	9
3.4 Definition of the walk angle.....	10
3.5 Description of the PDC bit structure.....	11
3.6 Bit A, B and C tested.....	11
3.7 Description of the five bit configurations tested.....	12
3.8 Side cutting angle vs. Operating parameters (WOB, RPM).....	15
3.9 Origin of the anisotropic side force.....	16
3.10 Cutting configurations and formation dip.....	18
3.11 Circular test schema.....	18
3.12 Results of a circular test.....	19
3.13 Schematic of biological neuron.....	21
3.14 Schematic diagram of ANN.....	22
4.1 Geological prognosis of the formation (selected from a well).....	27
4.2 Histogram of Inclination of total dataset.....	35
4.3 Histogram of Weight on bit (WOB) of total dataset.....	35

LIST OF FIGURES (continued)

Figure	Page
4.4 Histogram of Rotational speed of total dataset.....	36
4.5 Histogram of Torque of total dataset.....	36
4.6 ANN model configuration (from MATLAB source code).....	39
4.7 ANN model workspace.....	39
4.8 Output from model testing (shown in the workspace matrix).....	40
4.9 Learning process of ANN.....	41
4.10 Schematic diagram of ANN model – Case 2.1.....	42
4.11 Histogram of Inclination of training sets.....	44
4.12 Histogram of Inclination of validating sets.....	45
4.13 Histogram of Inclination of testing sets.....	45
4.14 Histogram of Weight on bit (WOB) of training sets.....	46
4.15 Histogram of Weight on bit (WOB) of validating sets.....	46
4.16 Histogram of Weight on bit (WOB) of testing sets.....	47
4.17 Histogram of Rotational speed of training sets.....	47
4.18 Histogram of Rotational speed of validating sets.....	48
4.19 Histogram of Rotational speed of testing sets.....	48
4.20 Histogram of Torque of training sets.....	49

LIST OF FIGURES (continued)

Figure	Page
4.21 Histogram of Torque of validating sets.....	49
4.22 Histogram of Torque of testing sets.....	50
4.23 Learning curve of model number 1.....	54
4.24 Learning curve of model number 12.....	54
4.25 Learning curve of model number 3.....	55
4.26 Learning curve of model number 5.....	56
4.27 Cross plot of Predicted vs. Actual walk rate (Model number 3 – Training sets).....	58
4.28 Cross plot of Predicted vs. Actual walk rate (Model number 3 – Validating sets).....	58
4.29 Cross plot of Predicted vs. Actual walk rate (Model number 5 – Training sets).....	59
4.30 Cross plot of Predicted vs. Actual walk rate (Model number 5 – Validating sets).....	59
4.31 Comparing Predicted vs. Actual walk rate by order (Model number 3 – Training sets).....	61
4.32 Gamma ray log (Dataset no. 28 of Model number 3 - Training sets).....	62
4.33 Gamma ray log (Dataset no. 58 of Model number 3 - Training sets).....	62
4.34 Gamma ray log (Dataset no. 66 of Model number 3 - Training sets).....	63
4.35 Gamma ray log (Dataset no. 74 of Model number 3 - Training sets).....	63

LIST OF FIGURES (continued)

Figure	Page
4.36 Comparing Predicted vs. Actual walk rate by order (Model number 3 – Validating sets)	64
4.37 Gamma ray log (Dataset no. 11 of Model number 3 – Validating sets).....	65
4.38 Gamma ray log (Dataset no. 13 of Model number 3 – Validating sets).....	66
4.39 Cross plot of Predicted vs. Actual walk rate (Model number 3 – Testing sets).....	67
4.40 Cross plot of Predicted vs. Actual walk rate (Model number 5 – Testing sets).....	67
4.41 Comparing Predicted vs. Actual walk rate by order (Model number 3 – Testing sets)	69
4.42 Schematic diagram of ANN model – Case 2.2	70
4.43 Learning curve of model number 1 (Case 2.2)	73
4.44 Learning curve of model number 6 (Case 2.2)	75
4.46 Comparing Predicted vs. Actual walk range by order (Model number 6 – Testing sets)	79
4.47 Comparing Predicted vs. Actual walk range by order (Model number 8 – Testing sets)	79
4.48 Bit walk range under low inclination range (18-35 deg)	81
4.49 Bit walk range under medium inclination range (35-45 deg).....	83
4.50 Bit walk range under high inclination range (45-56 deg).....	84

CHAPTER I

INTRODUCTION

Directional drilling is important in many today's wells. Not only it requires an ability to drill directionally, but also accuracy in hitting the reservoir target precisely to minimize the operation cost and maximize the production. Hence, there have been many applications for controlling inclination and direction of the drilling well. Adjustable Gauge Stabilizer (AGS) is normally used as a tool to control inclination while direction is controlled by steerable motor. The reservoir located at the deep section, 6-1/8" in particular, of the well in the Gulf of Thailand where petroleum reservoirs usually reside, exceptionally contains high temperature that the rubber part of the direction control tool is not able to effectively handle. As a result, AGS is solely used in the operation to control inclination without a directional control tool in place. This study is then attempting to address and model the bit directional behavior with the available controllable parameters by using an Artificial Neural Network (ANN) as a tool. Consequently, an ability to control bit directional deviation, referred in this study as bit walk, using the controllable drilling parameters without the existence of steerable motor could be established. The modeling is carried out by using the field data from the Gulf of Thailand to train the ANN building the bit walk predictive tool. The study is divided into two perspectives of predicting bit walk direction (left or right) and quantity.

Past studies were reviewed to obtain parameters affecting bit walk as well as comprehending their causes and effects. The parameters are categorized into many areas concerning bit model, bottom hole assembly (BHA) configuration, drill string mechanics, drilling parameters, and formation. However, not all of these are studied simultaneously in the bit walk prediction model. Only certain areas are selected to meet the objective of drilling runtime predictive tool that some parameters are not readily available at the drilling runtime, but can be collected after the drilling operation is finished through well log data acquisitions which mainly are the information associated with formation characteristics. The commonly used bit model and BHA configuration are selected without making change throughout the study. Formation is scoped to focus on the one closed to a petroleum reservoir. The

formation represents lower Miocene age with Fluvial channel depositional environment.

Procedures in creating the bit walk predictive tool are to be described step by step in each following chapter. Chapter 2 outlines the review of past studies on parameters affecting bit walk and summary made by each researcher. Chapter 3 explains the meaning and geometry of bit walk as well as describing the causes and effects of each parameter in details. As a result, important parameters affecting bit walk are identified to be the inputs of the ANN model. Moreover, ANN theory and concept are discussed. Chapter 4 mainly focuses on the model development and any conditions applied to this specific case. Firstly, field data are analyzed to ensure a qualified distribution before inputting into the model for training. Secondly, the ANN model is trained, validated and tested with several configurations. Results and analysis are also discussed in this chapter. Chapter 5 ends with conclusion and recommendation for future works.



ศูนย์วิทยทรัพยากร
จุฬาลงกรณ์มหาวิทยาลัย

CHAPTER II

LITERATURE REVIEW

This chapter describes the past studies related to parameters and conditions affecting bit walk concerning several areas, such as bit model, gauge, profile, Bottom Hole Assembly (BHA) configuration, drilling parameters, and formation characteristics and anisotropy. The studies have been conducted through number of methods including field data observation, mathematical model, and experiment through drilling bench.

Perry (1986) conducted a field data observation and survey from the drilling operations of several wells drilled in the Gulf of Thailand by different type of bit profiles coupled with the change in drilling parameters. The objective was to observe how much bit walk was affected. The case study focused on 8-1/2" hole section covering Fluvio-deltaic depositional environment formation. Bit profiles were divided into 5 types (A-E), ranging from very flat to ballistic profile. Weight on bit (WOB) and Rotational speed (RPM) were taken into account as part of drilling parameters variation. The results from the observation showed that most of the bits usually turn left at their optimum drilling parameters. Flat profile bit exhibited a tendency to a right walk.

Bannerman (1990) studied a walk rate prediction on 23 wells in the Alwyn North Field, in the North Sea by Means of Data Analysis and 3D Computer Model. By analyzing data from both the 17-1/2" and 12-1/2" phases, an attempt was made to explain the variation of walk rates from well to well. The study found that bit walk was affected by several factors, namely BHA type, number and diameter of stabilizers, hole size, inclination, coefficient of friction. Another conclusion drawn which is in line with Perry is that walk rate or walk tendency is not affected by bit gauge length.

Millhiem and Warren (1978) studied the side cutting characteristics of bits and stabilizers through full-scale, automated, drilling apparatus. Side cutting was measured in rate of displacement. The tests were conducted in Bedford Limestone and Carthage Marble. The paper also expressed the effect of drilling operation parameters

and rate of penetration on the displacement from the testing. The side force displacement data from the lab test can be used in conjunction with the finite element BHA program to develop a model for bit trajectory prediction.

Ernst, Pastusek and Lutes (2007) conducted several tests on full scale drilling laboratory to investigate the effects of drilling parameters on the steerability of PDC bits. Rock samples were taken from the field classified as medium and hard limestone. They mostly represented homogenous blocks. The lab results were consistent with field results. Rotational speed (RPM) and weight on bit were found to create an effect on bit steerability. Formation hardness also established a significant effect as formation hardness increases, the ability of bit to drill laterally decreases.

Walker (1986) concluded factors controlling hole angle and direction which were quoted from the paper of Williamson and Lubinski (1986). Factors are such as bit geometry, BHA configuration, borehole shape and curvature, operating parameters. This paper mainly discussed on the BHA analysis which is the interaction between formation and types of BHA configuration. BHA analysis was carried out through the 2-D BHA model. Result revealed that each assembly behaves in a predictable manner for typical operating conditions and hole angles.

Menand, Sellami et. al (2003) presented a comprehensive analysis of the directional behavior of PDC bits, covering the effect of bit profile, gauge cutters and gauge length. Numerical simulations and laboratory tests have been carried out to better understand the mechanisms of PDC bit deviation and to evaluate the most important parameters affecting the directional behavior of PDC bits. The results obtained from the full-scale directional-drilling bench demonstrated that the bit profile, gauge cutters and gauge length exhibit a significant effect on the walking tendency of the PDC bits.

Chen, Collins and Thomas (2008) provided a reexamination on several past papers studied on PDC bit walk in both directional and horizontal wells. Furthermore a computerized numerical model was built and verified. The model could calculate bit walk and walk force with consideration of bit gauge geometry, hole size, formation compressive strength, steering mechanism of the Rotary Steerable System (RSS), bit rotational speed, penetration rate, dogleg severity. The study mainly

focused on PDC bit drilled with steerable system. It was concluded that the application of the bit model together with the BHA model to solve field problems has shown significant benefits.

Ho (1987) firstly summarized several previous studies concerning rock-bit interaction. Those studies were in the form of either 2D or 3D mathematical model. This paper is different from others that it incorporated both rock-bit and BHA analysis program into a single model called as a new rock-bit interaction model. By doing such, the model is able to predict directional behavior of the bit in the forward mode as well as generating anisotropy index of bit and formation through the inverse mode. The field data were used to generate average bit and formation anisotropy index through the inverse mode. The indexes were used in the forward mode to predict bit directional behavior accordingly. The results showed that, in average, the roller cone bit is quite anisotropic ($I_b = 0.194$), while the formation is quite isotropic ($I_r = 0$)

Maldla, Campinas and Sampaio (1989) tried to create another rock bit interaction model with an attempt to complete some gaps of Ho's model. In Ho's model, bit anisotropy index is a function not only of the bit type but also of the bit conditions. So, it could be changed throughout its life. Ho's model suppresses this uncertainty by averaging the index. The alternative model in this paper was verified by field data from 15 directional wells drilled in the offshore Campos Basis area in Brazil. The well trajectory prediction for 5 planned wells showed a capability in predicting bit walk rate, while not in some cases due to lacking of data on dip and strike of the formation.

Boualleg, Sellami and Menand (2006) set a study focusing on anisotropic rock in two cases which are interbedded and laminated rocks. The paper coupled a 3D bit-rock model with a 3D bottomhole assembly (BHA) model enabling the prediction of tortuosity occurrence (inclinal and directional deviation). The theoretical model was validated and calibrated on full-scale bench concerning many types of rocks. The model was concluded to be helpful for BHA and bit selections and design to minimize the effect of the formation anisotropy.

CHAPTER III

THEORIES AND CONCEPTS

3.1 Bit directional tendency (Bit walk)

Directional drilling is a three dimensional process that the bit penetrates along both X and Y plane as shown in Figure 3.1. Bit demonstrates an inclination angle in the inclination plane Y, while presents a direction angle in direction plane X. Inclination angle is measured in a degree from vertical deviation and apparent direction angle is measured in degree of azimuth. Bit walk rate is the change of direction angle per a specified drilling depth, commonly measured in degree per 30 meters or 100 feet. This study uses degree per 30 meters as a unit of measurement.

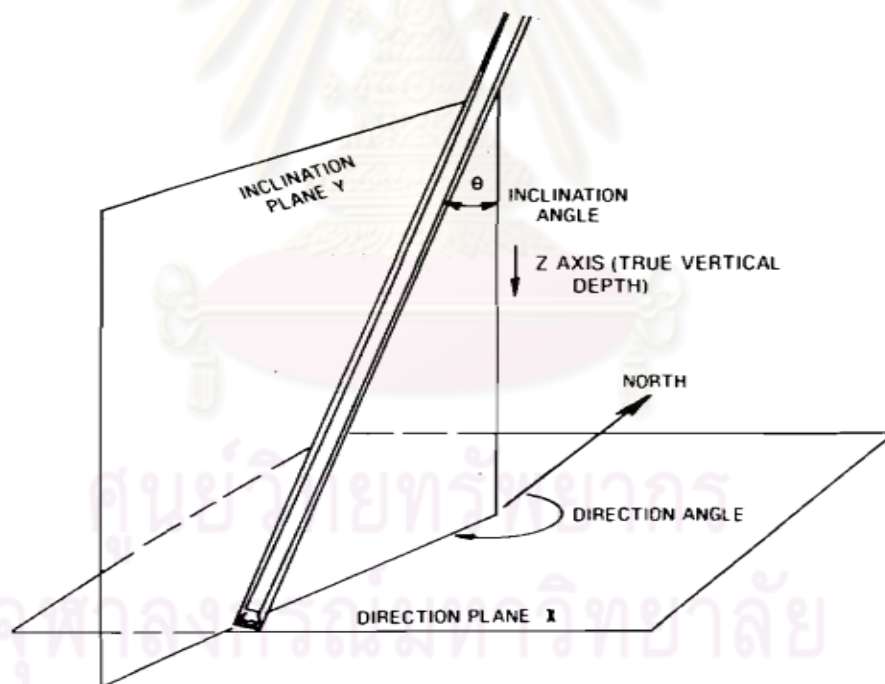


Figure 3.1: Inclination and direction angle (Bourgoyne Jr. A.T. *et al.*, 1984)

In practice, well geometry design is divided into several sections while inclination and direction angle are varied in each section as shown in Figure 3.2. Inclination angle in a tangent section of the well is usually controllable through the size adjustment of the stabilizer to establish build or drop of the inclination angle. Direction angle can be controlled by a steerable motor. However, this directional control tool is not applicable with certain formation conditions especially ones having high temperature where the rubber part of the tool is not able to operate effectively. This is the case in the Gulf of Thailand studied in this thesis. In this case, without a directional control tool in place, the bit travels in direction plane governing by certain factors described in the following section.

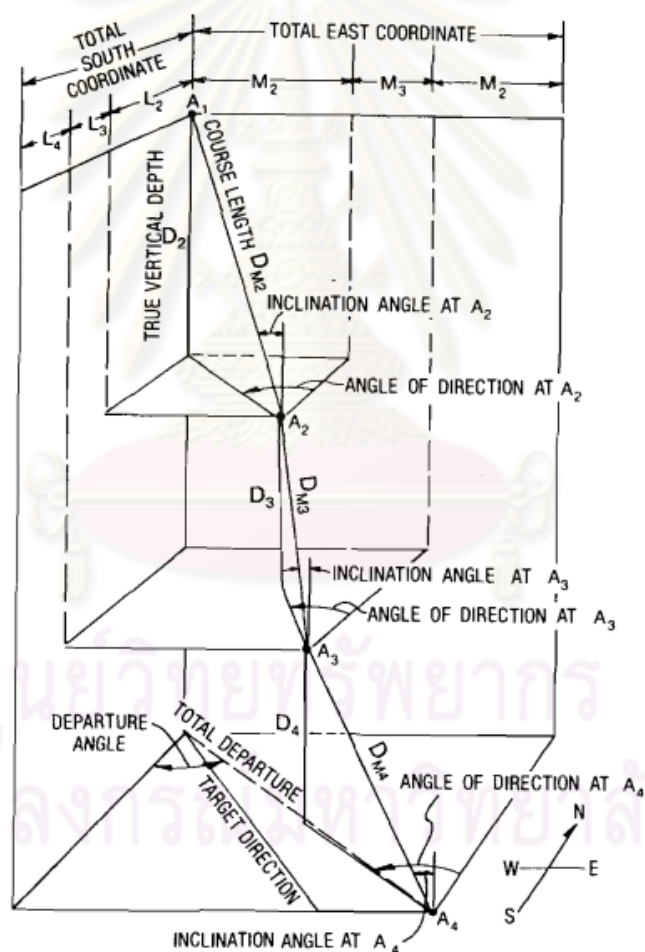


Figure 3.2: Drilling section (Bourgoyne Jr. A.T. *et al.*, 1984)

3.2 Factors affecting bit walk

Factors affecting bit walk have been extensively studied by many researchers. Some of them have been summarized in this topic, with a special emphasize on the factors that are used for the model in this study.

3.2.1 Bit Model

This section shows the summary and latest information conducted by some researchers on the factors affecting bit walk tendency. This topic focuses on the bit model and its configuration such as bit profile, active and passive gauge. The conclusions on how these parameters affect bit walk tendency are summarized through field or laboratory test as well as mathematical model.

Perry (1986) has conducted the real operation over 200 rotary bit runs in low-toxic oil base mud in the Gulf of Thailand. This was to observe how bit profile and gauge give an effect on the walk direction. All of the bits shown in figure 3.3 have exhibited a left walk tendency, except bit D that has a natural tendency to walk right in approximate. This happens at the condition of bits' optimum drilling parameters, namely 8 to 17 Klbs of weight on bit and 190-220 RPM of rotational speed. It is noticed that Bit D has a relatively flat profile comparing with other bits shown in Figure 3.3. The author has concluded that flat profile bit has a tendency to walk right than ones having ballistic profile. Also another conclusion drawn is that the bit gauge length as shown in table 3.1 does not seem to affect the bit walk. And the number of gauge cutters is about the same for bit type A, a "left walker", and bit type D, a "right walker".

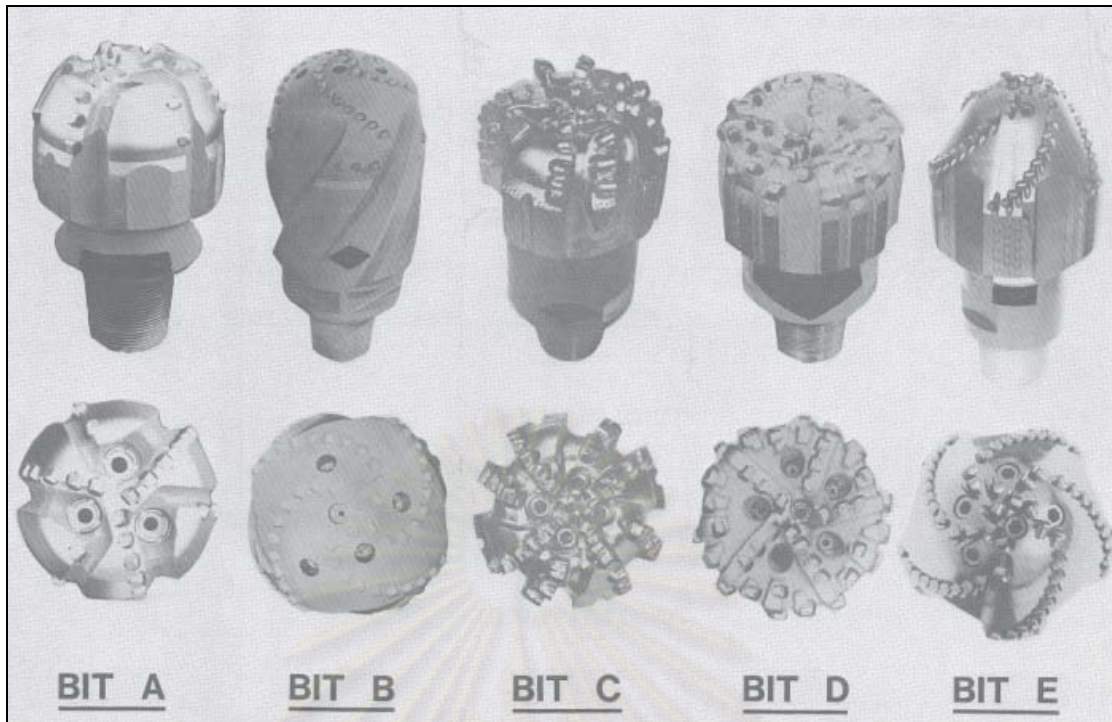


Figure 3.3 Bit used in the drilling operation (Perry, 1986)

Table 3.1: Bit configuration (Perry, 1986)

Bit	Body Type	Total no. cutters	No. gauge cutters	Length of gauge (in.)
A	Steel	24	6	2.5
B	Steel	37	16	6.0
C	Matrix	36	9	3.0
D	Steel	41	5	3.0
E	Steel	42	10	3.3

Menand, Sellami, et. al (2003) have developed a 3D theoretical rock-bit interaction model to reproduce the drilling test results observed from the field data and drilling-bench equipments. The author came up with the indicator to identify the walk tendency of the bit. It is called as bit steerability (B_s) corresponding to the ability of a bit to initiate a lateral deviation when submitted to lateral and axial forces. The bit steerability (B_s) can be defined as the ratio of lateral to axial drillability.

$$B_s = \frac{D_{lat}}{D_{ax}} \quad (3.1)$$

The lateral drillability (D_{lat}) is defined as the lateral displacement per bit revolution over the side force. The axial drillability (D_{ax}) is the axial penetration per bit revolution over the weight on bit (WOB). Bit steerability (B_s) which is equivalent to the bit anisotropic index is generally in the range of 0.001 to 0.1 for most PDC bits, depending on the cutting profile, gauge cutters, and gauge-pad characteristics. Lateral displacement and walk angle can be viewed in the figure 3.4 shown below. A bit with a high steerability means a strong tendency for lateral deviation. The rock-bit interaction model takes into account the three bit parts that interact with formation namely cutting structure, active gauge (trimmers or gauge cutters) and passive gauge (gauge pad), as shown in figure 3.5.

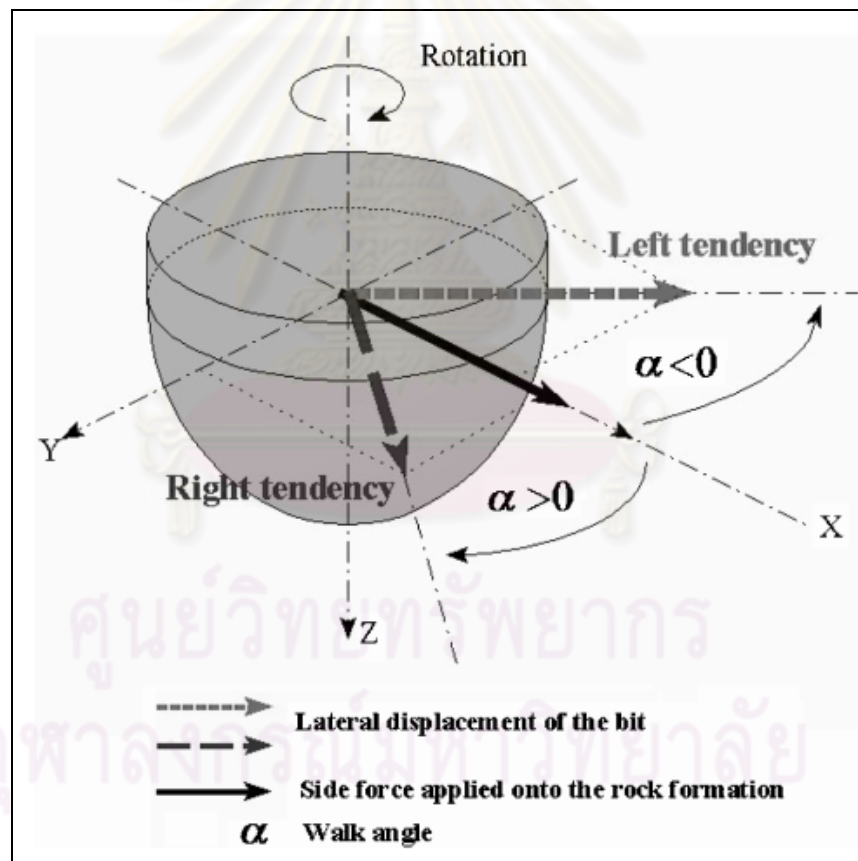


Figure 3.4: Definition of the walk angle (Menand *et. al*, 2003)

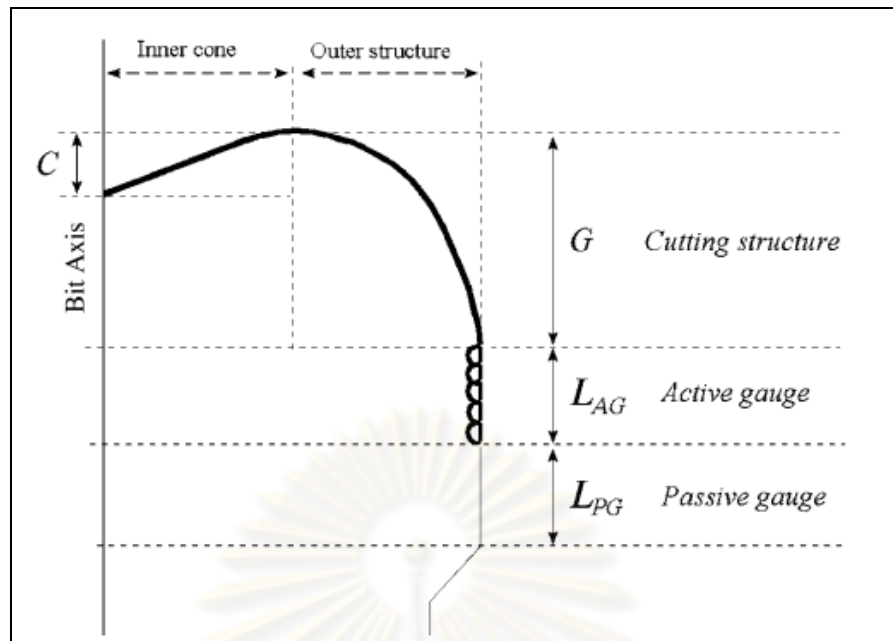


Figure 3.5: Description of the PDC bit structure (Menand *et. al*, 2003)

Three PDC bits having different profiles have been tested on the directional drilling bench namely bit A, B and C as shown in figure 3.6. The common characteristics of the bits are a 215.9 mm diameter, eight highly spiraled blades with 13.3 mm PDC cutters, and four nozzles. To evaluate the effect of the three different parts of the bit (cutting structure, active and passive gauges), each bit was tested with five different configurations, as shown in figure 3.7. Firstly, each bit was tested with passive gauge length ($L_{PG} = 101.6, 50.8$ and 25.4 mm). Then, the bits were tested with only their active gauge and cutting structure (no passive gauge). Lastly, each bit was tested with only the cutting structure (without any active or passive gauge).

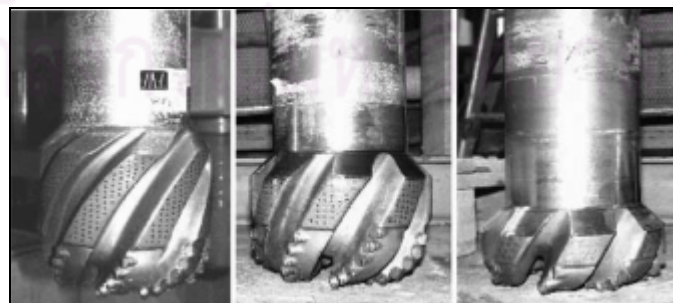


Figure 3.6: Bit A, B and C tested (Menand *et. al*, 2003)

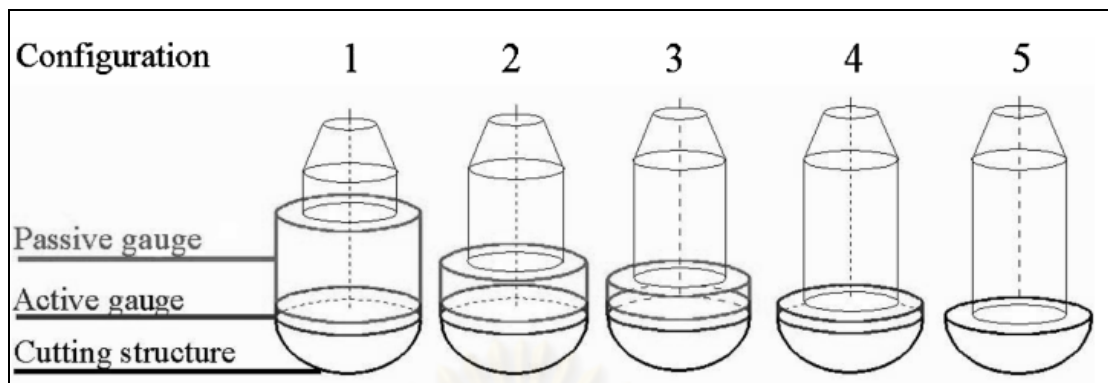


Figure 3.7: Description of the five bit configurations tested.

The result is summarized as shown in the table 3.2. From the various bit tested, it can be noticed that the bit steerability highly increases with the reduction of the passive gauge length. Consequently, it is concluded that passive gauge length highly contribute to the steerability or walk tendency of the bit. In addition, active gauge and bit profile also play the contributions. The active gauge contributes to the bit steerability with the same perspective as passive gauge. And bit profile is known as the flatter the profile is, the more steerable the bit is. Researchers can take into account of these parameters once a walk prediction model has to be developed.

Table 3.2: Bit steerability and walk angle from varying bit models and configurations (Menand *et. al*, 2003)

BIT STEERABILITY AND WALK ANGLE COMPUTED FROM THE 3D ROCK-BIT MODEL						
	Bit A		Bit B		Bit C	
	Steerability	Walk angle	Steerability	Walk angle	Steerability	Walk angle
Configuration 1 (CS+AG+PG = 101.6 mm)	0.032	-11°	0.016	-10°	0.012	-11°
Configuration 2 (CS+AG+PG = 50.8 mm)	0.080	-11°	0.033	-11°	0.038	-12°
Configuration 3 (CS+AG+PG = 25.4 mm)	0.110	-12°	0.118	-11°	0.093	-12°
Configuration 4 (CS+AG)	1.6	-12°	1.1	-12°	0.5	-12°
Configuration 5 (CS)	5.4	+23°	9.2	+7°	3.5	-30°

NOTE: CS = cutting structure, AG = active gauge, and PG = passive gauge.

3.2.2 Bottom Hole Assembly (BHA)

Each component of the drillstring has a unique stiffness that contributes to the overall performance of the BHA. The stiffness or rigidity of any component is a function of its modulus of elasticity and its moment of inertia. The weight of each component of the BHA affects the assembly's behavior. This weight is a function of the size and specific weight of the component and must include the buoyancy effect of the drilling fluid. In general, stabilizer placement and size are major factors in deviation control. The effects of location, size, shape, and properties of the BHA components on hole angle and direction can be analyzed by available BHA models (Walker, 1986). However, this study does not focus on the variation of the BHA configuration. In contrary, the configuration of the BHA remains in a particular set up according to the practice and actual operation that BHA configuration is usually not modified throughout the drilling operation in the 6-1/8" section.

3.2.3 Well geometry

The shape and curvature of the borehole has been the subject of much analysis, and the interaction between borehole trajectory and BHA elastic deflection can now be modeled in three dimensional spaces. The curvature of the borehole can cause the BHA to be deflected in a complex shape nearly independent of the BHA components (Walker, 1986). There was a proposal of a general rock-bit interaction model verified by field data which indicates an inverse relationship between well inclination and walk rate (Maldla and Sampaio, 1989) as

$$K \propto \frac{(I_b, I_r)}{\sin(\alpha)} \quad (3.2)$$

where

- I_b = bit anisotropy
- I_r = rock (formation) anisotropy
- α = inclination angle
- K = walk rate

3.2.4 Drilling operating parameters

According to Ernst, Pastusek and Lutes (2007), with regards to operating parameters, weight on bit (WOB) is well-known to be beneficial in increasing the desired turn rate under certain drilling conditions. It is proposed that most of the weight on bit effects is actually due to its influence on rate of penetration and bit tilt. There is a general consensus in the industry that increasing the rotational speed of the bit provides more opportunities to cut the formation in a given amount of time. Also by slowing the forward ROP of the bit from reducing the weight on bit, side cutting time would be increased resulting in high steerability. Drillers have long known that controlled drilling parameters (weight on bit and rotational speed) could be used in order to effect build, drop and walk rates of a bit and BHA system. With the use of full scale drilling laboratory, the effects of drilling parameters have been investigated. The test apparatus simulates the bit tilt and side loading normally induced by a BHA inside the wellbore. Lateral displacements are recorded within thousands of an inch. The testing method produces well defined results that are consistent with field results. During the test, the resultant lateral displacement drilled and vertical depth drilled were recorded. The same bit design was used for all tests. The test results are shown in figure 3.8 which is the result of varying rotational speed and ROP (representing WOB) in the Bedford (Indiana) Limestone demonstrating medium hardness. Side cutting angle also represents a walk tendency. It is shown in the figure that at a constant rotational speed, side cutting angle is decreased when ROP is increased. While at a constant ROP, low rotational speed has a tendency to exhibit high side cutting angle. ROP is directly proportional with WOB. Therefore, in this case, it is summarized that WOB and rotational speed generally exhibit an inverse relationship with the walk tendency.

จุฬาลงกรณ์มหาวิทยาลัย

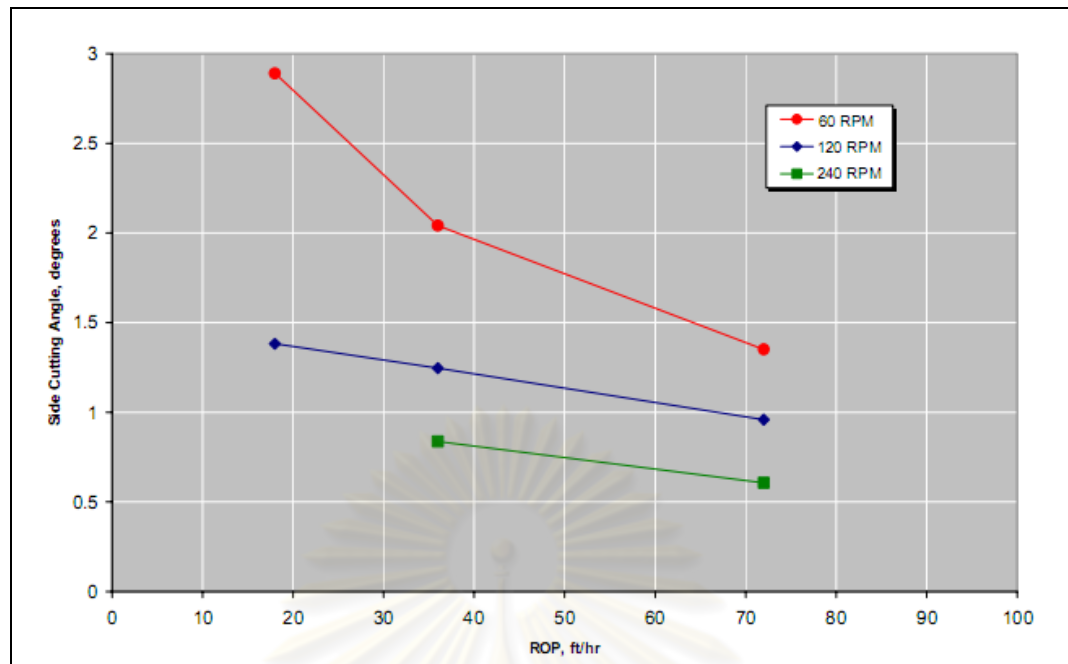


Figure 3.8: Side cutting angle vs. Operating parameters (WOB, RPM) (Ernst, Pastusek and Lutes, 2007)

3.2.5 Formation characteristics

3.2.5.1 Formation anisotropy

According to Boualleg, Sellami and Menand (2006), Interbedded formations hard/soft or soft/hard are a major cause of borehole tortuosity. Cases history have demonstrated that this tortuosity induces a higher torque and drag, running tubular problems, stabilizers wear, pipe damage and trajectory controlling problems. In some fields, shale formations have a tendency to cause wellbore deviations to undesired directions. To understand these phenomena of tortuosity, an experimental drilling program has been carried out on a full scale bench using various PDC bits in different formations (hard/soft, soft/hard with different interface angles). The interface angle is also known as dip angle of the formation. These described characteristics represent the anisotropy of the formation. It is well recognized today, by the drilling industry, that deviations of well trajectories are influenced by the BHA design, borehole curvature and inclination, weight on bit, bit characteristics, and formation anisotropy. The last one is subjected to be discussed in this section. Deviation of the wellbore could be written in a function form as

$$\text{Deviation} = f(\text{BHA}, \text{Bit}, \text{wellbore geometry}, \text{WOB}, \text{formation anisotropy}) \quad (3.3)$$

The author focused on the effect of the formation anisotropy and especially on the following cases.

- Interbedded rocks: consisting in a sudden change of the rock's mechanical characteristics.
- Laminated rocks: presenting an orthotropic mechanical behavior. Mostly shales belong to this category.

Interbedded rocks

Considering a PDC bit drilling an isotropic rock, all PDCs cut similarly the same rock, so there is no reason to generate a side force except that imbalance force if the bit is not balanced. However, as seen in figure 3.9, when the bit drills sequence of hard/soft or soft/hard rock, some PDCs cut the hard rock and others cut the soft one resulting in a side force during the drilling of the interface.

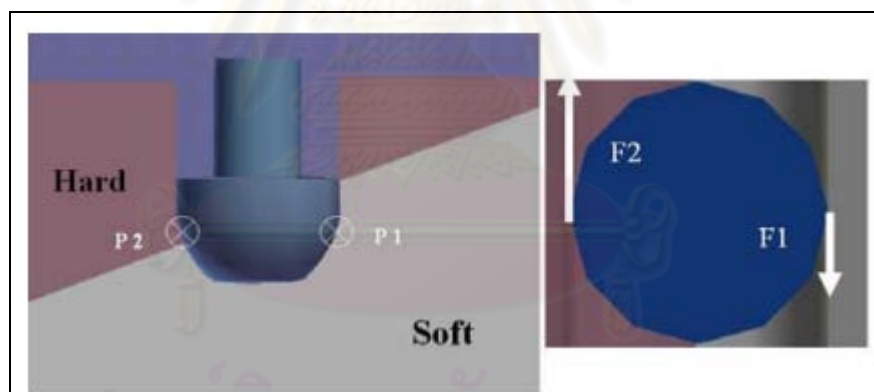


Figure 3.9: Origin of the anisotropic side force (Boualleg, Sellami and Menand 2006)

From testing with the interbedded rock, the side force on the bit depends generally on the interface angle between the hard and soft rock. From the observation, drilling through a sequence with a higher dip angle causes more significant force and deviations as the bit remains a longer time drilling through the interface. The sequence of rock (soft to hard or hard to soft) also influences the side force and deviations. Some tests have proved that the hard to soft transition produces less effort and deviation. This is explained by the fact that when the bit starts to touch the soft rock, the gauge is still in the hard one and has more difficulty to generate deviation.

Laminated rocks

Ecole des Mines de Paris has developed a complete model which takes into account build-up edge of crushed materials chamfer and back cutter force. The Model uses limit analysis and Mohr-Coulomb criterion to calculate the specific energy R_{eq} defined as the ratio of horizontal cutting force over the cutting area. For laminated rock, the specific energy depends also on the orientation of the formation dip defined by the unit normal (\vec{n}) It can be seen from the figure 3.10 below that it is easier to cut the rock in the configuration 1 than in the configuration 2. To calculate the specific energy, we assume that the stress state in the chip is homogeneous. In this case, the specific energy can be formally expressed as

$$R_{eq} = R_{eq}(\vec{n}, \alpha_1, \alpha_2, \bar{\alpha}_1, \bar{\alpha}_2, \omega_c, \theta_f) \quad (3.4)$$

Where

$$\begin{aligned} R_{eq} &= \text{specific energy} \\ \vec{n} &= \text{normal to dipping plane} \\ \alpha_1, \alpha_2, \bar{\alpha}_1, \bar{\alpha}_2 &= \text{material parameters} \\ \omega_c &= \text{rake angle} \\ \theta_f &= \text{rock-cutter friction angle} \end{aligned}$$

This model, taking into account the 3D variation of dip orientation (\vec{n}), has been validated with circular tests. These tests consist in cutting a circular groove (figure 3.11) with a PDC in an orthotropic rock. The PDC cuts the rock in different configurations referred by the angular position θ . Figure 3.12 presents a comparison between the experimental and theoretical results. It shows the evolution of the specific energy vs. the angle θ for a test carried out with 8 mm PDC diameter in the Angers schist (laminated rock). It can be noted, in this case of orthotropic rock, that the specific energy is very sensitive to the angular position. This sensitivity that cannot be observed in isotropic rock is the origin of the side force on the bit. It can be seen that the cutting forces depend on the PDCs radial positions on the bit. If we consider two PDCs at the same level and with different radial positions, they have different reactions resulting in a side force creating a walk tendency to the bit consequently.

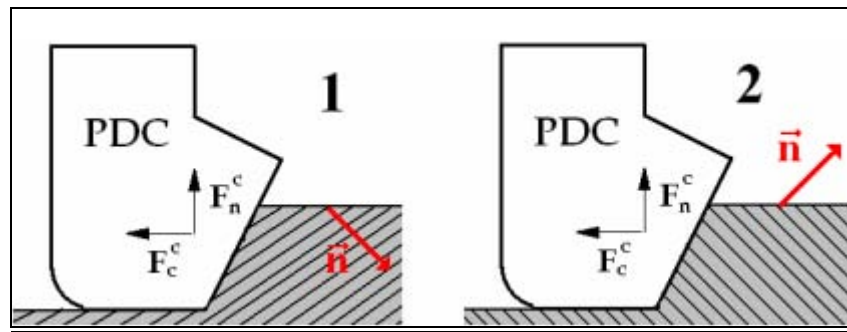


Figure 3.10: Cutting configurations and formation dip (Boualleg, Sellami and Menand, 2006)

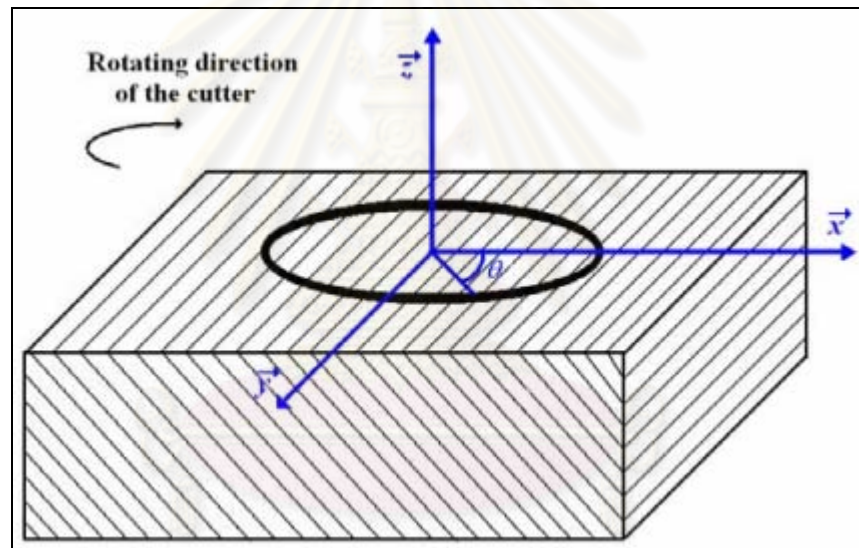


Figure 3.11: Circular test schema (Boualleg, Sellami and Menand, 2006)

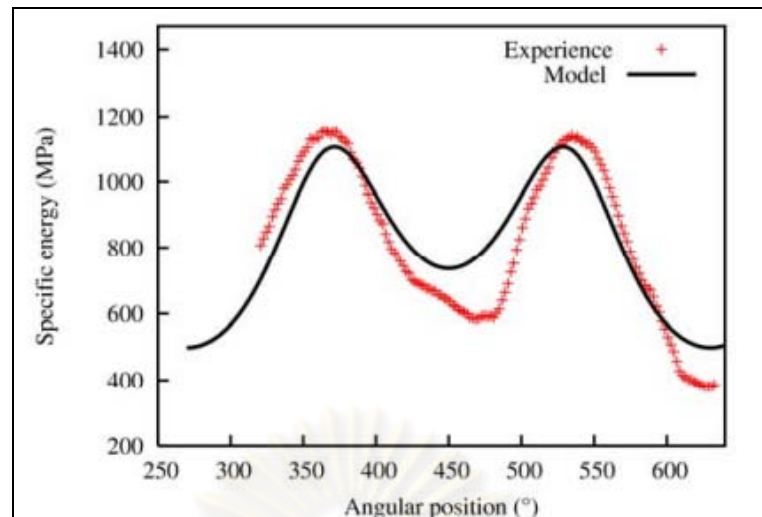


Figure 3.12: Results of a circular test (Boualleg, Sellami and Menand, 2006)

3.2.5.2 Formation hardness

Formation hardness has a significant effect on PDC bit steerability. As formation hardness increases, the ability of bit to drill laterally decreases (Ernst, Pastusek and Lutes, 2007). This also makes the bit walk rate decrease as a result. This has been summarized from the drilling bench testing. In this study, formation hardness information could be derived from the bit torque. According to Wolcott and Bordelon (1993), the bit torque can be used to identify the formation lithology into porous, shaly and tight. This corresponds to the hardness of formation as low, medium and high respectively. Torque will increase in soft formation because of good tooth penetration and therefore decrease in hard formations.

3.3 Artificial Neural Network

Artificial neural network (ANN) has been found acceptance in solving real world problems in many disciplines. ANN learns to create a representation of complex relationship between input and output samples by utilizing processing characteristics of biological system such as nonlinearity, high parallelism, fault and failure tolerance, and capability to generalize. ANN has been utilized in many forms of applications such as modeling, classification, pattern recognition (Basheer and Hajmeer, 2000). The idea of ANN was motivated from the biological nerve cell called neuron. Interconnection of billion of neurons composes a human nervous system.

ANN applies the same concept by interconnecting several neurons together with a connection link that can be newly established or updated to form a knowledge learning process. Figure 3.13 shows the components of biological neuron comprising of three major functional units namely dendrites, cell body and axon. The dendrites receive signals from other neurons and pass on to the cell body. After receiving the signal, cell body sums total incoming signals and fire an electrochemical signal when threshold is reached. The axon receives signals from the cell body and carries through the synapse to the dendrites of neighboring neurons. The connections between artificial neuron analogously represent axon and dendrites while connection weights represent the synapses. ANN as well as biological network learns the knowledge through adjusting magnitude of weight or synapses' strengths. There are many types of artificial neural networks invented by several researchers. For this study, Backpropagation ANN (BPANN), known as one of the most famous artificial neural network architecture and algorithm, is selected as a tool. In every iteration of BPANNs, it performs two steps; 1) forward activation of the signal to produce an output. 2) backward the computed error to modify weight by the feedforward error-backpropagation learning algorithm. Basic elements are one input, one output and a certain number of hidden layers. Each layer consists of processing units or neurons. Signals are passed from the neurons of input layer through hidden layer before arriving output layer. Each neuron of one layer to another is interconnected with connection link having its own associated weight. Figure 3.14 demonstrates a diagram of ANN. Each circle represents neuron interconnected with the link where weight is stored. The neurons receive weighted inputs from previous layer, summing and pass on through a threshold function having a sigmoidal shape. The output from sigmoid function ranges between 0 and 1, when input is a large negative and positive number respectively. Mathematical description of the neuron output is written as

$$O_j = \frac{1}{1 + e^{-\varepsilon_j}} \quad (3.5)$$

$$\varepsilon_j = \sum w_{ji} O_i \quad (3.6)$$

where O_j is the output from a neuron in the j^{th} layer and ε_j is the summation of weighted inputs of the previous layer (input layer in this case), while w_{ji} is the associated weight of connection link between neurons of i^{th} and j^{th} layer. BPANN is

iterated to perform learning process to adjust the weight based on the error calculated from a difference between real sample and network generated output. The weight updating method is written as

$$w_{ji}(t) = w_{ji}(t-1) + \Delta w_{ji}(t) \quad (3.7)$$

$$\Delta w_{ji} = \eta \delta x_{ji} + \mu \Delta w_{ji}(t-1) \quad (3.8)$$

where $\Delta w_{ji}(t)$ is the updated weight at t^{th} iteration, η is the learning rate, and μ is the momentum coefficient. δ is the error criterion. Giving an example of neuron at the output layer, error criterion is calculated from

$$\delta = (x_k - y_k) x_k (1 - x_k) \quad (3.9)$$

where y_k is the real sample output and x_k is the ANN output. Then an error criterion is propagated back through each neuron of the network and re-updates the weight of connection link used in the next iteration. ANN training is stopped by a condition, commonly using Mean Square Error (MSE) as a criterion to verify the model output against validation set of data. Details on how to calculate mean square error is described in the next chapter.

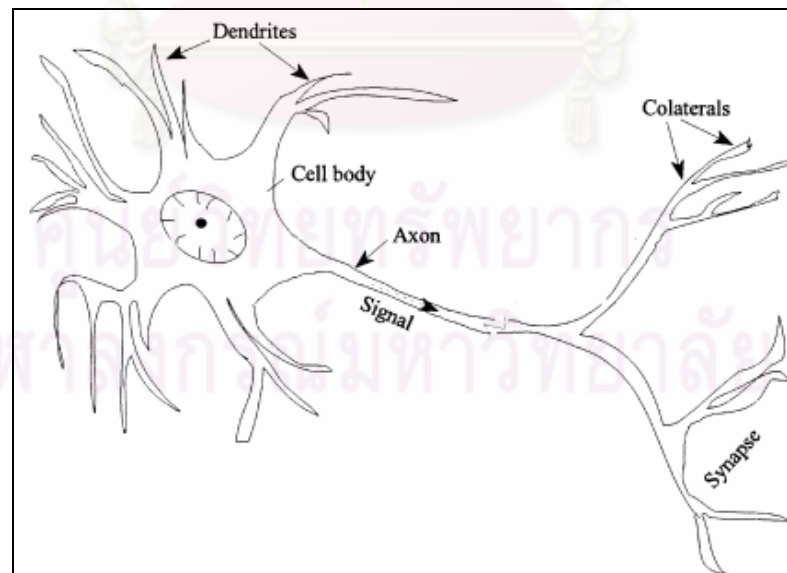


Figure 3.13: Schematic of biological neuron (Basheer and Hajmeer, 2000)

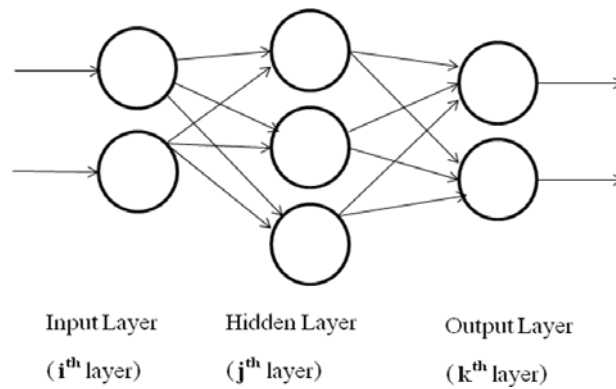


Figure 3.14: Schematic diagram of ANN

Although the error backpropagation algorithm has been a significant milestone in neural network research area of interest, it has been known as an algorithm with a poor convergence rate (Wilamowski *et. al.*, 2001). One of the attempt to improve the speed of the error backpropagation is to use the Levenberg-Marquardt (LM) optimization technique. LM algorithm is widely accepted as the most efficient one in terms of realization accuracy. LM algorithm has a similar concept of weight update to the normal error backpropagation algorithm. The weight updates are calculated using the following equation.

$$w_{t+1} = w_t - (J_t^T J_t + \eta_t I)^{-1} J_t^T E_t \quad (3.10)$$

Where

$w = [w_1 w_2 \dots w_N]^T$ consists of all weights of the network

J is the Jacobian of m output errors with respect to n weights of the neural network.

Jacobian matrix can be written as follow

$$\mathbf{J} = \begin{bmatrix} \frac{\partial e_{11}}{\partial w_1} & \frac{\partial e_{11}}{\partial w_2} & \dots & \frac{\partial e_{11}}{\partial w_N} \\ \frac{\partial e_{21}}{\partial w_1} & \frac{\partial e_{21}}{\partial w_2} & \dots & \frac{\partial e_{21}}{\partial w_N} \\ \vdots & \vdots & & \vdots \\ \frac{\partial e_{K1}}{\partial w_1} & \frac{\partial e_{K1}}{\partial w_2} & \dots & \frac{\partial e_{K1}}{\partial w_N} \\ \vdots & \vdots & & \vdots \\ \frac{\partial e_{1P}}{\partial w_1} & \frac{\partial e_{1P}}{\partial w_2} & \dots & \frac{\partial e_{1P}}{\partial w_N} \\ \frac{\partial e_{2P}}{\partial w_1} & \frac{\partial e_{2P}}{\partial w_2} & \dots & \frac{\partial e_{2P}}{\partial w_N} \\ \vdots & \vdots & & \vdots \\ \frac{\partial e_{KP}}{\partial w_1} & \frac{\partial e_{KP}}{\partial w_2} & \dots & \frac{\partial e_{KP}}{\partial w_N} \end{bmatrix}$$

I is an identity unit matrix

η is a learning rate

And lastly,

$E = [e_{11} \dots e_{K1} \quad e_{12} \dots e_{K2} \quad \dots \quad e_{1P} \dots e_{KP}]^T$ is the cumulative error vector (for all patterns)

Where

$$e_{kp} = d_{kp} - o_{kp} \quad k = 1, \dots, K \quad p = 1, \dots, P$$

d_{kp} is the desired value of the k^{th} output and the p^{th} pattern, o_{kp} is the actual value of the k^{th} output and the p^{th} pattern, N is the number of the weights, P is the number of pattern, and K is the number of the network outputs.

This LM algorithm is used in this study as a network training algorithm for calculating the error and back propagate to update the weight of the network. This should help the network to reach the convergence quicker than the normal back propagation algorithm.

CHAPTER IV

BIT WALK PREDICTION MODEL DEVELOPMENT

This chapter firstly covers an outline of the specific case and conditions applied to this study. Secondly, it describes the ANN tool, methodology and each case study in ANN model development. Thirdly, the chapter discusses the result and analysis. Certain parameters affecting bit walk behavior are selected for this study. The study mainly focuses on the available parameters which can be controlled or monitored at the drilling site. Field data used as the ANN inputs comes from several sources. They are all compiled into a single format to facilitate the model development. Procedures and methods on information compiling and reformatting are also described. Furthermore, ANN model development is divided into cases. Each of which contains the ANN configurations adjusted to be suitable for the format and condition of dataset. The developed models passing the validating criteria are selected for performance testing with the real field data in order to locate the best network configuration. Finally, results from the ANN model prediction are discussed and analyzed.

4.1 Model Parameters and Conditions

The previous chapter demonstrates the factors affecting bit walk in many aspects. However, the model development of this study does not take into considerations of all parameters. As the development mainly focuses on the practicality and usability of the model in the real operation where selected parameters can be controlled or monitored at the drilling site or predefined at the well planning phase. In addition, the model is intended to scope down to focus on the frequently used drilling equipment and configurations. Formation is specific to the one where the petroleum reservoir is resided. Drilling operation in the formation closest to the reservoir is required to exhibit the accuracy in order to meet the reservoir target in an acceptable range maximizing the production.

4.1.1 Bit type

According to the IADC classification of PDC bit, the selected PDC bit for this study is under M423 type. And this bit type is used throughout the study. The explanation of the codes is shown in table 4.1.

Table 4.1: IADC classification of the PDC bit

Code	Description
M	Bit body: Matrix
4	Formation type: Medium
2	Cutting structure: PDC, 19mm
3	Bit profile : Medium profile

4.1.2 BHA configuration

This study focuses on a single type of BHA configuration and component. This is according to the actual drilling operation that this BHA set up is normally used with the selected PDC bit type.

Table 4.2: BHA components

Item#	Details	Size(in)	Length(m)
1	Bit	6.125	0.240
2	Near bit stabilizer	4.750	0.710
3	Extension Sub	5.000	0.590
4	AGS	5.000	3.180
5	MWD tool	5.000	9.470
6	Steel screen sub	4.750	1.900
7	String Stabilizer	4.750	1.520
8	Drill collar	4.750	36.880

4.1.3 Drilling parameters

Weight on bit (WOB) and Rotational speed (RPM) are selected for the inputs of the model. These two parameters are known to be the common parameters adjustable while performing drilling operation by a directional driller. They have exhibited the relationships with bit walk as previously described. Moreover, another model input, torque, is used as an indirect indicator of formation characteristic and hardness. Torque is not a directly adjustable drilling parameter. It is recorded by the drilling measurement system as a result of the change in drilling parameters and effect from the formation in each interval.

4.1.4 Wellbore inclination

Wellbore inclination is selected to be another important parameter affecting bit walk. It is normally predetermined at well design phase and can be minimally adjusted during the drilling operations using AGS tool.

4.1.5 Formation

The study focuses on the formation closest to the petroleum reservoir. The specific formation represents lower Miocene age with Fluvial channel depositional environment. It is a red bed unit composed of red and reddish gray clay stone, siltstone and sandstone. Individual sand beds can be as thick as 20 meters in total. Sand tends to be medium to coarse-grained. Thin sand bed of thickness less than 5 meters can also be presented. An example of geological prognosis of a well is shown in figure 4.1.

ศูนย์วิทยทรัพยากร
จุฬาลงกรณ์มหาวิทยาลัย

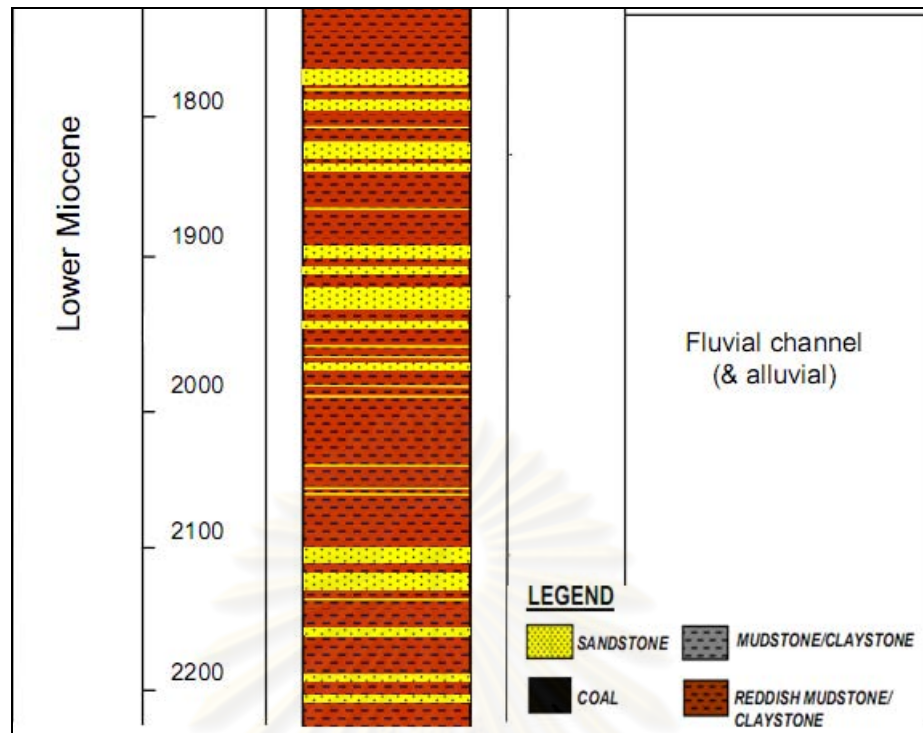


Figure 4.1: Geological prognosis of the formation (selected from a well)

4.2 Data compilation and formatting

Field data are collected from the drilling operation of 13 wells drilled in the Gulf of Thailand area. They are mapped with the geological prognosis to determine the dataset from the operation performed in the studied formation. Information concerning parameters either controlled or resulted from the drilling operation is measured and captured in the “drilling parameters ascii file”. The parameters and unit of measurements in this file are such as 1) Measured and true vertical depth in meters 2) Weight on bit (WOB) in Kilo pounds (Klbs) 3) rotational speed in revolution per minute (RPM) 4) Torque in Kilo pound * feet (Klbs*ft) 5) Rate of penetration in meters/hours (m/hr) 6) pump pressure in pound per square inches (psi) 7) flow rate measured in liters/minutes (l/min) 8) Mud weight in specific gravity (SG). The frequency of each data collection is 0.5 meter. Moreover, another important measurement is associated with the inclination and direction angle of the bit. These are captured in the “definitive survey” file. And the data collection is carried out every 30 meters.

Since the information from the definitive survey is in a different scale from the drilling parameters, namely the survey is measured every 30 meters while the drilling parameters are measured every 0.5 meters. Consequently, these two sources have to be aligned into the same unit of measurement by averaging the drilling parameters to be in accordance with the survey domain. Table 4.3 demonstrates the averaging procedure of the drilling parameters which are sampled from an interval of a drilled well. From the measured depth of 1623.71 and 1652.51 m, degree of azimuth is measured from the definitive survey as 140.23 and 139.88 degree respectively. Bit walk rate is calculated by the difference of degree of azimuth per measured interval length. In this case bit walk rate equal $-0.35 \text{ deg/ } 28.8 \text{ m}$ ($139.88 - 140.23$) deg/ ($1652.51-1623.71$) m. Each measured interval may be varied, but every bit walk rate has to be in the same interval domain. Therefore, bit walk rate produced from every dataset has to be aligned into the same unit that is a deg/30m . Bit walk rate as $-0.35 \text{ deg/} 28.8 \text{ m}$ is normalized to a deg/30m unit giving a result of -0.365 deg/30m . The negative sign represents the left direction, as there is a reduction in the degree of azimuth while the positive sign represents the right direction. Drilling parameters measurement frequency is higher than the survey. Hence, they have to be averaged to match the interval of the survey. The results from the average are displayed. In summary, from the interval of 1623.71 to 1652.51m, Bit walk rate is $0.365 \text{ deg/ } 30\text{m}$ to the left direction given drilling parameters as WOB = 5.59 Klbs, Rotational Speed = 209.00 RPM and Torque = 5897.88 Klbs*ft.

Table 4.3: Measured parameters from Drilling Parameters Ascii and Definitive Survey

Drilling Parameters Ascii				Definitive Survey		
MD (m)	WOB (Klbs)	Rotational Speed (RPM)	Torque (Klbs*ft)	MD (m)	Inclination (deg)	Azimuth (deg)
1624.00	6.00	202.00	6201.00	1623.71	15.33	140.23
1624.50	6.00	204.00	6087.00			
1625.00	6.00	204.00	5929.00			
1625.50	6.00	203.00	6231.00			
1626.00	6.00	205.00	5990.00			
1626.50	6.00	202.00	6165.00			
1627.00	6.00	204.00	5994.00			
1627.50	6.00	205.00	6108.00			
1628.00	5.00	208.00	5697.00			
1628.50	6.00	206.00	6022.00			
1629.00	6.00	205.00	5941.00			
1629.50	6.00	205.00	5925.00			
.	.	.	.			
.	.	.	.			
.	.	.	.			
1646.50	4.00	212.00	5701.00			
1647.00	4.00	212.00	5514.00			
1647.50	4.00	212.00	5477.00			
1648.00	4.00	212.00	5705.00			
1648.50	4.00	211.00	5872.00			
1649.00	4.00	212.00	5603.00			
1649.50	4.00	211.00	5847.00			
1650.00	4.00	211.00	5827.00			
1650.50	4.00	212.00	5733.00			
1651.00	3.00	211.00	5632.00			
1651.50	4.00	211.00	5636.00			
1652.00	4.00	211.00	5754.00			
1652.50	4.00	211.00	5843.00	1652.51	15.15	139.88
Average	5.59	209.00	5897.88			-0.35 deg/28.8 m
						-0.365 deg/30m

} Bit walk rate

4.3 Bit walk prediction model development

The study on bit walk behavior in this thesis concerns two perspectives, namely bit walk quantity and direction. Bit walk quantity is, in other word, presented as bit walk rate. Bit walk direction is represented in either left or right deviation. Three case studies are presented. Firstly, case 1 is an attempt to address parameters potentially affecting bit walk direction and builds a model if the availability of data allow. Secondly, case 2.1 is a study on bit walk rate. For this case, absolute bit walk rate is modeled and later analyzed on the result and error occurred. Thirdly, case 2.2 is also in the area concerning bit walk rate but not focusing on predicting the absolute value of the bit walk rate, rather it tries to predict bit walk rate in range. Result and error analysis of this case are also discussed. Artificial neural network (ANN) is used as a tool to create a bit walk rate prediction model on case 2.1 and 2.2. The model is also verified against the real field data as well as checked for the alignment with the theories proposed by other researchers regarding factors affecting bit walk.

4.3.1 Case 1 – Bit walk direction

4.3.1.1 Bit walk direction data analysis

From the observation of the total 140 dataset extracted from 13 wells of drilling operations in the Gulf of Thailand, there are only 20 right walk instance out of the total 140 dataset. This is calculated as approximately 14 percent of right walk instance out of the totals. The rest represents left walk instance. It is well known by the information from the bit manufacturer that the selected PDC bit model mentioned in the previous section normally exhibits left walk tendency. Therefore, it is worth to study what could be the effects on the 20 instances of right walk. All of the 20 dataset are analyzed to observe the factors that could be related to the walk direction and 7 of them are captured for the examples as shown in table 4.4. The observation is carried out by matching two dataset having similar quantity of the parameters that could affect the bit walk, one with left walk and another with right walk presentation.

Table 4.4: Comparison of left and right bit walk dataset

Dataset #	Inclination (deg)	WOB (Klbs)	Rotational speed (rpm)	Torque (Klbs*ft)	AGS size (in.)	Walk rate (deg/30m)	Walk direction
1	15.33	3.67	214	6036	2.25	0.52	Right
2	15.55	4.09	212	6356	2.25	0.52	Left
3	18.72	12.03	222	9792	5.00	0.36	Right
4	18.24	12.91	220	9444	5.00	0.36	Left
5	21.98	12.38	220	9634	5.00	0.18	Right
6	21.98	14.14	222	9740	5.00	0.35	Left
7	22.78	14.03	221	9592	5.00	0.47	Right
8	22.65	11.34	220	9570	5.00	0.35	Left
9	23.35	12.76	142	8824	5.00	0.71	Right
10	23.60	13.03	163	13586	5.00	0.82	Left
11	31.77	13.25	223	9403	5.00	0.18	Right
12	31.32	13.10	223	9873	5.00	0.70	Left
13	55.24	12.28	220	9097	2.25	0.18	Right
14	55.51	10.98	220	9369	2.25	0.18	Left

4.3.1.2 Results and Discussion

The result turns out that given the two datasets where each parameter has nearly the same quantity namely inclination, weight on bit (WOB), rotational speed (RPM), torque and AGS size (diameter). However, walk results in a total different direction. One walks to the left while another one walks to the right. The examples can be referred to dataset#1 and #2, and also other two adjacent datasets shown in Table 4.4. Dataset#1 representing right walk, demonstrates inclination angle as 15.33 deg, weight on bit as 3.67 Klbs, rotational speed as 213.58, torque as 6035.65 Klbs*ft, and AGS size as 2.25 m. Whereas dataset#2, representing left walk, demonstrates inclination angle as 15.55 deg, weight on bit as 4.09 Klbs, rotational speed as 211.64, torque as 6356.28 Klbs*ft, and AGS size as 2.25 m. Both of them demonstrates an equal walk quantity but different in the direction. It could be noticed between the two dataset that the parameters are not exactly equal, but the difference are not significant. Giving an example of weight on bit 3.67 Klbs of dataset#1 and 4.09 Klbs of dataset#2, dataset#2's weight on bit is different from dataset#1's by 11%. However, this should not result in a total different in the walk direction. Therefore, it could be inferred that there are other parameters governing the walk direction that are not presented which could be the information that are not available in this study mainly

related to the formation characteristics such as dip angle and anisotropy indicator of the formation. Giving another example between dataset#5 and #6, parameters of the two dataset are quite close but result in a different walk direction. Even though the walk quantity is not exactly equal, the difference in direction has already confirmed the effect of the unrepresented parameters related to the formation characteristics as mentioned above. And this case is concluded that ANN model is not used for the walk direction prediction due to unavailability of the information. However, the preliminary factors that could affect the walk direction are determined which are related to the formation characteristics.

4.3.2 Case 2 – Bit walk quantity (rate)

The 20 dataset of right walk are excluded from the total 140 dataset. As a result, 120 dataset of left walk are remained. These left walk dataset are to be inputted into the ANN model to create the prediction model stating the relationship between the parameters and walk quantity (rate). Parameters that are selected for the model inputs are inclination, weight on bit (WOB), rotational speed (RPM), and torque. In this study, the left walk prediction model is created in two different cases. Firstly, case 2.1 attempts to predict the absolute value of walk rate, result and error analysis by comparing the predicted and desired output are to be discussed to evaluate the performance of the model. Secondly, case 2.2 attempts to predict the walk rate in range, rather than trying to find an absolute value of walk rate. Results and error analysis are also discussed to evaluate the performance. These two different cases are built and compared to find the most appropriate approach how to best utilize the model. Some example dataset that are used for both cases are shown in table 4.5. And ranges of each parameter are summarized in the table 4.6.

Table 4.5: Walk rate parameters (example dataset)

Dataset#	Inclination (deg)	WOB (Klbs)	Rotational speed (rpm)	Torque (Klbs*ft)	Walk rate (deg/30m)
1	55.23	12.42	180	11434	0.15
2	48.28	11.71	214	12062	0.17
3	27.01	11.71	222	12839	0.18
4	53.97	8.26	180	11939	0.19
5	45.90	12.68	179	12794	0.35
6	21.11	13.31	217	10075	0.36
7	55.22	11.72	179	10782	0.55
8	31.32	13.10	223	9873	0.70
9	40.71	12.72	185	11884	0.71
10	22.38	14.48	220	9965	0.82
11	36.42	14.47	140	12107	0.86
12	46.43	12.67	223	11757	0.88
13	43.00	13.64	188	11973	1.06
14	24.29	12.00	160	13586	1.15
15	23.07	13.45	146	13862	1.17
16	25.92	11.90	208	14345	1.22
17	48.15	11.72	222	11660	1.23

Table 4.6: Walk rate parameters and their ranges

Item	Parameter	Unit	Minimum	Maximum
1	Inclination	deg	18.24	55.23
2	Weight on bit	Klbs	8.25	15.45
3	Rotational speed	rpm	105	228
4	Torque	Klbs*ft	6298	14483

Histograms of all parameters, as shown in figure 4.2 to 4.5, are plotted to observe the distribution pattern and also used for excluding some dataset that are not in accordance with the majority of the entire dataset. The result of the histogram plot

shows that there are some numbers of dataset existed at the lower end of the histogram and they are to be excluded which are ones having WOB as 8.26, 8.31 and 8.54 Klbs (3 sets), Rotational Speed as 104.63, 123.93 and 129.83 rpm (3 sets) and torque as 6297.53, 6450.47 Klbs*ft (2 sets). Therefore, a total of 112 sets of data are remained after the screening process. Their ranges are shown in table 4.7. These 112 sets of data are to be used for the ANN model training to be discussed in the following topics.



ศูนย์วิทยทรัพยากร
จุฬาลงกรณ์มหาวิทยาลัย

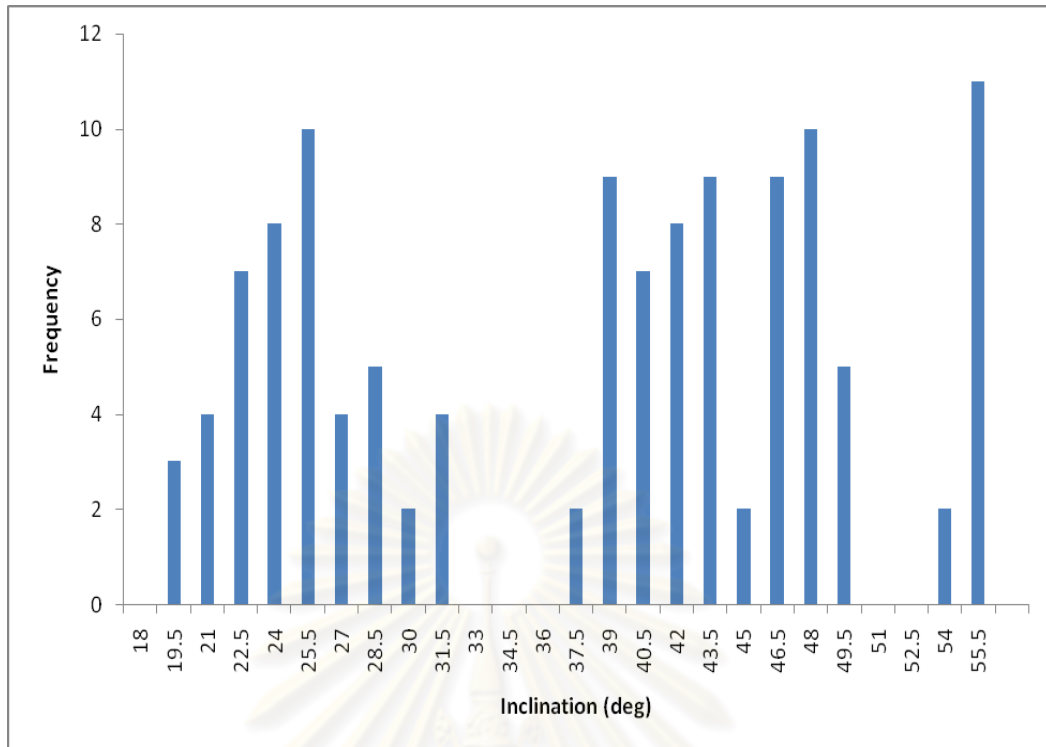


Figure 4.2: Histogram of Inclination of total dataset

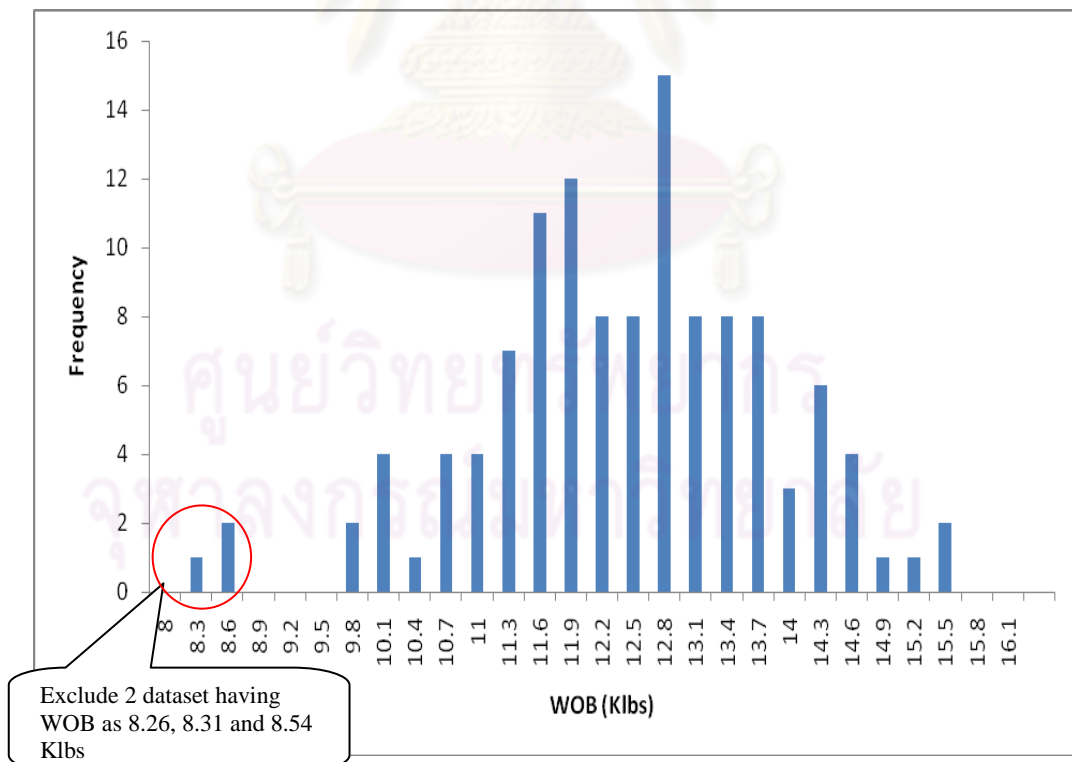


Figure 4.3: Histogram of Weight on bit (WOB) of total dataset

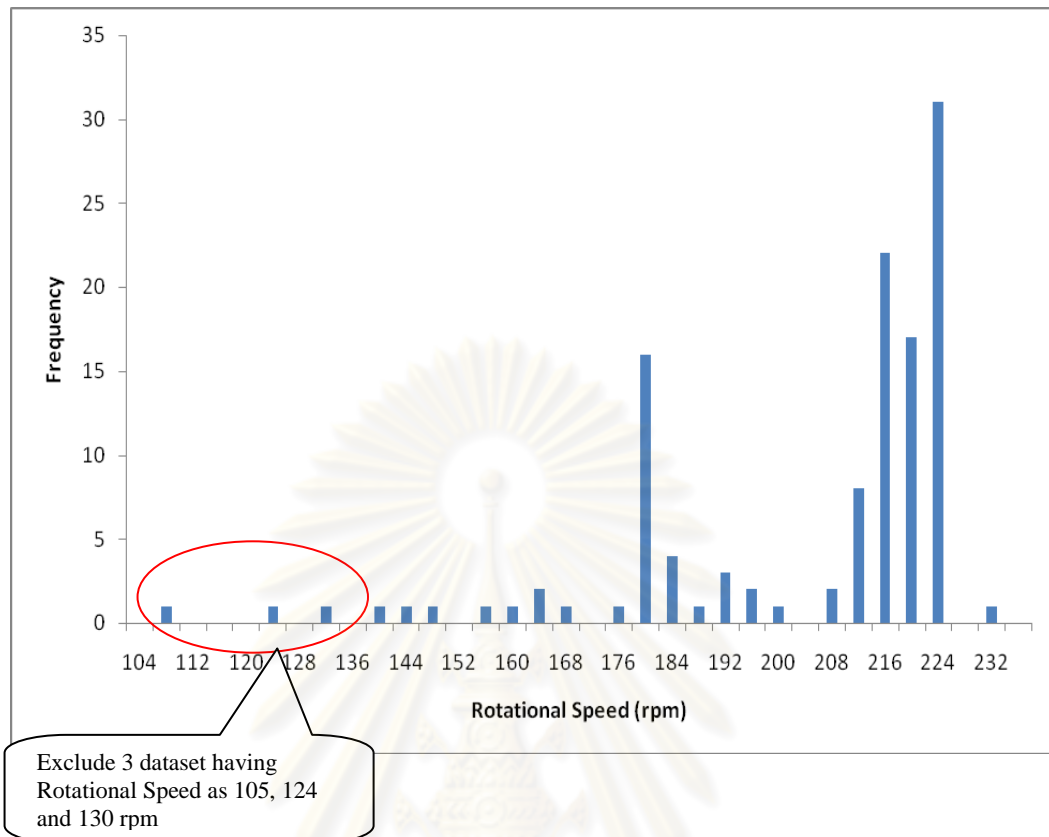


Figure 4.4: Histogram of Rotational speed of total dataset

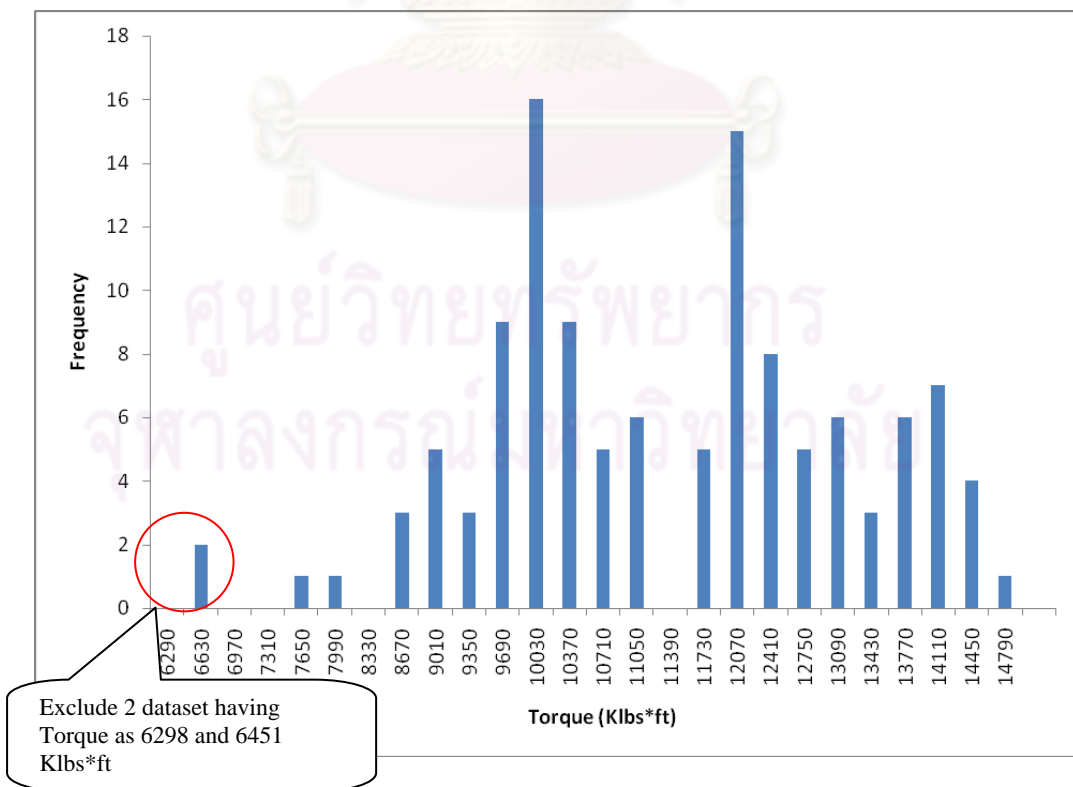


Figure 4.5: Histogram of Torque of total dataset

Table 4.7: Walk rate parameters and their ranges (after screening)

Item	Parameter	Unit	Minimum	Maximum
1	Inclination	Deg	18.24	55.23
2	Weight on bit	Klbs	9.54	15.45
3	Rotational speed	rpm	140	228
4	Torque	Klbs*ft	7492	14483

MATLAB software, which is an integrated platform for Engineering and Science research in various areas, is used for the ANN model development, training as well as result analysis. The software was developed by The MathWorks Inc. The software license is shared for the Engineering students provided by the Engineering computer center. The ANN library of the software is utilized for the model creation. The software is capable of developing several types of ANN networks and configurations namely transfer function, training algorithm, learning rate, momentum, number of cycles run, performance evaluation criteria. The partial model source code can be found in the figure 4.6. The captured code is intended to explain the general usage of MATLAB ANN library and how they are applied in this study for the model development.

From the MATLAB code, Section 1 describes the general definition of the network including specification of numbers of neurons in each layer, learning rate, momentum. Learning rate can be set to any number in the range from 0 to 10, while momentum can be set to any number in the range from 0 to 1.0. These definitions are varied and adjusted case by case in order to create the model that is able to produce minimum errors relatively to others. In addition, the definition includes dataset which are divided into training: validating: testing based on 4:1:1 ratio which make the total dataset of 112 divide into 76:18:18 respectively. Input dataset in this section covers training and validating set as they are used for the model training process where training sets are feed into the model and validating sets are used for validating in each training cycle as well as stopping once the model reach convergence criteria. The dataset can be inserted directly into the ANN model source code or using the MATLAB features to open a connection with spread sheet software.

Section 2 covers the network building where the network's specific configurations are described. These configurations are kept constant model to model covering the automatic initialization of network weight, transfer function, training function and stopping criteria. The model is stopped when the minimum error criteria is reached, in this case written in the code as "goal". The model is to be trained no further than 100,000 cycles, as known as epochs. The input and output sets from section 1 are divided into training and validating sets using in the model learning process. These two sets are kept unchanged in each model building. This is to make sure that each network configurations are tested on the same dataset. The "divideblock" command is used for this matter.

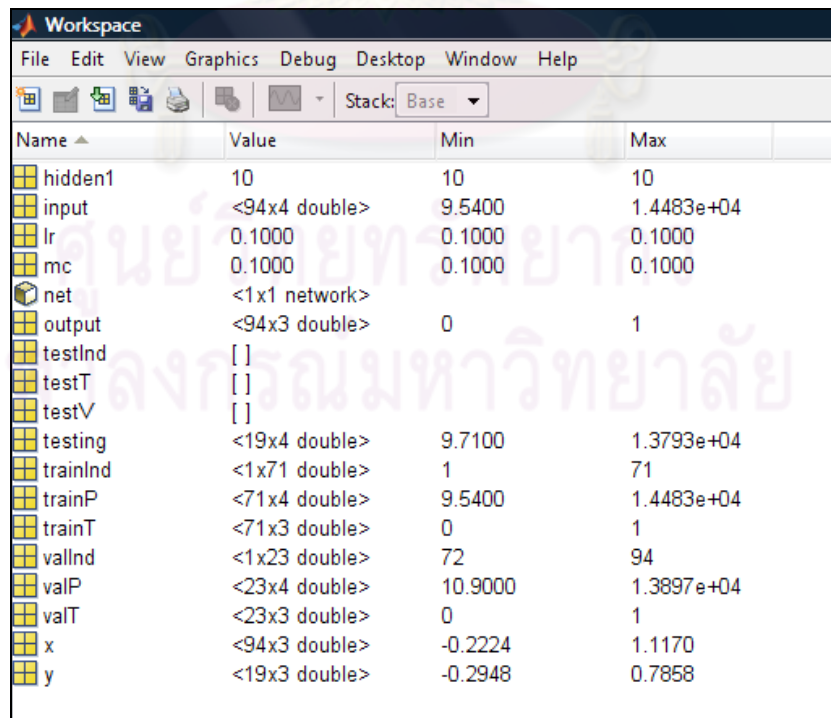
Section 3 covers the model running process. Network that has been obtained the configuration together with input and output sets divided into the specified ratio are input into the "train" function of MATLAB. The predicted output is also simulated by inputting the dataset that were not participated in the model learning process. Moreover, the training and validating set that were used for model development are feed into the model again to see the model prediction performance. MATLAB has the feature to display the outputs from simulating the network through the workspace window as shown in figure 4.7. The network shown as "net" can also be saved for future use in the prediction with new testing dataset. Other parameters can be displayed in matrix or table format as shown in figure 4.8.

```

1 % Section 1 - Definition
2 % - No. of neurons
3 hidden1 = 10;
4 hidden2 = 20;
5 % - Learning rate and Momentum
6 lr = 0.1;
7 mc = 0.1;
8 % - Dataset (train, validate, test)
9 input = [];
10 output = [];
11 testing = [];
12 % Section 2 - Network building
13 net = newff(input, output, [hidden1,hidden2], {'logsig'});
14 % - Weigth initialization
15 net = init(net);
16 % - Training function
17 net.trainFcn = 'trainlm' ;
18 % - Configuration
19 net.trainParam.lr = lr;
20 net.trainParam.mc = mc;
21 net.trainParam.goal = 1e-5;
22 net.trainParam.epochs = 100000;
23 % - Dataset partitioning
24 net.divideFcn = 'divideblock';
25 [trainP,valP,testV,trainInd,valInd,testInd] = divideblock(input, 0.75, 0.25, 0);
26 [trainT,valT,testT] = divideind(output,trainInd,valInd,testInd);
27 % Section 3 - Training, validating and testing process
28 net = train(net,input,output);
29 y = sim(net, testing);
30 % - Results output
31 y = y';
32 x = sim(net, input);
33 x = x';
34 trainP = trainP';
35 valP = valP';
36 testV = testV';

```

Figure 4.6: ANN model configuration (from MATLAB source code)



Name	Value	Min	Max
hidden1	10	10	10
input	<94x4 double>	9.5400	1.4483e+04
lr	0.1000	0.1000	0.1000
mc	0.1000	0.1000	0.1000
net	<1x1 network>		
output	<94x3 double>	0	1
testInd	[]		
testT	[]		
testV	[]		
testing	<19x4 double>	9.7100	1.3793e+04
trainInd	<1x71 double>	1	71
trainP	<71x4 double>	9.5400	1.4483e+04
trainT	<71x3 double>	0	1
valInd	<1x23 double>	72	94
valP	<23x4 double>	10.9000	1.3897e+04
valT	<23x3 double>	0	1
x	<94x3 double>	-0.2224	1.1170
y	<19x3 double>	-0.2948	0.7858

Figure 4.7: ANN model workspace

y <19x3 double>			
	1	2	3
1	0.3816	0.4006	0.1963
2	0.3707	0.4283	0.1822
3	0.3243	0.6135	0.0534
4	0.3031	0.3711	0.3910
5	0.3296	0.3396	0.3286
6	0.3780	0.3751	0.2338
7	0.3628	0.2946	0.3006
8	0.5460	0.0659	0.0013
9	0.4905	0.4455	-0.0825
10	0.4033	0.1111	0.5268
11	0.2327	0.5479	0.2692
12	0.5333	0.5758	-0.2948
13	0.3870	0.4074	0.1834
14	0.3528	0.2991	0.1770
15	0.4048	0.2440	0.2009
16	0.2835	0.4043	0.4065
17	0.1696	0.0205	0.7858
18	0.3865	0.2624	0.2607
19	0.1668	0.7714	0.1772

Figure 4.8: Output from model testing (shown in the workspace matrix)

The ANN's learning process and stopping criteria are discussed in details. Figure 4.9 is an example of error output graph while conducting networks training. At the beginning of training cycle, the error criteria measured in mean square error (MSE) is reducing for both training and validating sets, while the training sets having less MSE minimally than validating sets. This is normal due to the high exposure of the networks to the training sets making the result lean towards the majority of data. However, after the best validating performance is reached, there is a big difference in the gap as well as the inverse trend between training and validating sets that training sets show ongoing of the reduction of error criteria, while validating sets show the increasing trend. This is according to a behavior called over fitting where networks produce a result that is lacking of ability to generalize. Therefore, the network in this case is stopped at the best validation performance line where optimum MSE and updated weights are obtained. Furthermore, if the networks are not converged into this condition, there are also other criteria to stop the networks training which are 1) the specified training goal as known as the minimum error criteria. The networks are stopped if this minimum error is reached. However, it might be difficult to reach the condition if the minimum error is set for too low. 2) the training cycles or epochs. The

networks are stopped if the maximum epoch is reached even though the optimum condition has not yet been met.

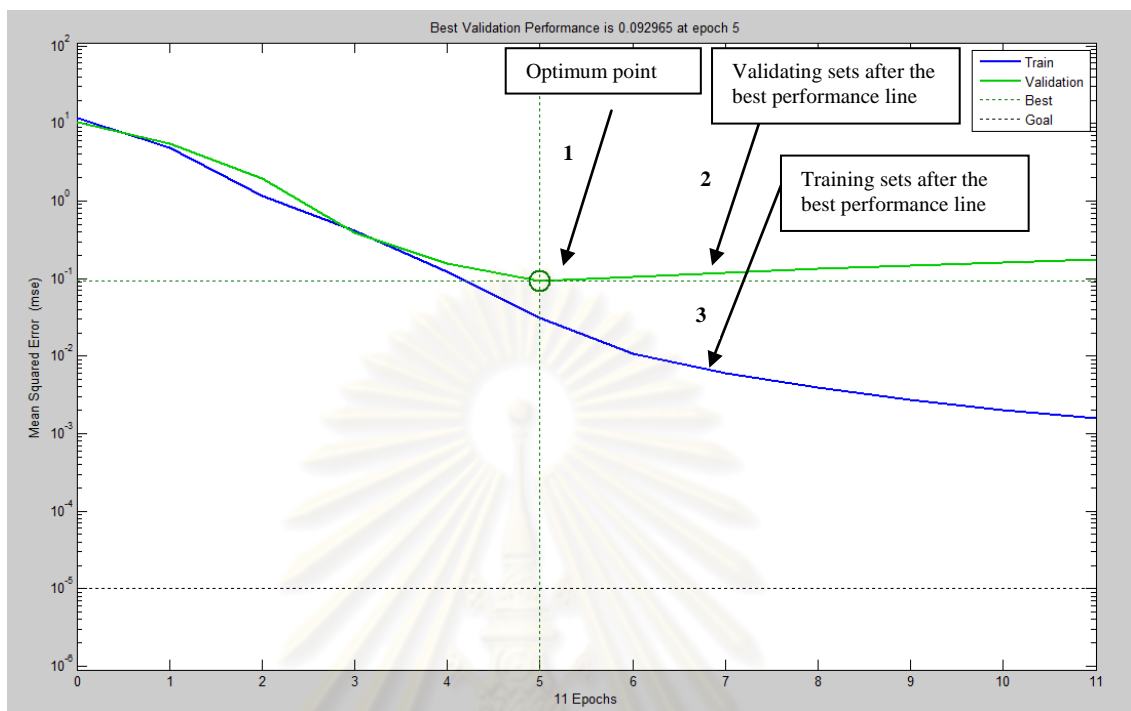


Figure 4.9: Learning process of ANN

The error criterion used which is the mean square error (MSE) is defined as

$$MSE = \frac{1}{N} \sum_{p=1}^N \sum_{i=1}^M (t_{pi} - O_{pi})^2 \quad (4.1)$$

Where

O_{pi} = the actual solution of the i^{th} output node on the p^{th} example.

t_{pi} = the target(predicted) solution of the i^{th} output node on the p^{th} example.

N = the number of training or validating examples.

M = the number of output nodes.

4.3.2.1 Case 2.1 – Bit walk quantity in absolute amount

In this case, factors or parameters affecting bit walk rate which were determined in previous topic are specified as the model inputs while the absolute walk rate is the output. The input layer contains four neurons, each of which represents inclination, weight on bit, rotational speed and torque. Hidden layer and number of neurons in each hidden layer are varied in order to seek for the best model producing least error. Figure 4.10 below illustrates the schematic diagram of the ANN model of this case.

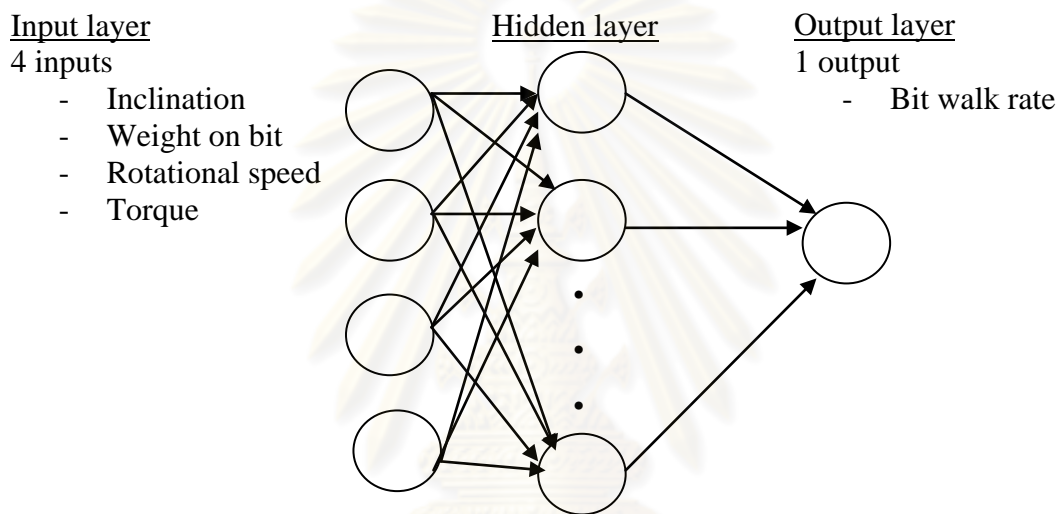


Figure 4.10: Schematic diagram of ANN model – Case 2.1

Examples of dataset used for training the model of this case are shown in the table 4.8. During the learning process, the networks try to predict the correct walk rate according to the input parameters. The difference between the predicted and actual walk rate are calculated as a criteria to adjust the networks' weights for improving the training accuracy in the following cycles.

Table 4.8: Examples of dataset used in the model learning process (Case 2.1)

Dataset#	Model Inputs				Model Output
	Inclination (deg)	WOB (Klbs)	Rotational speed (rpm)	Torque (Klbs*ft)	Walk rate (deg/30m)
1	55.23	12.42	180	11434	0.15
2	48.28	11.71	214	12062	0.17
3	27.01	11.71	222	12839	0.18
4	53.97	8.26	180	11939	0.19
5	45.90	12.68	179	12794	0.35
6	21.11	13.31	217	10075	0.36
7	55.22	11.72	179	10781	0.55
8	31.32	13.10	223	9873	0.70
9	40.71	12.72	185	11884	0.71
10	22.38	14.48	220	9965	0.82
11	36.42	14.47	140	12107	0.86
12	46.43	12.67	223	11757	0.88
13	43.00	13.64	188	11973	1.06
14	24.29	12.00	160	13586	1.15
15	23.07	13.45	146	13862	1.17
16	25.92	11.90	208	14345	1.22
17	48.15	11.72	222	11660	1.23

4.3.2.1.1 Data preprocessing

In order to ensure the efficiency in generalization of the model, dataset that are partitioned into training, validating and testing sets should present a similar distribution and cover possible ranges of information as much as possible. Consequently, histograms of all input parameters for three partitioned dataset (training, validating and testing) are plotted to observe the distribution and reshuffled among partitioned group if necessary. The distributions of these partitioned dataset are kept unchanged throughout the training process. This is to ensure that the only changes applied are the network configuration such as learning rate, momentum and number of neurons. Histograms are shown in figure 4.11 to 4.22 The histograms of

each parameter also demonstrate similar distributions to that of the original data as shown in Figure 4.2 to 4.5 in the previous section. Moreover, statistical representations which are the mean, quartile and standard deviation are also calculated for the training, validating and testing sets of the four parameters. This is shown in the table 4.9. From the comparison of these statistical values of all sets, they exhibit a similar result. For example, the mean values of inclination for training, validating and testing sets are 36.98, 38.59 and 36.40 deg respectively. Another example is the standard deviation of the WOB. They are 1.22, 1.35 and 1.23 for training, validating and testing sets respectively. These values of inclination and WOB are shown to be closed among each other showing that the training, validating and testing sets have the same trend and figure. These similar trends of training, validating and testing sets also happen with other parameters.

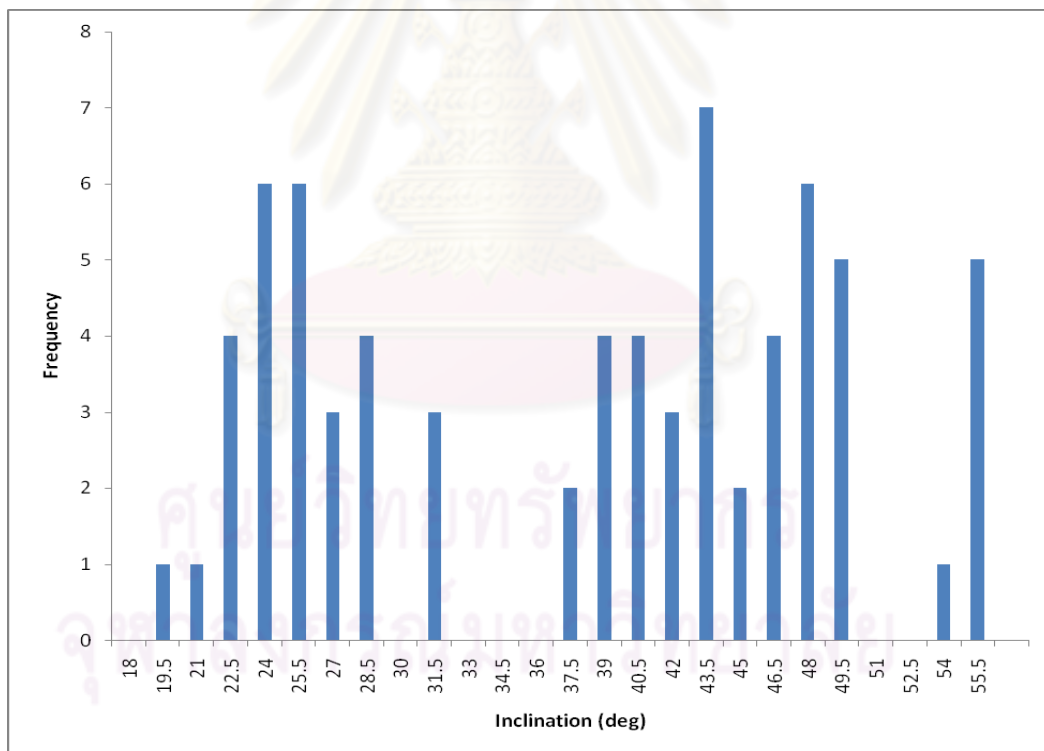


Figure 4.11: Histogram of Inclination of training sets

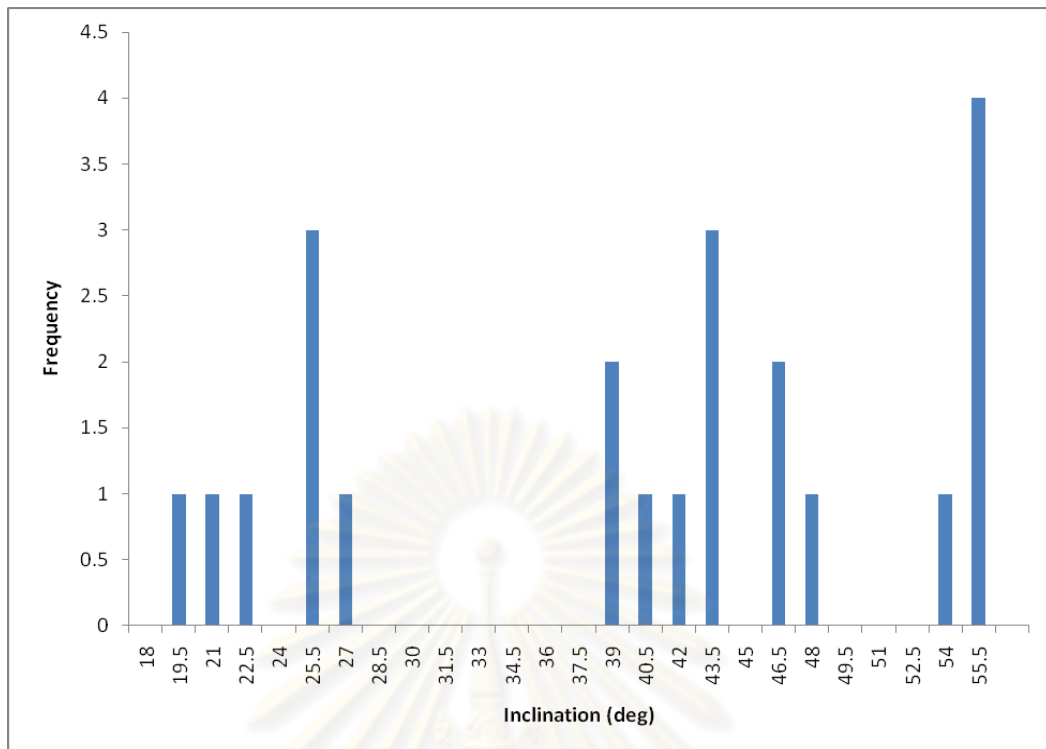


Figure 4.12: Histogram of Inclination of validating sets

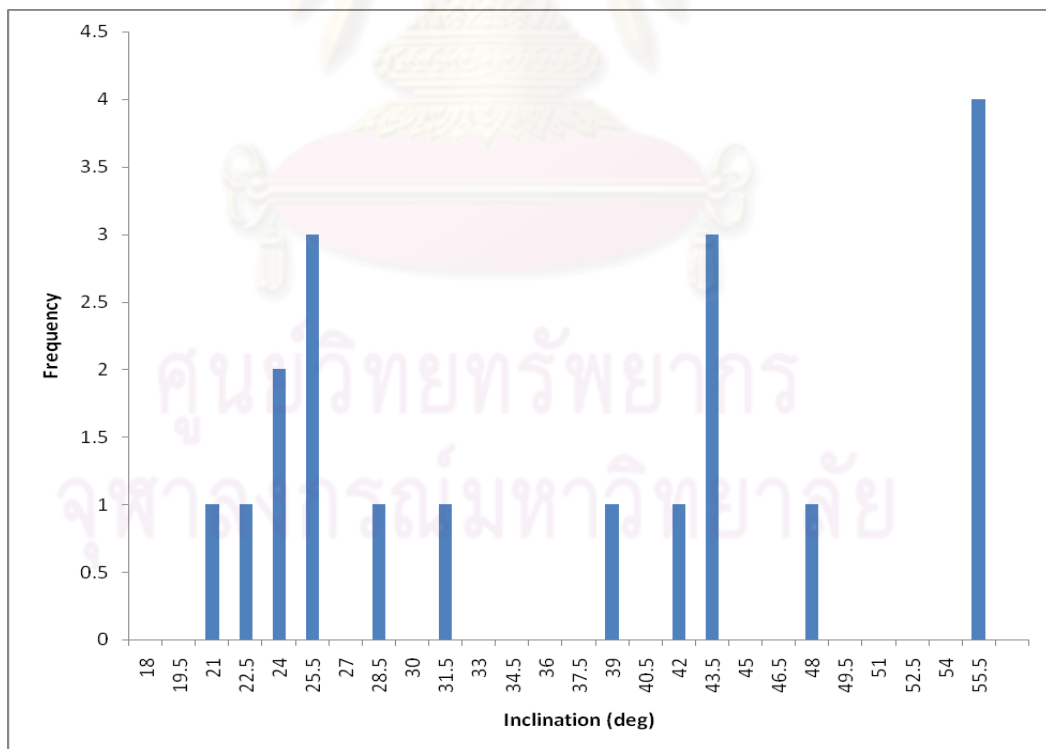


Figure 4.13: Histogram of Inclination of testing sets

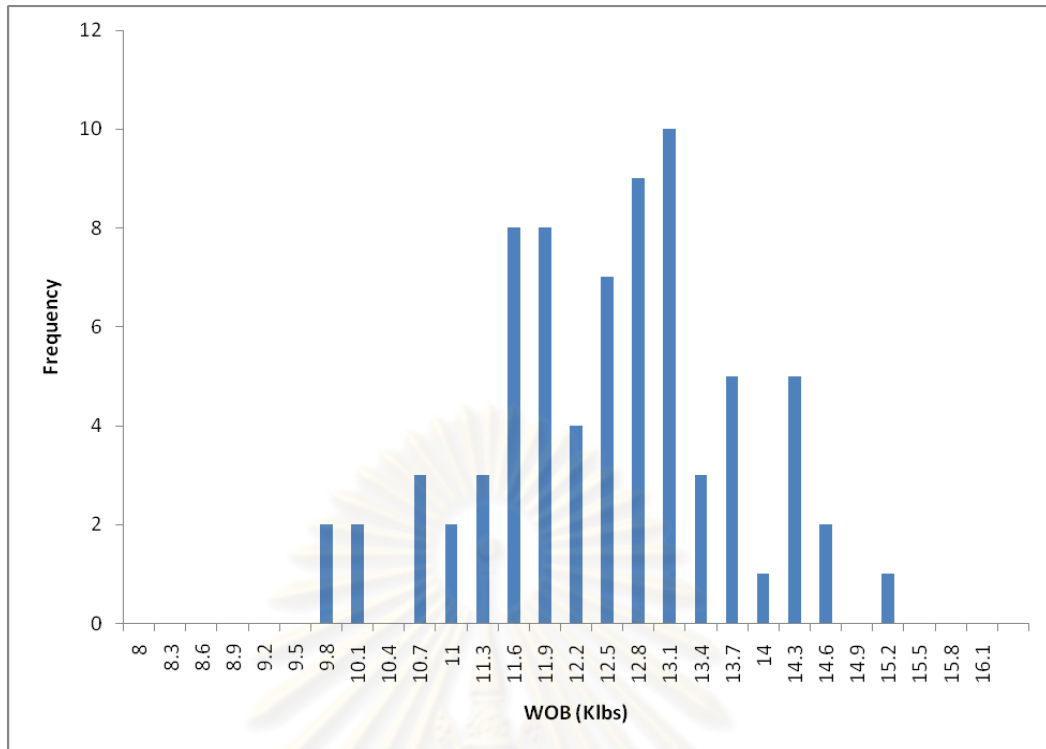


Figure 4.14: Histogram of Weight on bit (WOB) of training sets

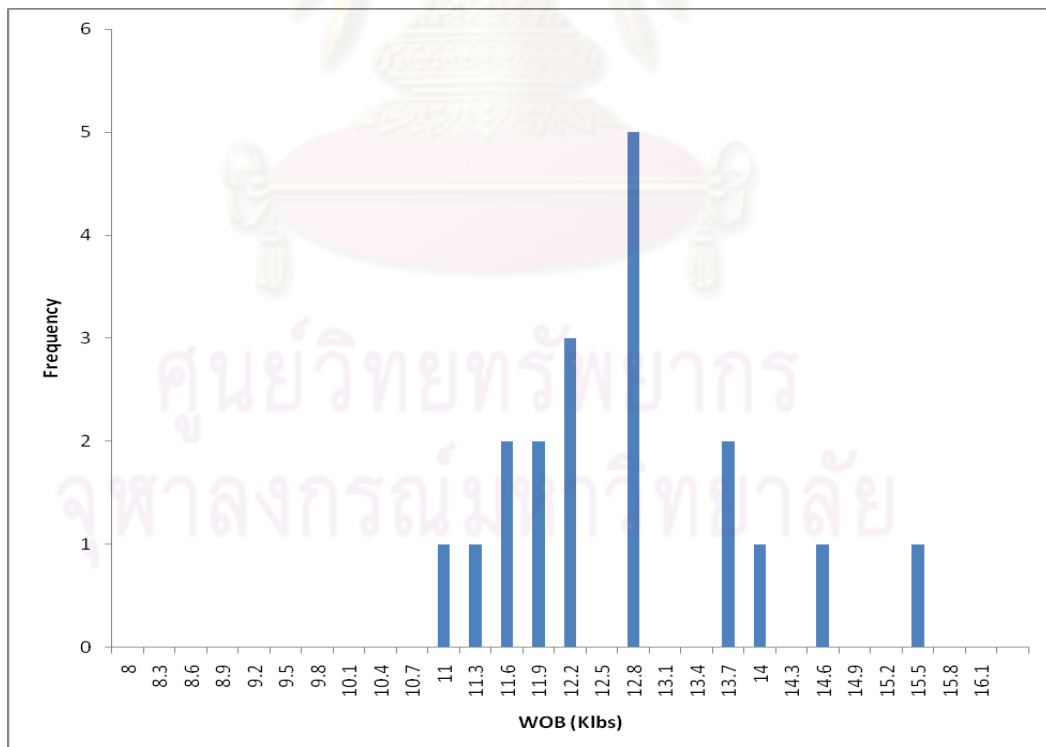


Figure 4.15: Histogram of Weight on bit (WOB) of validating sets

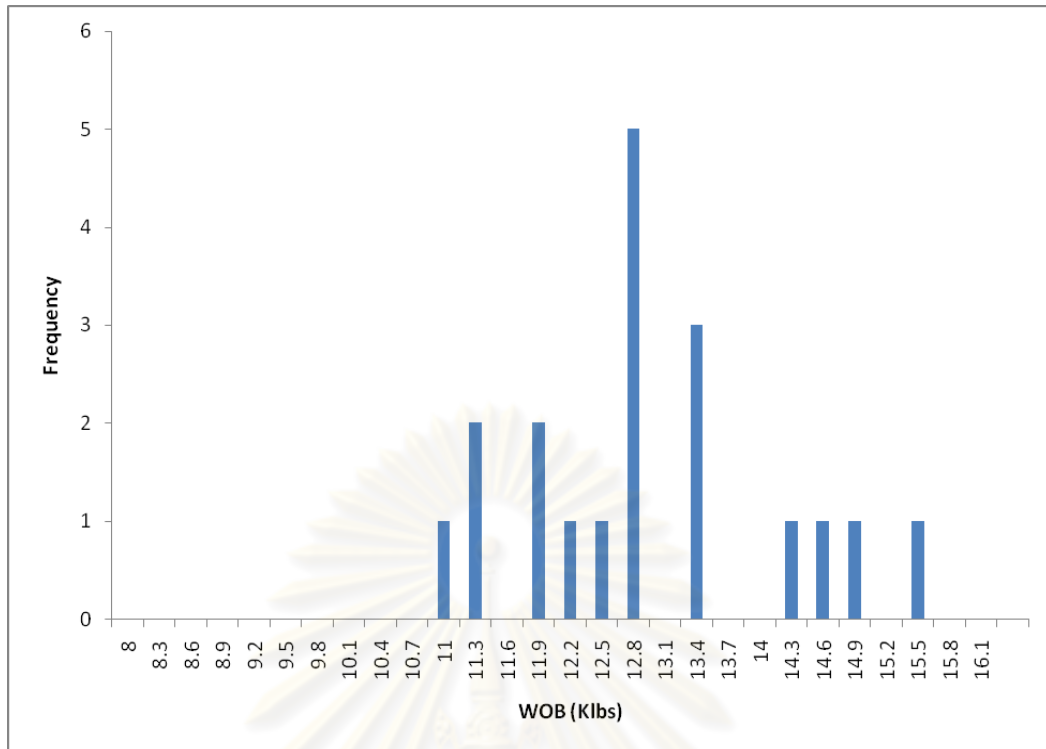


Figure 4.16: Histogram of Weight on bit (WOB) of testing sets

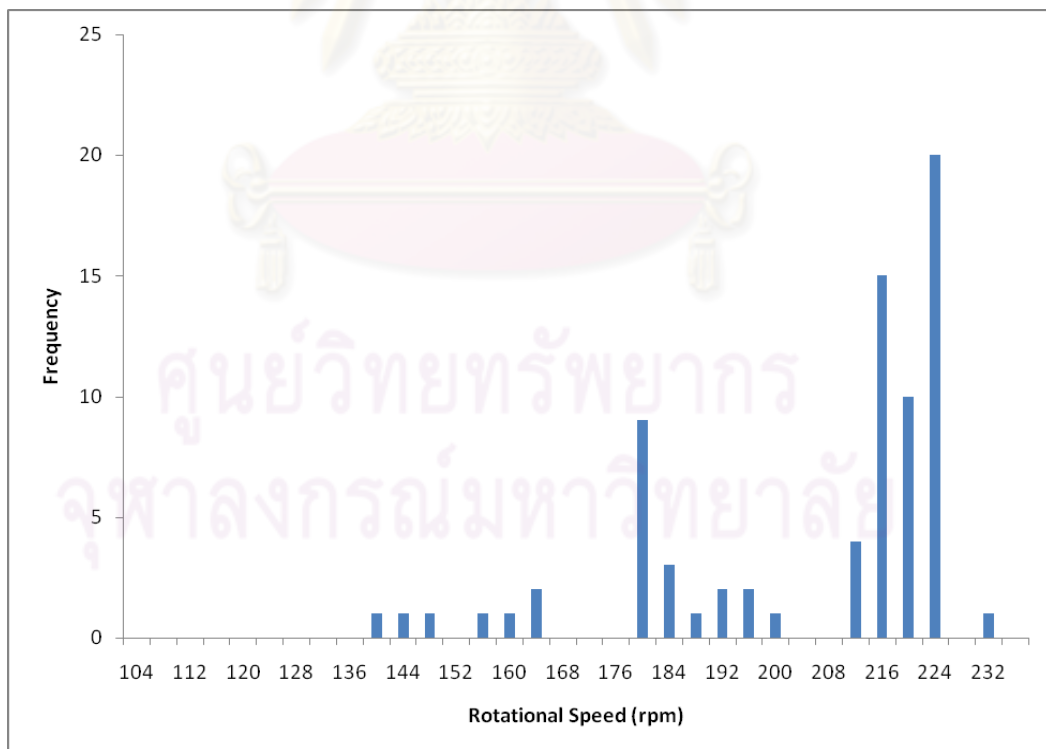


Figure 4.17: Histogram of Rotational speed of training sets

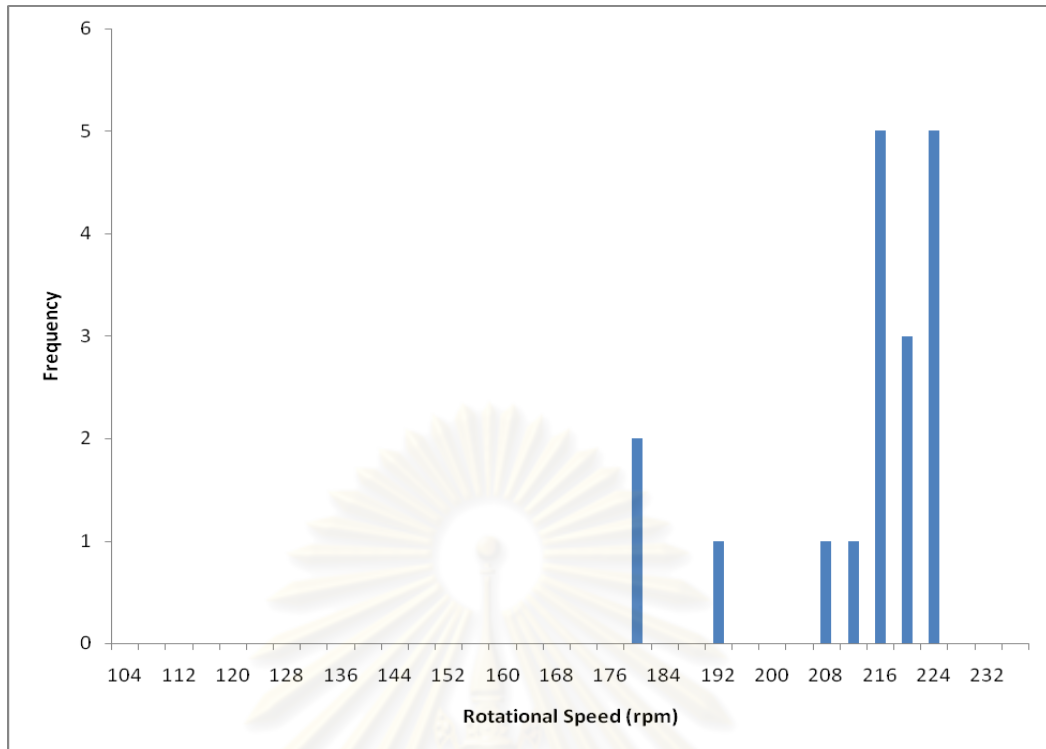


Figure 4.18: Histogram of Rotational speed of validating sets

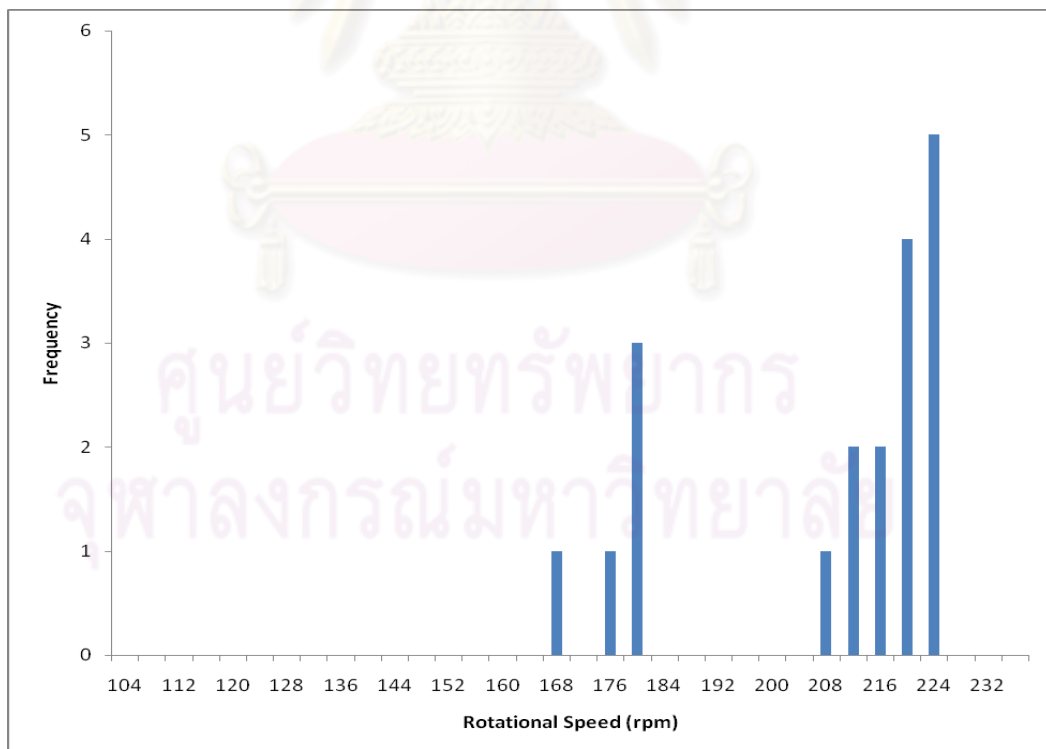


Figure 4.19: Histogram of Rotational speed of testing sets

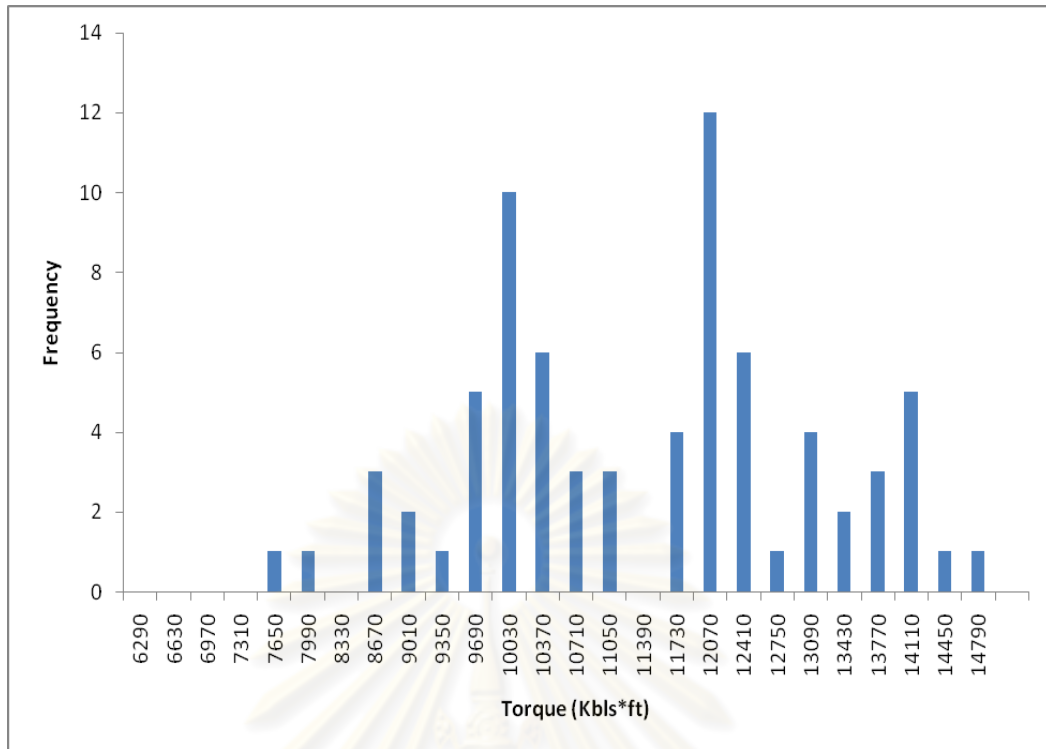


Figure 4.20: Histogram of Torque of training sets

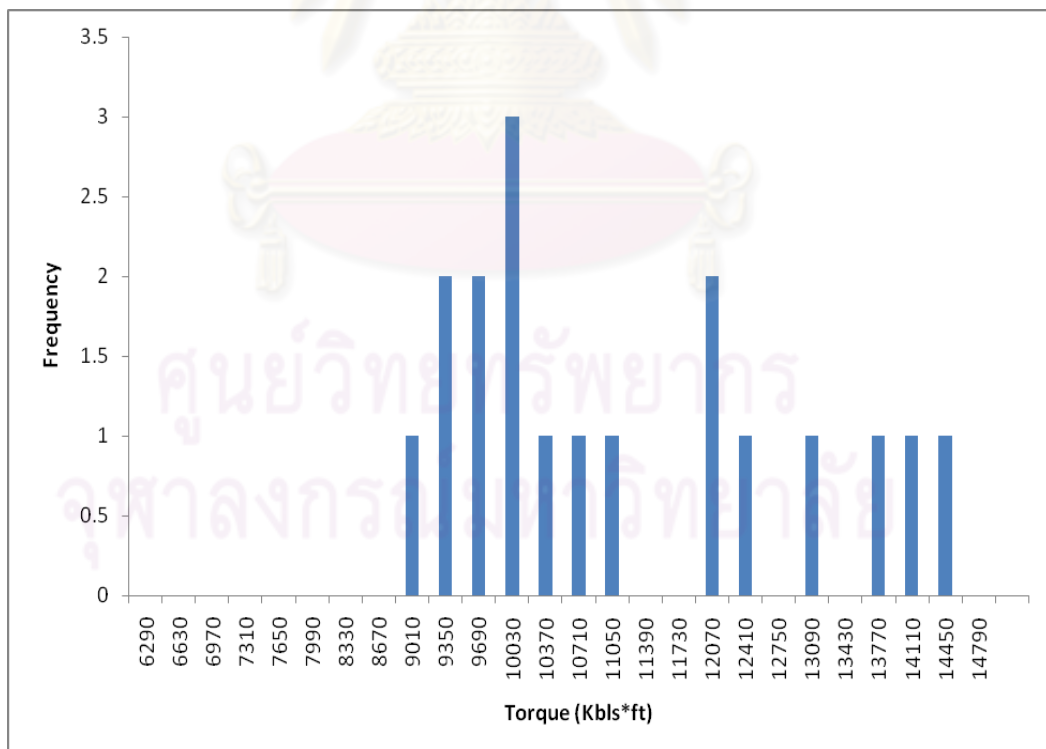


Figure 4.21: Histogram of Torque of validating sets

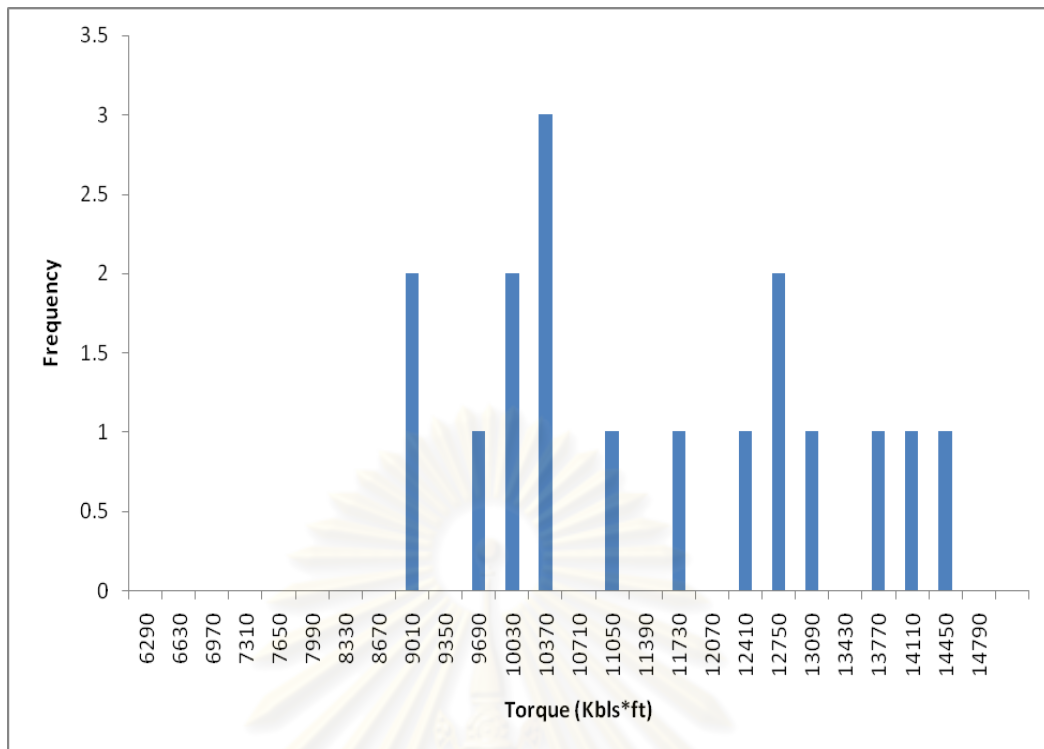


Figure 4.22: Histogram of Torque of testing sets

Table 4.9: Summary of statistical representation of training, validating and testing sets

Statistical representations	Dataset type	Inclination (deg)	WOB (Klbs)	Rotational Speed (rpm)	Torque (Klbs*ft)
Mean	Training	36.98	12.33	204	11241
	Validating	38.59	12.22	205	11011
	Testing	36.40	12.79	199	11513
1 st Quartile	Training	25.77	11.48	187	9880
	Validating	25.45	11.28	198	9750
	Testing	24.70	11.84	179	10067
3 rd Quartile	Training	46.17	13.10	221	12246
	Validating	46.43	13.07	219	12067
	Testing	45.69	13.40	221	12713
Standard deviation	Training	10.80	1.22	22.96	1714.11
	Validating	11.87	1.35	22.52	1625.34
	Testing	11.76	1.23	27.43	1744.22

4.3.2.1.2 Model training

In this case, ANN model configurations namely number of hidden layers, number of neurons in each layer, learning rate and momentum are varied on a trial and error basis to locate the best configuration making the model converge as well as yielding the lowest MSE. 17 model runs are tried with different configurations. The results are summarized in the table 4.10 as shown below.

Table 4.10: Model configuration – Case 2.1

Model #	No. of neurons		Learning rate	Momentum	MSE
	Hidden layer1	Hidden layer 2			
1	6	0	0.6	0.6	0.0357
2	6	0	0.2	0.2	0.0369
3	9	0	0.2	0.2	0.0345
4	9	0	0.2	0.5	0.0497
5	9	0	0.2	0.1	0.0353
6	12	0	0.2	0.2	0.0446
7	15	0	0.2	0.2	0.0387
8	15	0	0.2	0.4	0.0583
9	18	0	0.2	0.2	0.0456
10	21	0	0.2	0.2	0.0478
11	24	0	0.2	0.2	0.0389
12	27	0	0.2	0.2	0.0685
13	30	0	0.2	0.2	0.0930
14	10	5	0.2	0.2	0.0375
15	20	5	0.2	0.2	0.0395
16	20	10	0.2	0.2	0.0493
17	30	20	0.2	0.2	0.0809

The trial starts with a single hidden layer and a minimum number of neurons and increase the neurons and hidden layer in the latters models. Jadid and Fairbrairn (1996) proposed the formula to suggest the number of hidden neurons which is

$$NHN = N_{TRN} / [R + (N_{INP} + N_{OUT})] \quad (4.2)$$

Where

NHN = Number of hidden neurons

N_{TRN} = Number of training sets

N_{INP} = Number of nodes in input layer

N_{OUT} = Number of nodes in output layer

R = Any value from 5 to 10

The first model is configured with the proposed number of neurons accordingly. Learning rate determines the acceleration of the weight updating. Setting it for too low will result in slow training, while too large of it could result in an unstable ANN model that the oscillation is occurred and the model is unconverged. Momentum is commonly used in weight updating to help the search escape local minima and reduce the likelihood of search instability. A high momentum will reduce the risk of the network being stuck in local minima, however it increases the risk of overshooting the solution.

Model number 1 starts with a single hidden layer with number of neurons as 6 according to the proposed formula. Learning rate and momentum are both set as 0.6. The model is run for about 11 epochs where the converged pattern is shown. At the 5th epoch, MSE of the validating sets reach the optimum point and start to increase after this point. Whereas the MSE of training sets are still continuously reducing as could be due to the overfitting behavior of the ANN model. (This is depicted in the figure 4.23.) Model number 2 still maintains the number of neuron and layer as the first one, but change the learning rate and momentum to be lower with the attempt to improve the training and reduce MSE. The next model, number 3, is tried with the increasing number of neurons but maintain the same learning rate and momentum. The increasing in the number of neurons in the model number 3 show that the training

result is improved and MSE is reduced to 0.0345. Model number 4 is an attempt to see a result of adding more momentum to the model to accelerate the training and help the model to escape from local minima. The momentum is increased from 0.2 to 0.5. This results in a higher MSE. The momentum is reduced to 0.1 in model number 5, this makes the model producing less MSE than the 4th case. Setting learning rate and momentum as 0.2 looks promising that it tends to produce a low MSE result. Consequently, they are applied to the following cases. Number of neurons are increased in model number 6, with the same learning rate and momentum. However, by increasing the number of the neurons in this case, the MSE at the optimum point of the model is not decreased relatively with the previous model having lower number of neurons. This same behavior happens with other following models from model number 6 to 13 where the number of neurons is increased given a single hidden layer configuration. This could be a result of the lack of generalization ability of the model that it is overfitted by the configuration of too many number of neurons relatively to the condition and number of dataset.

The model number 12 with number of neurons as 27 is selected for an example. It is shown in figure 4.24 that the training sets of the entire curve starting from the beginning until the end of training exhibit a better performance (lower in MSE) than the validating sets. After the best performance line or the optimum point, the MSE of validating sets comparing with training sets show a big difference in the MSE. This is according to the large number of neurons setting which make the network overfitted to the training sets and tend to lose the ability to generalize when the error criterion is checked against the validating sets. Model number 14 is tried with two hidden layers with number of neurons as 10 and 5 respectively. Learning rate and momentum are set to 0.2. The network of this case is trained until MSE does not improve further, or as it reaches optimum point. The MSE at the optimum point is 0.0375 which is lower comparing with those configuration of one single layer with several number of neurons (model number 6 to 13). Model number 14 to 17 are tried with the increasing number of neurons given two hidden layers. Learning rate and momentum are kept constant at 0.2 as they were proved to yield a good training result, examples were shown in the model number 3 to 5. The result from model number 14 to 17 turn out that increasing number of neurons in two hidden layers could not produce a lower MSE.

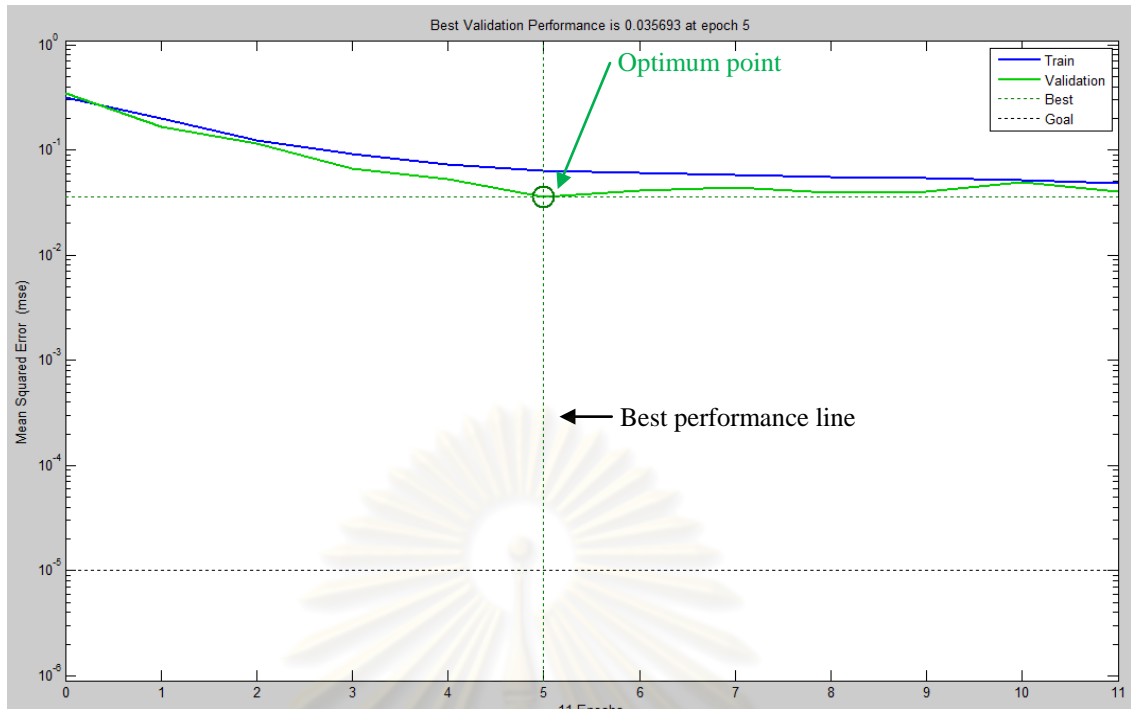


Figure 4.23: Learning curve of model number 1

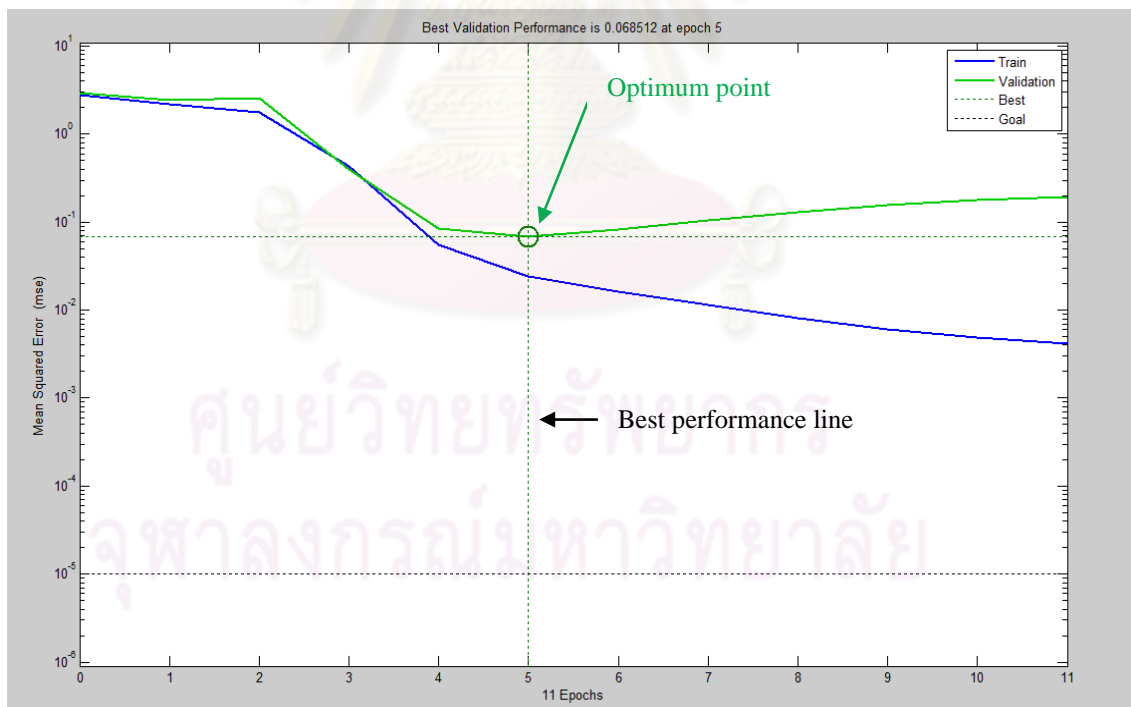


Figure 4.24: Learning curve of model number 12

From the total of 17 runs, two models which generate the lowest MSE are picked up to further verify for locating best model representing the absolute walk rate

prediction model. Model number 3 and 5 are shown to produce the two lowest MSE as 0.0345 and 0.0353 respectively. Model number 3 is equipped with a single hidden layer with 9 hidden neurons and learning rate and momentum are set as 0.2. Model number 5 is also equipped with the same configurations as the model number 3 except that the momentum is set as 0.1. The learning curve of model number 3 and 5 are depicted in the figure 4.25 and 4.26 respectively. Model number 3 is trained for 12 epochs until ensuring that the optimum condition arises at the 6th epoch where the optimum MSE is shown as 0.0345. Model number 5 also has a similar trend with the model number 3, but only different that the model reaches the optimum condition at the 8th epoch.

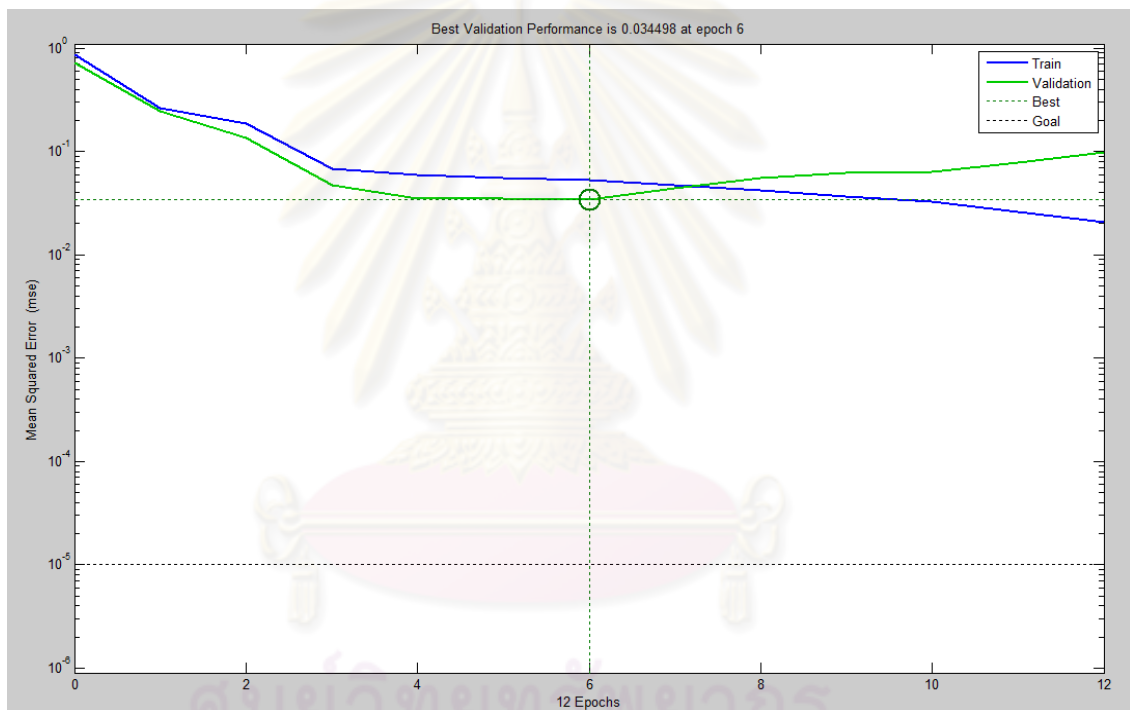


Figure 4.25: Learning curve of model number 3

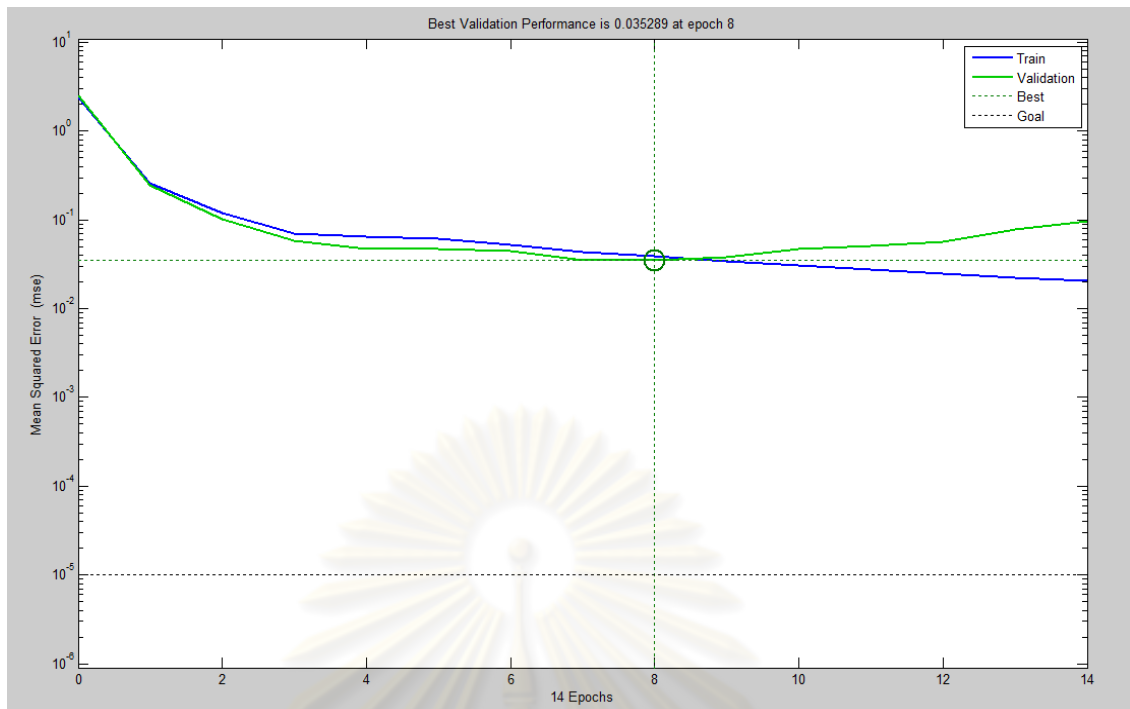


Figure 4.26: Learning curve of model number 5

The two models yielding the lowest MSE, namely model number 3 and 5 are tested with the training and validating dataset to see how well the models are able to predict the result based on the information models have experienced. The result from the model (predicted walk rate) is compared with the actual walk rate. The comparison is carried out by the cross plot between predicted and actual walk rate for the training and validating dataset. Figure 4.27 and 4.28 represents model number 3 while figure 4.29 and 4.30 represents model number 5. Moreover, the comparison result in another perspective is shown in table 4.11 and 4.12. The information in the table represents the percentage of error between the predicted and actual walk rate. Error differences are grouped into 5 ranges which are 0-10%, 10-20%, 20-30%, 30-40% and >40%. The fraction shows the percentage of dataset that belongs to each error range.

Regarding model number 3, the cross plot in figure 4.27 shows the difference between predicted and actual walk rate. The “ $y=x$ ” line refers to the correct prediction. However, this correct prediction is not regularly occurred. Therefore, r (Correlation coefficient) is calculated to see how well the predicted walk rate is correlated with the actual one. In this case of the comparison between predicted and

actual walk rate of training sets of model number 3, r is equal to 0.85. Another perspective of comparison could also be seen from table 4.11, for model number 3, there are 14% (fraction = 0.14) of training sets that produce the difference between predicted and actual walk rate in the range of 0-10%. Moreover, there are 20%, 16%, 18%, and 32% (fraction = 0.20, 0.16, 0.18 and 0.32) of training sets that produce the difference between predicted and actual walk rate in the range of 10-20%, 20-30%, 30-40%, and >40% respectively. The same cross plot and table comparison concept applies to the validating sets. The cross plots of validating sets are displayed in figure 4.28, while the table comparisons of predicted and actual walk rate is displayed in table 4.12.

Regarding model number 5, the cross plot in figure 4.29 shows the difference between actual and predicted walk rate. The “ $y=x$ ” line refers to the correct prediction. However, this correct prediction is not regularly occurred. Therefore, r (Correlation coefficient) is calculated to see how well the predicted walk rate is correlated with the actual one. In this case of the comparison between actual and predicted walk rate of training sets of model number 5, r is equal to 0.79. Another perspective of comparison could also be seen from table 4.11, for model number 3, there are 24% (fraction = 0.24) of training sets that produce the difference between predicted and actual walk rate in the range of 0-10%. Moreover, there are 25%, 11%, 9%, and 31% (fraction = 0.25, 0.11, 0.09 and 0.31) of training sets that produce the difference between predicted and actual walk rate in the range of 10-20%, 20-30%, 30-40%, and >40% respectively. The same cross plot and table comparison concept applies to the validating sets. The cross plot of validating sets is displayed in figure 4.30, while the table comparison of predicted and actual walk rate for validating sets is displayed in table 4.12.

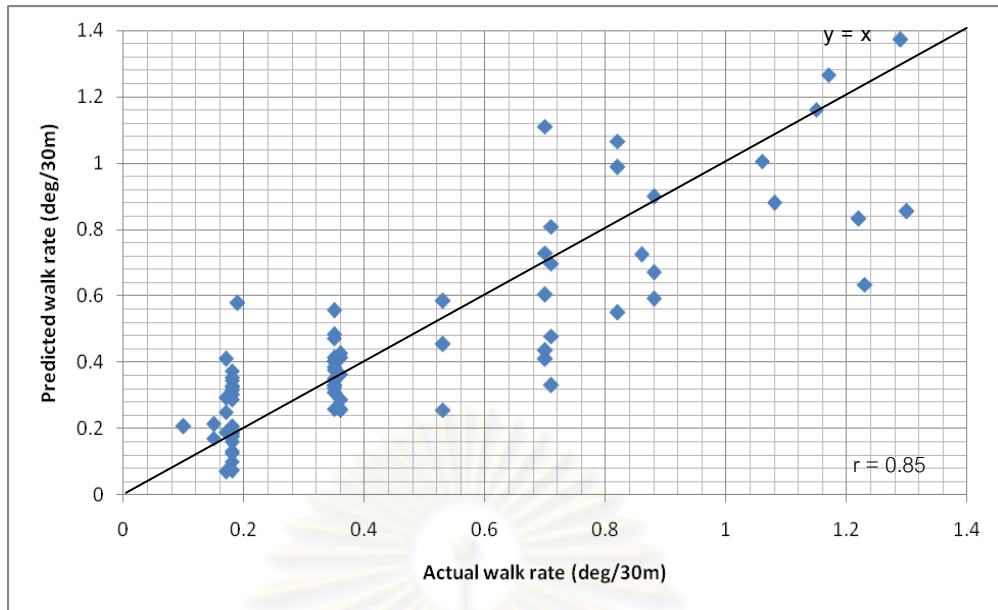


Figure 4.27: Cross plot of Predicted vs. Actual walk rate (Model number 3 – Training sets)

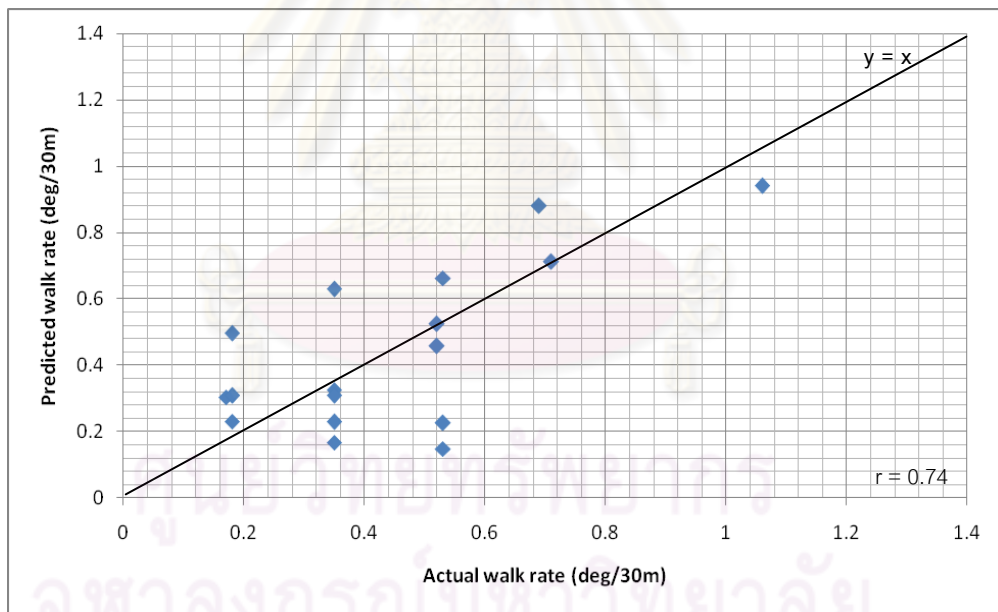


Figure 4.28: Cross plot of Predicted vs. Actual walk rate (Model number 3 – Validating sets)

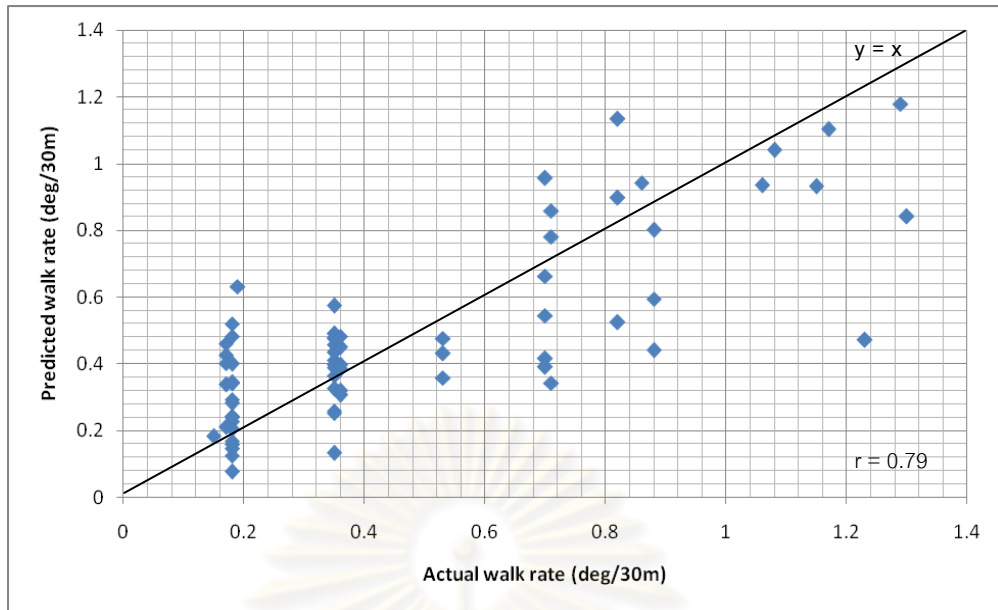


Figure 4.29: Cross plot of Predicted vs. Actual walk rate (Model number 5 – Training sets)

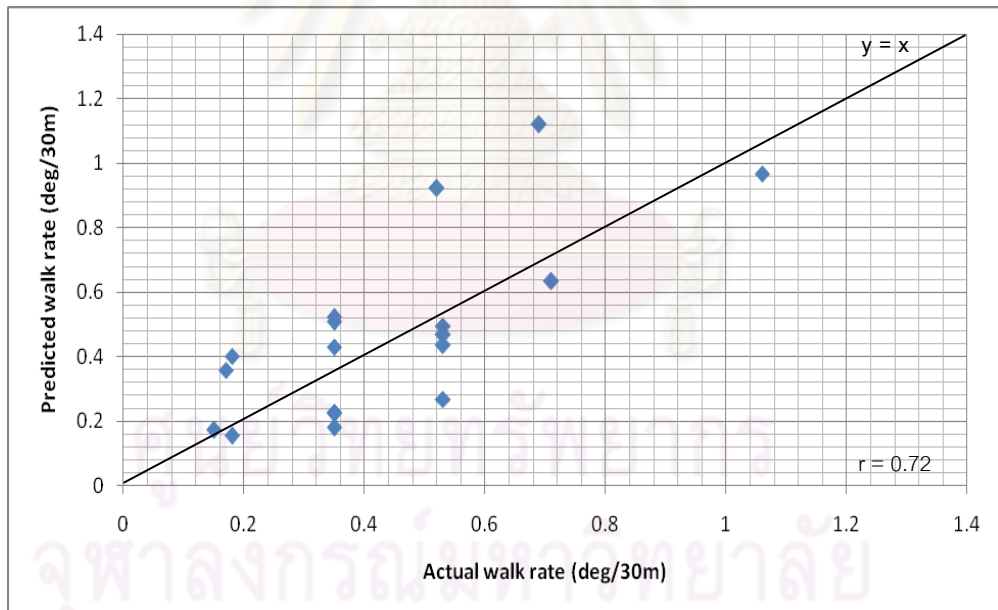


Figure 4.30: Cross plot of Predicted vs. Actual walk rate (Model number 5 – Validating sets)

Table 4.11: Error fraction (Training sets)

Training Sets							
Model#	Number of neurons		Fraction of dataset in each error range				
	Hidden layer 1	Hidden layer 2	0-10 %	10-20 %	20-30 %	30-40 %	>40 %
3	9	0	0.14	0.20	0.16	0.18	0.32
5	9	0	0.24	0.25	0.11	0.09	0.31

Table 4.12: Error fraction (Validating sets)

Validating Sets							
Model#	Number of neurons		Fraction of dataset in each error range				
	Hidden layer 1	Hidden layer 2	0-10 %	10-20 %	20-30 %	30-40 %	>40 %
3	9	0	0.17	0.22	0.04	0.22	0.35
5	9	0	0.17	0.13	0.13	0.13	0.44

As seen from the prediction result, the model does not exhibit a high accuracy. Therefore, further work is carried out to analyze what could cause the error in the prediction. From the past studies, it can be seen that formation characteristics contribute quite significantly on the quantity of bit walk. Model 3 possesses a higher correlation coefficient (r) indicating stronger relationship between predicted and actual walk rate than model number 5. As a result, it is selected as a representative to study the formation effect. The comparisons between predicted and actual walk rate of model number 3 are alternatively plotted by dataset number. This is to give a closer view on the quantity difference between predicted and actual walk rate dataset by dataset. From the training sets of model number 3 (figure 4.31), the dataset exhibiting an error between the predicted and actual walk rate of more than 50% are selected for study. The dataset is checked against the gamma ray log on the specified depth interval and well. The 50% difference between predicted and actual walk rate could be divided into two cases, namely, either the actual is lower or higher than the predicted value. From analyzing the gamma ray well log, there is no gamma ray pattern to explain the former case. However, for the latter case that the actual is higher than predicted value, there are some patterns from the gamma ray log found which is in connection with the theory regarding laminated rock that usually represents the

shale formation. Figure 4.32 to 4.35 show the gamma ray log representing the interval of each dataset in table 4.13. If Gamma ray is higher than 80 API, the formation is considered as shale (Hilchie, 1978). It can be seen from the gamma ray of all 4 dataset that they are all in the shale domain. And they all exhibit the high fluctuation in gamma ray log. This shows the characteristic of laminated rock that there are several format of rocks gradually formed into shale layer. Therefore, if this kind of gamma ray pattern is found, high walk rate could be implied. However, in the drilling operation, such information might not be readily provided. So, geological prognosis could be used for this matter that if the continuous shale pattern is found, there is a likelihood of high walk rate occurrence.

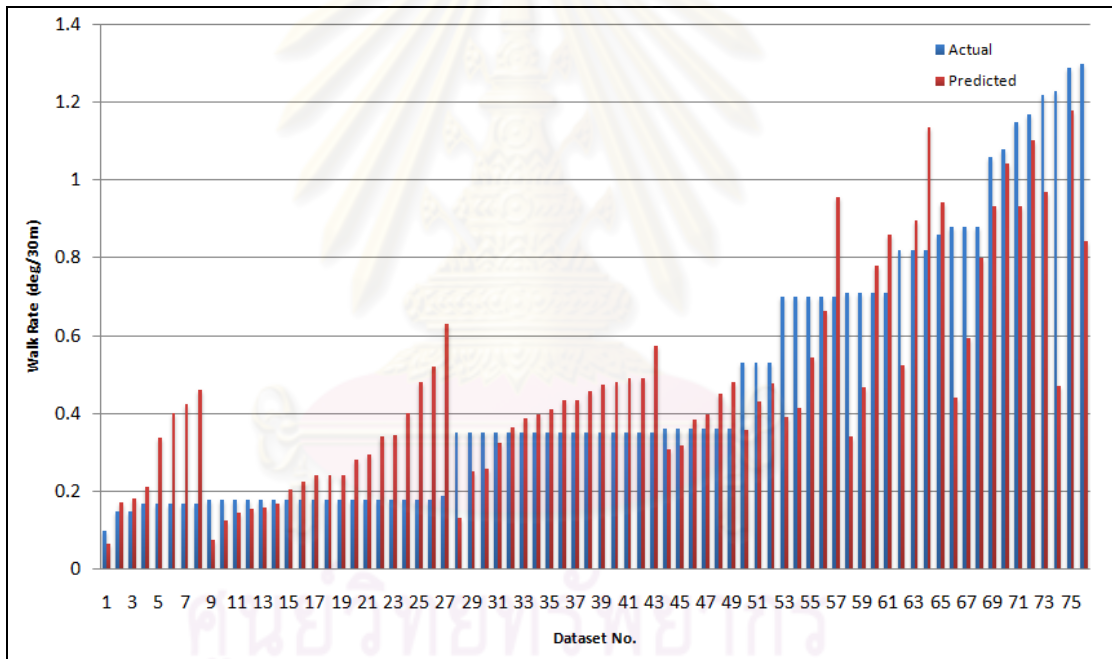


Figure 4.31: Comparing Predicted vs. Actual walk rate by order (Model number 3 – Training sets)

Table 4.13: Details dataset (Model number 3 – Training sets)

Dataset no.	Inclination (deg)	WOB (Klbs)	Rotational Speed (RPM)	Torque (Klbs*ft)	Actual walk rate (deg/30m)	Predicted walk rate (deg/30m)
28	42.2	10.57	221	7492	0.35	0.13
58	25.33	12.21	221	8936	0.71	0.34
66	46.43	12.67	223	11757	0.88	0.44
74	48.15	11.72	222	11660	1.23	0.47

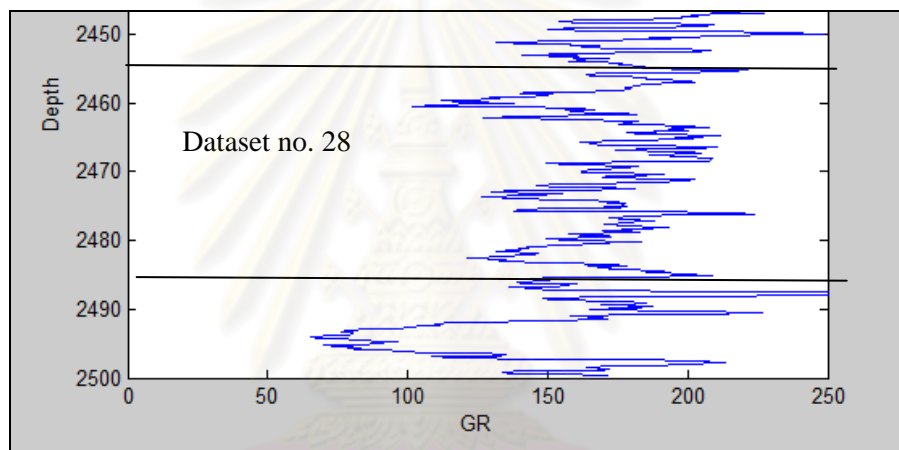


Figure 4.32: Gamma ray log (Dataset no. 28 of Model number 3 - Training sets)

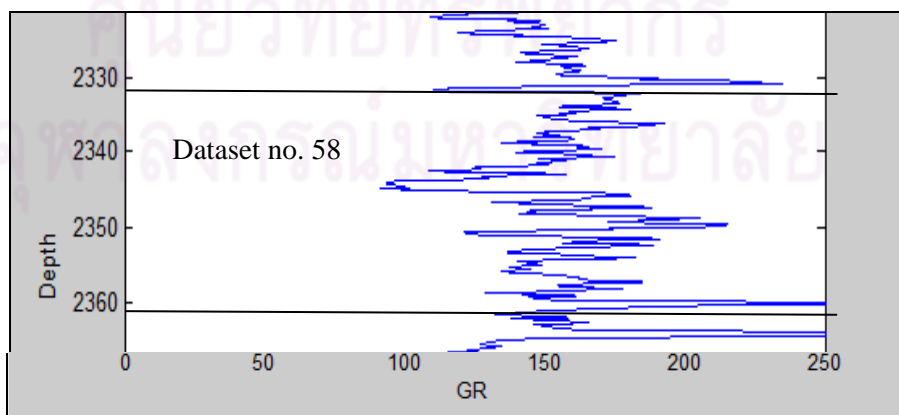


Figure 4.33: Gamma ray log (Dataset no. 58 of Model number 3 - Training sets)

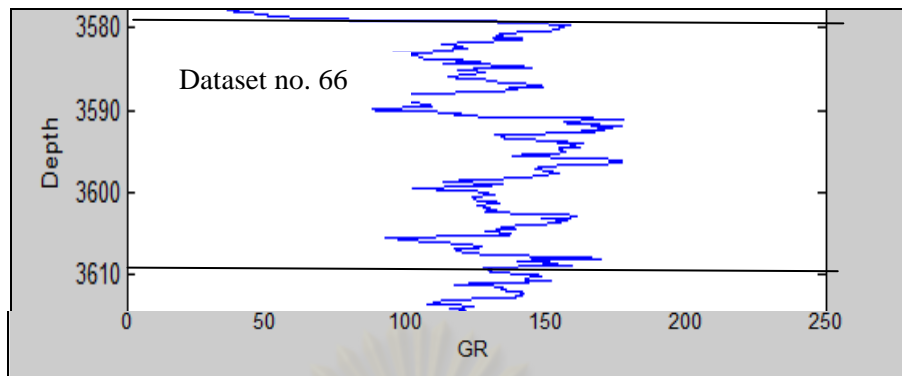


Figure 4.34: Gamma ray log (Dataset no. 66 of Model number 3 – Training sets)

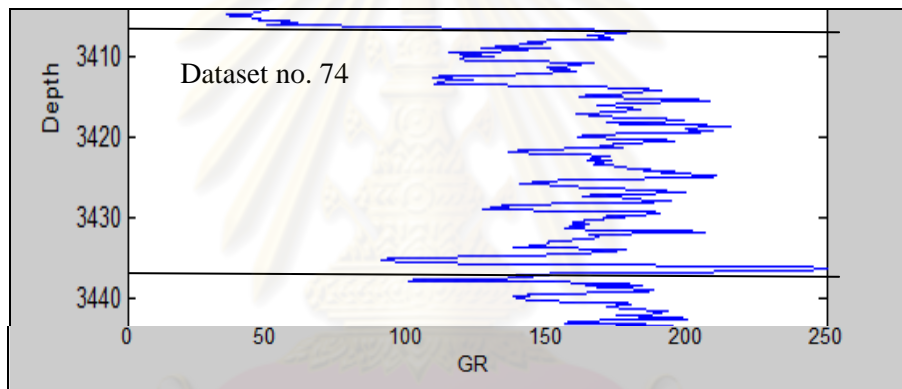


Figure 4.35: Gamma ray log (Dataset no. 74 of Model number 3 – Training sets)

The comparisons between predicted and actual walk rate of validating sets of model number 3 are alternatively plotted by dataset number. This is to give a closer view on the quantity difference between predicted and actual walk rate dataset by dataset. From the validating sets of model number 3 (figure 4.36), the dataset exhibiting an error between the predicted and actual walk rate of more than 50% are selected for study. The dataset is checked against the gamma ray log on the specified depth interval and well. The 50% difference between predicted and actual walk rate could be divided into two cases, namely, either the actual is lower or higher than the predicted value. From analyzing the gamma ray well log, there is no gamma ray pattern to explain the former case. However, for the latter case that the actual is higher

than predicted value, there are some patterns from the gamma ray log found which is in connection with the theory regarding laminated rock that usually represents the shale formation. Figure 4.37 to 4.38 show the gamma ray log representing the interval of each dataset in table 4.14. If Gamma ray is higher than 80 API, the formation is considered as shale. It can be seen from the gamma ray of the two dataset that they are all in the shale domain. And they all exhibit a high fluctuation in gamma ray log. However, the dataset number 13 extends minimally into the sand formation after the depth of 2620 meters but the majority of the interval is still in shale domain. This can be summarized as same as the case of the dataset of the training sets that if this kind of gamma ray pattern is found, high walk rate could be implied. And the information could be viewed through the geological prognosis. Moreover, the summary of formation effect from the training and validating sets cases should also give a precaution of implied error created by the formation anisotropy characteristics at some drilling interval when testing the model with testing dataset or any new actual data from the drilling operation.

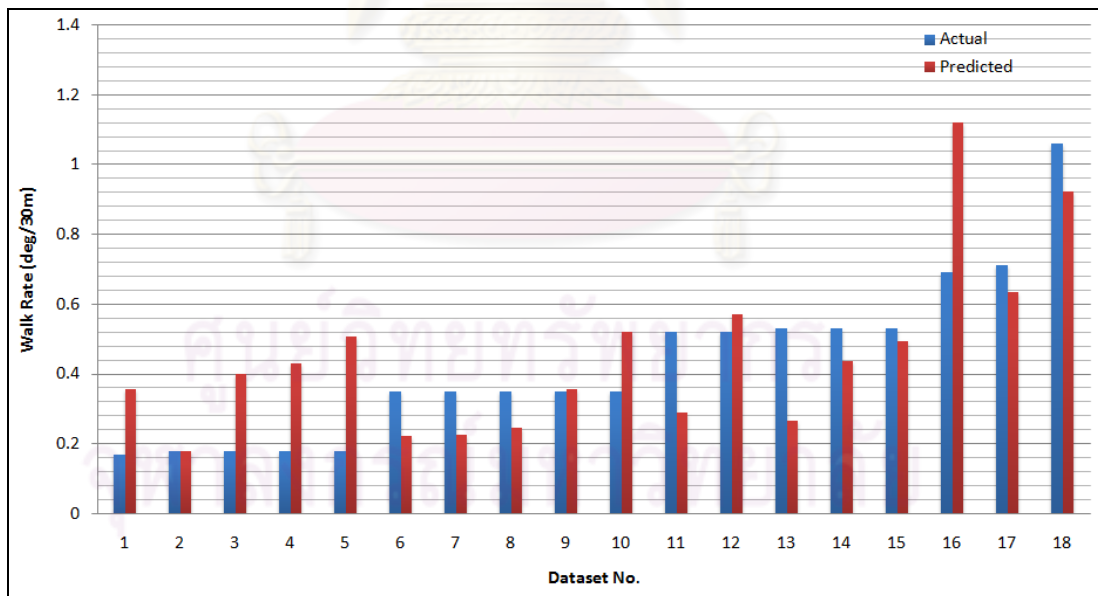


Figure 4.36: Comparing Predicted vs. Actual walk rate by order (Model number 3 – Validating sets)

Table 4.14: Details dataset (Model number 3 – Validating sets)

Dataset no.	Inclination (deg)	WOB (Klbs)	Rotational Speed (RPM)	Torque (Klbs*ft)	Actual walk rate (deg/30m)	Predicted walk rate (deg/30m)
11	41.68	9.97	223	13862	0.52	0.29
13	41.19	11.79	217	8966	0.53	0.27

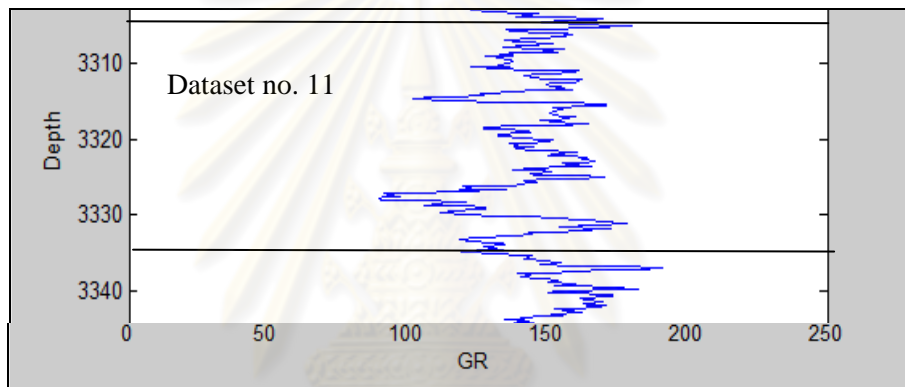


Figure 4.37: Gamma ray log (Dataset no. 11 of Model number 3 – Validating sets)

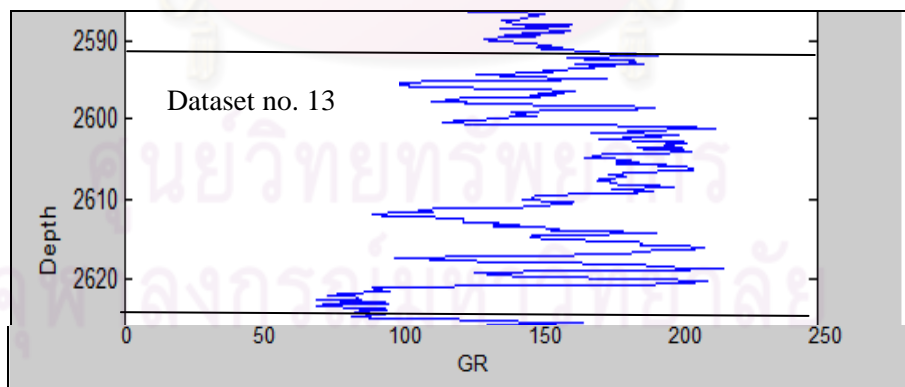


Figure 4.38: Gamma ray log (Dataset no. 13 of Model number 3 – Validating sets)

4.3.2.1.3 Model testing results and discussion

Model number 3 and 5 are tested with the testing dataset. The result from the model (predicted walk rate) is compared with the actual walk rate. The comparison is carried out by the cross plot between predicted and actual walk rate for the testing dataset. Figure 4.39 represents model number 3 while figure 4.40 represents model number 5. Moreover, the comparison result in another perspective is shown in table 4.15. The information in the table represents the percentage of error between the predicted and actual walk rate. Error differences are grouped into 5 ranges which are 0-10%, 10-20%, 20-30%, 30-40% and >40%. The fraction shows the percentage of dataset that belongs to each error range.

Regarding model number 3, the cross plot in figure 4.39 shows the difference between predicted and actual walk rate. The “ $y=x$ ” line refers to the correct prediction. However, this correct prediction is not regularly occurred. Therefore, r (Correlation coefficient) is calculated to see how well the predicted walk rate is correlated with the actual one. In this case of the comparison between predicted and actual walk rate of training sets of model number 3, r is equal to 0.71. Another perspective of comparison could also be seen from table 4.15, for model number 3, there are 11% (fraction = 0.11) of training sets that produce the difference between predicted and actual walk rate in the range of 0-10%. Moreover, there are 11%, 26%, 16%, and 36% (fraction = 0.11, 0.26, 0.16 and 0.36) of training sets that produce the difference between predicted and actual walk rate in the range of 10-20%, 20-30%, 30-40%, and >40% respectively.

Regarding model number 5, the cross plot in figure 4.40 shows the difference between actual and predicted walk rate. The “ $y=x$ ” line refers to the correct prediction. However, this correct prediction is not regularly occurred. Therefore, r (Correlation coefficient) is calculated to see how well the predicted walk rate is correlated with the actual one. In this case of the comparison between actual and predicted walk rate of training sets of model number 5, r is equal to 0.70. Another perspective of comparison could also be seen from table 4.15, for model number 3, there are 14% (fraction = 0.14) of training sets that produce the difference between predicted and actual walk rate in the range of 0-10%. Moreover, there are 5%, 16%, 23%, and 42% (fraction = 0.05, 0.16, 0.23 and 0.42) of training sets that produce the

difference between predicted and actual walk rate in the range of 10-20%, 20-30%, 30-40%, and >40% respectively.

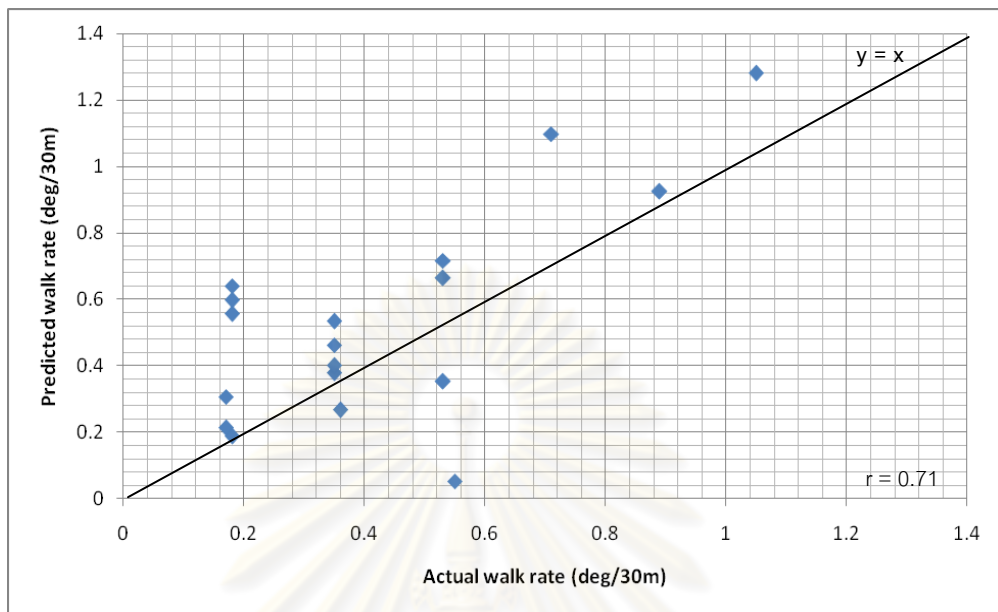


Figure 4.39: Cross plot of Predicted vs. Actual walk rate (Model number 3 – Testing sets)

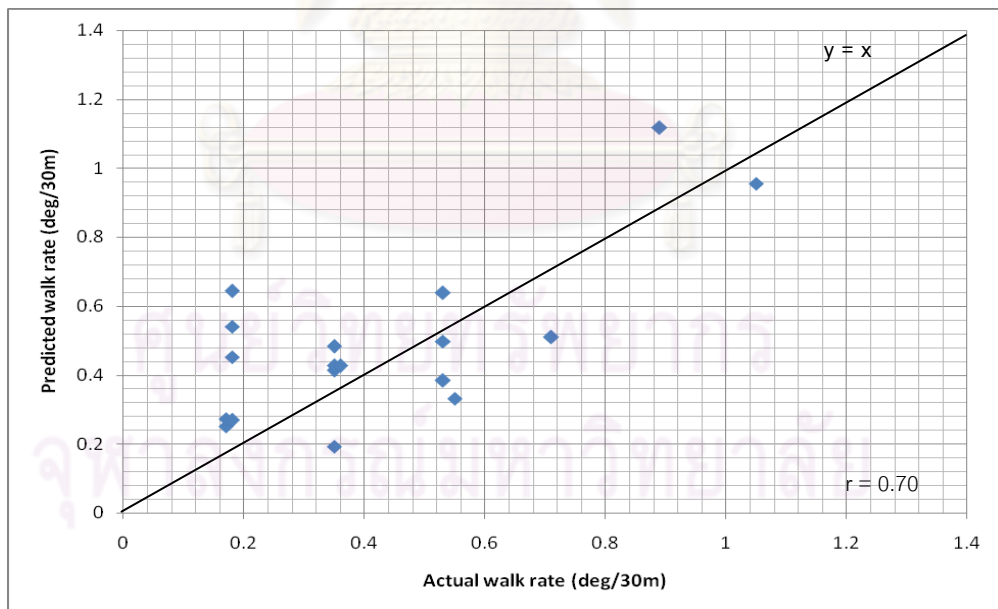


Figure 4.40: Cross plot of Predicted vs. Actual walk rate (Model number 5 – Testing sets)

Table 4.15: Error fraction (Testing sets)

Testing Sets							
Model#	Number of neurons		Fraction of dataset in each error range				
	Hidden layer 1	Hidden layer 2	0-10 %	10-20 %	20-30 %	30-40 %	>40 %
3	9	0	0.11	0.11	0.26	0.16	0.36
5	9	0	0.14	0.05	0.16	0.23	0.42

Model number 3 and 5 are compared to locate which one is better in terms of prediction performance. r values prescribed at the bottom right of each figure between 4.39 and 4.40 are used for the prediction performance comparison. Figure 4.39 representing testing sets of model number 3 give a value of r as 0.71. Figure 4.40 representing testing sets of model number 5 give a value of r as 0.70. Comparing the cross plot representing testing sets between model number 3 and 5 using r values, it is found out that model number 3 yields slightly better result than another one. As a result, model number 3 is selected to represent the absolute bit walk quantity prediction (Case 2.1).

Figure 4.41 shows the comparison between predicted and actual walk rate of testing sets of model number 3. It is alternatively plotted by dataset number. This is to give a closer view on the quantity difference between predicted and actual walk rate dataset by dataset. It is shown in the figure that there is no existence of the case where the actual is significantly higher than the predicted value. However, from the gamma ray pattern found in the case of training and validating sets, it could be implied that if the continuous shale formation is found throughout the specified drilling interval from the geological prognosis, high walk rate could be implied and precaution that the model could likely yield a lower prediction value than the actual case has to be taken place.

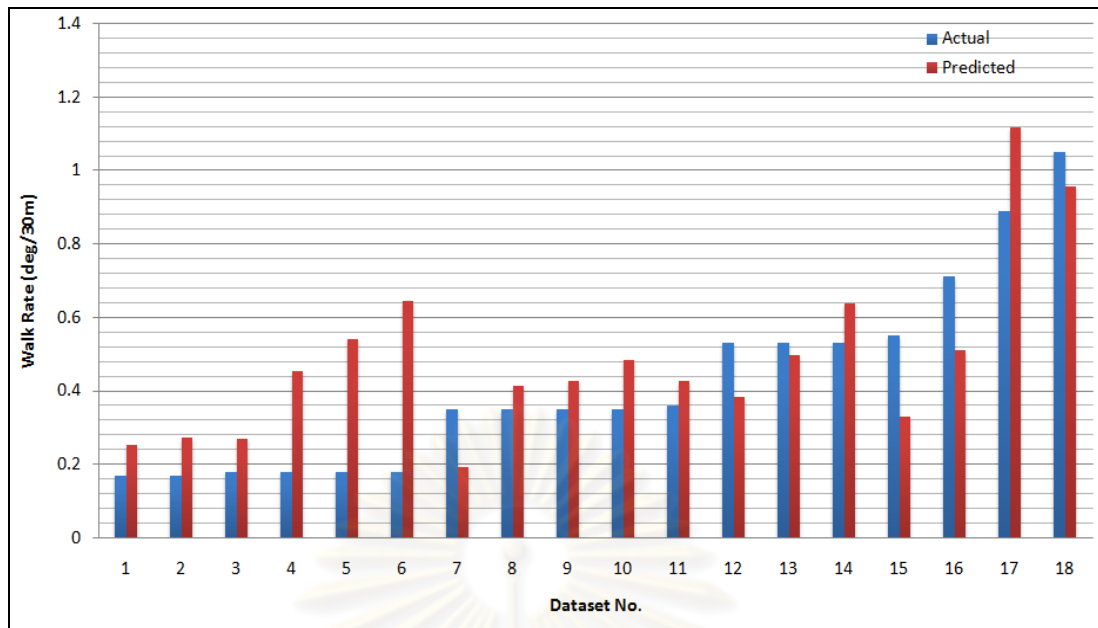


Figure 4.41: Comparing Predicted vs. Actual walk rate by order (Model number 3 – Testing sets)

As observed from the entire dataset, it could be noticed that the actual walk rate exhibits a clustering pattern that there are certain number of dataset yielding the same amount of the actual walk rate. Moreover, according to the error from the testing shown in either cross plot or error fraction (figure 4.39, 4.40 and table 4.15), it could be seen that both models do not exhibit a high accuracy in the prediction. This could be because there are certain effects from the formation. For examples, the drilling interval that experience high formation anisotropies could result in a higher walk rate than usual while drilling in the interval where low anisotropies are experienced will give an opposite result. Even though the formation anisotropies could give an effect to the walk rate, but it is based on the assumption that it should generally gives a moderate effect to the walk rate that it could make the walk rate to be higher or lower than usual in certain range. With these given two reasons above, there is an attempt to establish another case study to try predicting bit walk rate in range rather than the absolute amount. The case study is described and analyzed in the following topic.

4.3.2.2 Case 2.2 – Bit walk quantity in range

This case is the extension of the previous case that it tries to model the bit walk rate given an output in range instead of the absolute walk amount. The rationale behind is to build a model that is best suitable with the information currently available. It has been known that the formation anisotropies contribute quite significantly in affecting the bit walk rate and they are the unknown parameters. The model of this case focus on predicting bit walk rate in range. This could more or less suppress the uncertainty created by the unknown parameters. The walk rate is grouped into three ranges namely group A covers a range of 0.1 to 0.3 deg/30m, group B covers a range of 0.3 to 0.7 deg/30m and group C covers a range of 0.7 to 1.3 deg/30m. The dataset belonging to each group of the walk rate are divided to nearly equally as 38, 40 and 34 respectively from the total of 112 dataset. The model is configured with an input layer consisted of four neurons representing inclination, weight on bit, rotational speed and torque. The output layer is consisted of 3 neurons representing group A, B or C of walk rate range. The number of hidden layers and neurons are varied to search for the configurations resulting in low error. The schematic diagram of the ANN model of this case is shown in figure 4.42.

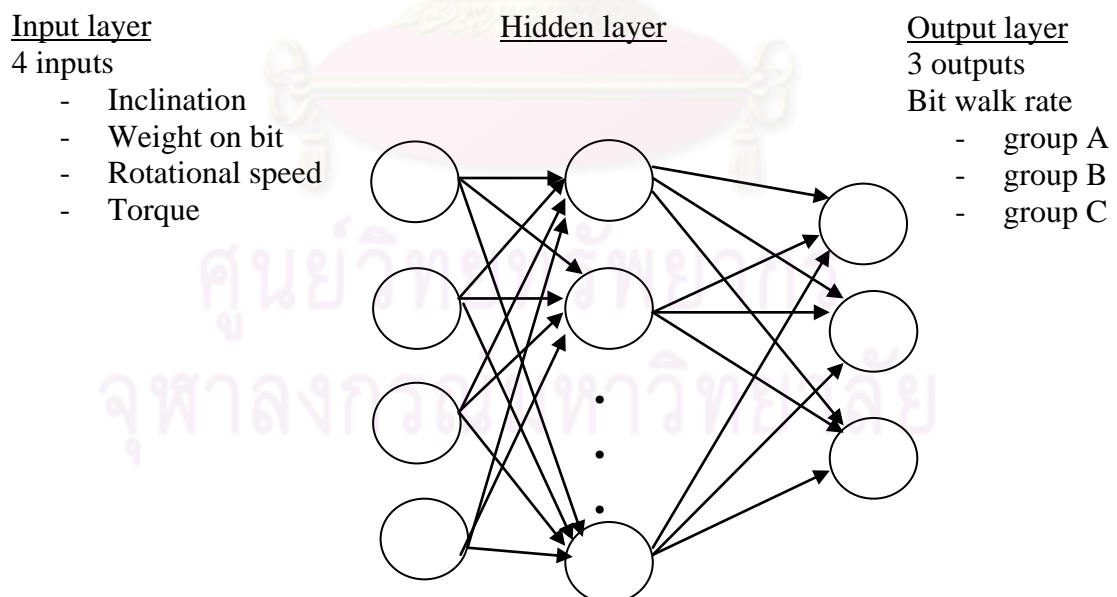


Figure 4.42: Schematic diagram of ANN model – Case 2.2

4.3.2.2.1 Data preprocessing

Table 4.16 demonstrates the examples of dataset that are grouped into three bit walk range. In order to apply these walk range groups with the ANN model, three neuron nodes at the output layer are required to represent all three cases of group A, B or C. The reformatting of the output is shown in table 4.17. For example, a walk rate as 0.17 deg/30m which is under group A is transformed into the ANN output where node1 has a value of 1, node2 as 0 and node3 as 0. Each node of the neurons could give a result ranging from 0 to 1. The details on how to translate the output from the model prediction back to the bit walk range are to be discussed in the results and discussion section.

Table 4.16: Model output in group

Dataset#	Model Inputs				Model Output	
	Inclination	WOB	Rotational speed	Torque	Walk rate	Group
	(deg)	(Klbs)	(rpm)	(Klbs*ft)	(deg/30m)	
1	48.28	11.71	214	12062	0.17	A
2	27.01	11.71	222	12839	0.18	A
3	53.97	8.26	180	11939	0.19	A
4	45.90	12.68	179	12794	0.35	B
5	21.11	13.31	217	10075	0.36	B
5	55.22	11.72	179	10782	0.55	B
6	31.32	13.10	223	9873	0.70	C
8	40.71	12.72	185	11884	0.71	C
9	22.38	14.48	220	9965	0.82	C

*Note: Group A = 0.1-0.3 deg/30m; Group B = 0.3-0.7 deg/30m; Group C = 0.7-1.3 deg/30m

Table 4.17: Output node representation

Group	Output layers		
	Node 1	Node 2	Node 3
A	1	0	0
B	0	1	0
C	0	0	1

*Note: Group A = 0.1-0.3 deg/30m; Group B = 0.3-0.7 deg/30m; Group C = 0.7-1.3 deg/30m

In order to ensure the efficiency in generalization of the model, dataset that are partitioned into training, validating and testing sets should present a similar distribution and cover possible ranges of information as much as possible. The same partitioned dataset with the case 2.1 are also applied to this case. Therefore, the histogram of each partitioned dataset can be referred to the figure 4.11 to 4.22 as shown in the case 2.1.

4.3.2.2 Model training

In this case, ANN model configurations namely number of hidden layers, number of neurons in each layer, learning rate and momentum are varied on a trial and error basis to locate the best configuration making the model converge as well as yielding the lowest MSE. 15 model runs are tried with different configurations. The results are summarized in the table 4.18 as shown below.

Table 4.18: Model configuration – Case 2.2

Model #	No. of neurons		Learning rate	Momentum	MSE
	Hidden layer1	Hidden layer 2			
1	3	0	0.20	0.2	0.1481
2	4	0	0.25	0.9	0.1469
3	4	0	0.20	0.2	0.1546
4	6	0	0.25	0.9	0.1450
5	7	0	0.25	0.9	0.1440
6	8	0	0.25	0.9	0.1396
7	9	0	0.25	0.9	0.1434
8	10	0	0.25	0.9	0.1269
9	15	0	0.25	0.9	0.1575
10	20	0	0.25	0.9	0.1629
11	25	0	0.25	0.9	0.1463
12	30	0	0.25	0.9	0.1628
13	20	10	0.25	0.9	0.1704
14	20	15	0.25	0.9	0.1721
15	20	20	0.25	0.9	0.1568

The trial starts with a single hidden layer and a minimum number of neurons and increase the neurons and hidden layer in the latter models. The first model is configured with the proposed number of neurons as 3 and hidden layer as 1 according

to the proposed formula by Jadid and Fairbairn (1996). The proposed formula calculates the number of neurons to be as 3 from the equation 4.2 as same as in the case 2.1. ($NHN = N_{TRN} / [R + (N_{INP} + N_{OUT})]$) N_{TRN} (No. of training sets) is equal to 76, N_{INP} is equal to 4, N_{OUT} is equal to 3, R could be any number from 5 to 10. The calculated NHN (No. of hidden neurons) is 4.5. The author suggested that this is an upper bound. So, we set the initial no. of hidden neurons to be lower than 4.5 which is 3. Learning rate determines the acceleration of the weight updating. Momentum is used in weight updating to help the search escape local minima and reduce the likelihood of search instability. Therefore, Learning rate and momentum of the first model is minimally set as 0.2. The model is run for about 12 epochs where the converge pattern is shown. At the 6th epoch, MSE of the validating sets reach the optimum point and start to increase after this point. Whereas the MSE of training sets are still continuously reducing as could be due to the overfitting behavior of the ANN model. This is depicted in the figure 4.43.

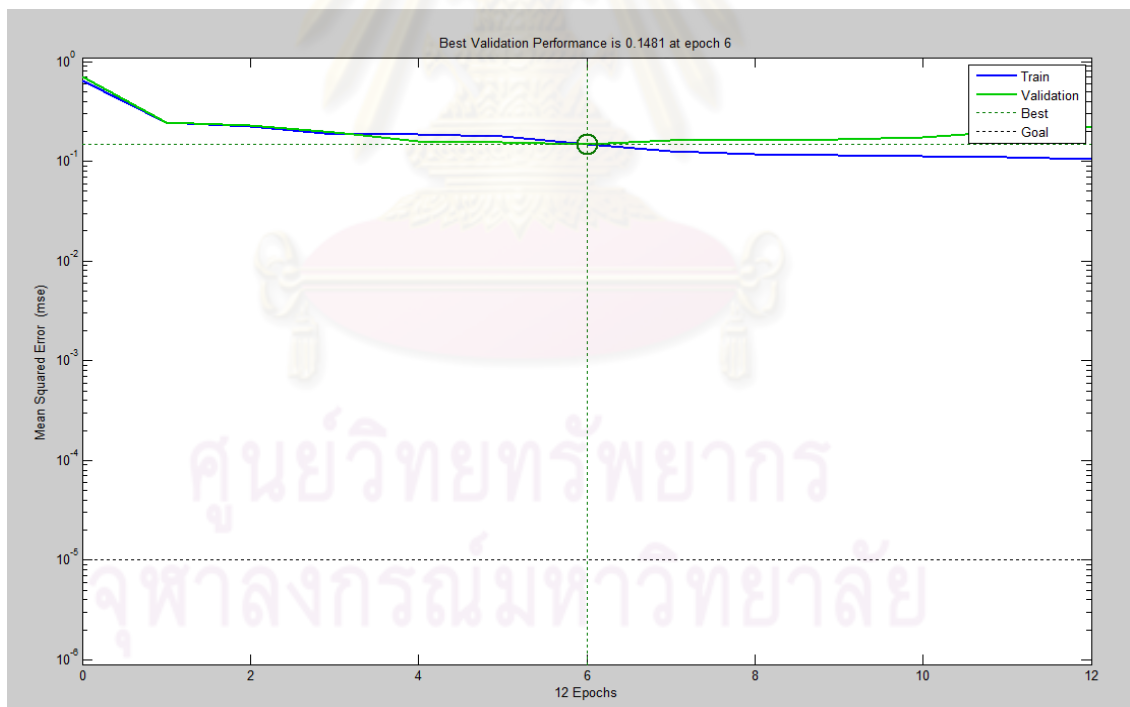


Figure 4.43: Learning curve of model number 1 (Case 2.2)

Model number 2 is increased the number of neurons to 4. Learning rate is set to 0.25 and momentum as 0.9. These learning rate and momentum setting follows the suggestion proposed by Swingler (1996) that setting such values are recommended for

every model configuration unless a good solution could not be obtained. This proposal is also tested by keeping the number of neurons and layers constant and vary the learning rate and momentum. Model number 2 having hidden layer as 1 , number of hidden neurons as 4, learning rate as 0.25 and momentum as 0.9, gives the result of MSE as 0.1469. For model number 3, number of neurons is set to 4 as same as model number 2, while learning rate is set to 0.2 and also the same for the momentum. The MSE results in the value of 0.1546. Model number 2 and 3 are compared, given the same number of neurons but different in learning rate and momentum. This is to test the model performance of model number 3 when learning rate and momentum is changed from 0.25 and 0.9 respectively. It turns out that MSE of model 3 is higher than that of model number 2. This could be generally conclude that learning rate as 0.25 and momentum as 0.9 yield a good result of MSE. Consequently, these configurations are also applied to other followed models. Number of neuron is increased to 6 in model number 4 with learning rate as 0.25 and momentum as 0.9. This results in a better model performance giving lower MSE as 0.1450. Model number 5 is configured with 7 number of neurons and one hidden layer. Learning rate is also set as 0.25 and momentum as 0.9. It results in the MSE as 0.1440. Additional number of hidden neurons have been put into the model for lowering the MSE. This is conducted in model number 6 to model number 15 with the same learning rate and momentum as 0.25 and 0.9 respectively. Model number 13 to 15 are configured with 2 hidden layers. However, the result does not show a better result of MSE than the model with one hidden layer.

From the entire testings, two outstanding models giving lowest MSE are captured for examples. They are model number 6 and 8. Model number 6 gives MSE as 0.1396 with a configuration of 1 hidden layer and 8 number of hidden neurons. Model number 8 gives MSE as 0.1269 with a configuration of 1 hidden layer and 10 number of hidden neurons. Learning rate and momentum for these two models are also set as 0.25 and 0.9 respectively. Model number 6, as shown in figure 4.44, from the beginning of the training cycles, MSE of training set start to decline in parallel with that of the validating set. Until the optimum point is reached at 2th epoch, where validating set start to produce higher MSE but training set still produce a lower MSE. This is according to the overfitting behavior that the network is extensively exposed to the training set making the network lack of the ability to generalize. This is tested

by the validating set that the MSE is increased after the optimum point. Model number 8 also exhibits a minimal MSE which is 0.1269. This is lower than the model number 6's. Its learning curve is shown in figure 4.45. The learning curve is similar to that of model number 6 but it is different only that the model number 8 converges at the 5th epoch where the MSE of training and validating sets start to set apart. Model number 6 and 8 are compared by testing the model with the entire dataset to see how good the model can predict the walk rate resulting in one of the predefined walk range. This is discussed in the next topic.

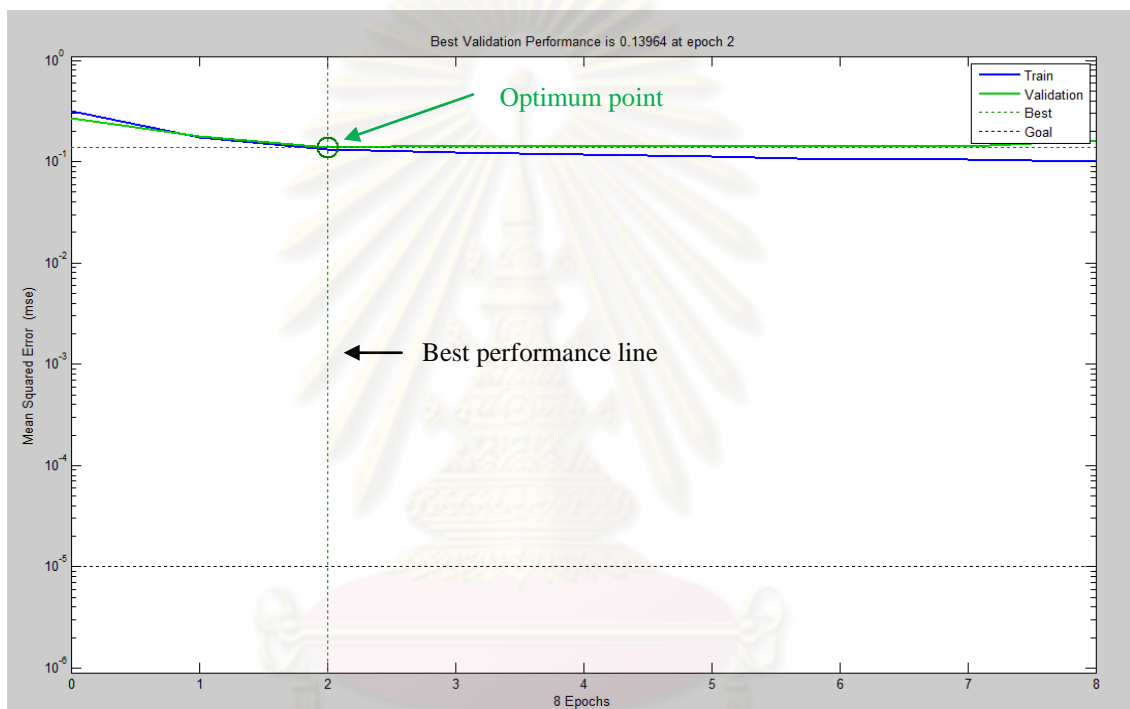


Figure 4.44: Learning curve of model number 6 (Case 2.2)

ศูนย์เวชศาสตร์พยากรณ์
จุฬาลงกรณ์มหาวิทยาลัย

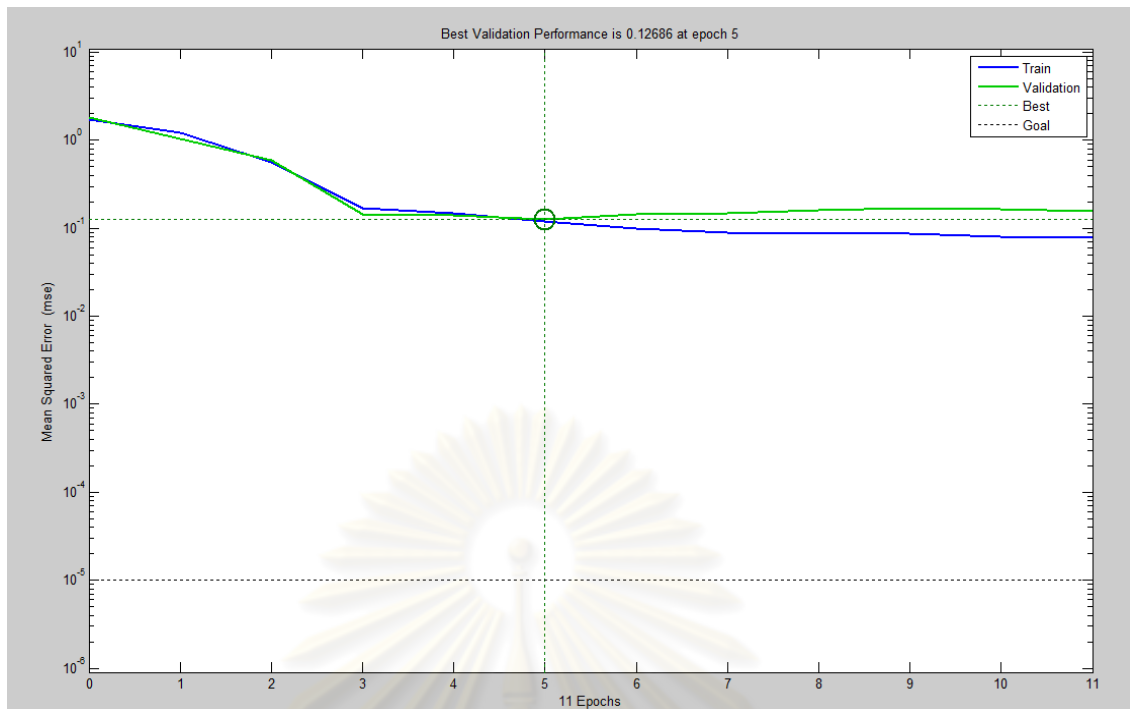


Figure 4.45: Learning curve of model number 8 (Case 2.2)

4.3.2.2.3 Model testing results and discussion

Below in table 4.19 is an example of results from the model prediction. The model gives the output of node 1, 2 and 3 in a range from 0 to 1. The model ideally gives the answer as 1 for the output node that represents the answer while returning 0 for other output nodes. In practice, the model does not give the absolute answer as 0 nor 1 but rather a number between 0 and 1 depending on the strength and condition of the inputs. In general, the threshold can be set up to transform the model output into a binary number, namely 0 or 1. For examples, for a model that exhibit a strong answer, threshold as 0.8 can be set up that higher than such is transformed to 1 else to 0. However, according to the observation of the outputs from the model prediction of this study, not every dataset exhibits a strong output. This can be seen from dataset number 3 and 4 in the table 4.19 that the node representing highest output gives an answer between 0.45 and 0.65. Therefore, transforming the model output to a binary number via a threshold regime as mentioned earlier is not applicable to the data of this study. As a result, the answer of the model is based on the maximum regime that the node out of the three exhibiting the highest value than the others is selected as the

answer of the model prediction. Table 4.20 shows how the model outputs in table 4.19 are transformed into a binary number to show which walk range the model predict for each dataset. For examples, the dataset number 1 in the table 4.18 shows that the model predicts the walk range as 0.3-0.7 deg/30m. In other words, from the input of dataset number 1, inclination as 39.83 deg, WOB as 11.53 Klbs, Rotational speed as 177.46 rpm and Torque as 12000.32 Klbs*ft yield a result of walk range as 0.3-0.7 deg/30m.

Table 4.19: Result from ANN model prediction (Case 2.2)

Dataset#	Model Inputs				Model Outputs		
	Inclination (deg)	WOB (Klbs)	Rotational speed (rpm)	Torque (Klbs*ft)	Node 1 (0.1-0.3 deg/30m)	Node 2 (0.3-0.7 deg/30m)	Node 3 (0.7 – 1.3 deg/30m)
1	39.83	11.53	178	12000	0.07900	0.83732	0.18072
2	26.57	11.62	214	13966	0.13872	0.02023	0.94844
3	18.24	12.91	220	9444	0.20973	0.64235	0.13884
4	20.09	11.88	179	9843	0.45062	0.35603	0.18924

Table 4.20: Result from ANN model prediction (after transforming to binary)

Dataset#	Model Inputs				Model Outputs		
	Inclination (deg)	WOB (Klbs)	Rotational speed (rpm)	Torque (Klbs*ft)	Node 1 (0.1-0.3 deg/30m)	Node 2 (0.3-0.7 deg/30m)	Node 3 (0.7 – 1.3 deg/30m)
1	39.83	11.53	178	12000	0	1	0
2	26.57	11.62	214	13966	0	0	1
3	18.24	12.91	220	9444	0	1	0
4	20.09	11.88	179	9843	1	0	0

This predicted output can be compared with the actual walk range. Not every dataset is correctly predicted by the neural network. The example of both correct and incorrect walk rate prediction is shown in table 4.21. Dataset number 1 shows the correct prediction as the result from the model gives a result of 0.3-0.7 deg/30m walk range, the actual result is also in this range. Dataset number 2 is the example of mismatch between the model prediction and the actual value, the model output predict

that these parameters result in walk range of 0.3-0.7 deg/30m, in fact the actual output of the input parameters is in walk range of 0.1-0.3 deg/30m. Therefore, a performance evaluation of the model has to be built. In this case, hit fraction is used for this matter. Hit fraction represents the proportion of correct prediction over total number of dataset. Giving an example from table 4.22 below, model number 8 gives a hit fraction of testing set as 0.72. This means that the model is able to 72% correctly predict the range of walk rate resulting in any of the walk ranges of 0.1-0.3, 0.3-0.7 or 0.7-1.3 deg/30m. From the comparison of the two models, model number 8 yields a better result than another one when testing the model with the testing sets. Figure 4.46 and 4.47 also show the comparison between predicted and actual walk range in details dataset by dataset which are the extension of the result in table 4.22.

Table 4.21: Example of the comparison between the predicted and actual walk range

Dataset#	Model Inputs				Model Outputs Vs. Actual		
	Inclination (deg)	WOB (Klbs)	Rotational speed (rpm)	Torque (Klbs*ft)	Node 1 (0.1-0.3 deg/30m)	Node 2 (0.3-0.7 deg/30m)	Node 3 (0.7 – 1.3 deg/30m)
1	39.83	11.53	178	12000	0	1	0
Actual					0	1	0
2	40.31	11.33	214	9620	0	1	0
Actual					1	0	0

Table 4.22: Hit fraction – Case 2.2

Model #	Hit fraction of testing dataset
6	0.67
8	0.72

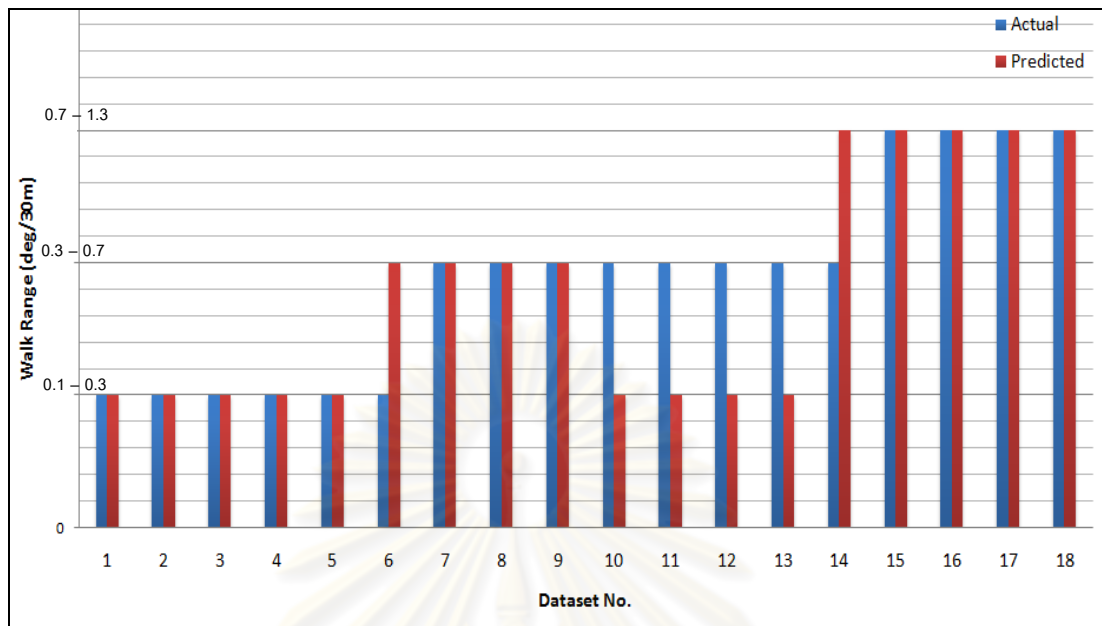


Figure 4.46: Comparing Predicted vs. Actual walk range by order (Model number 6 – Testing sets)

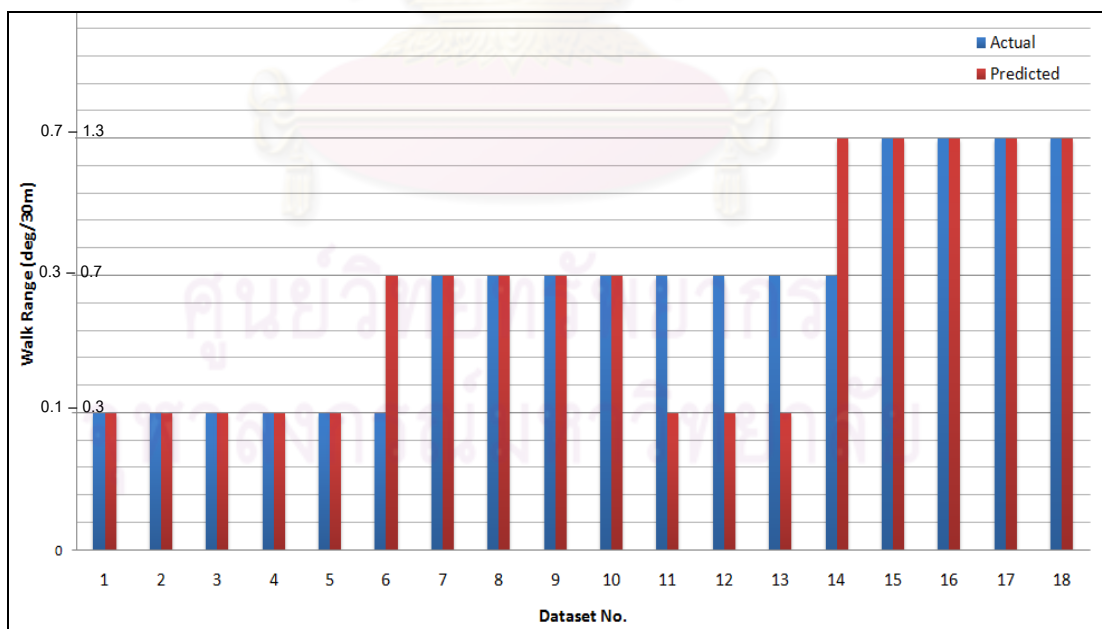


Figure 4.47: Comparing Predicted vs. Actual walk range by order (Model number 8 – Testing sets)

From the model prediction result, it is seen that some incorrect prediction is still occurred even though it is to the less extent than the case 2.1. The explanation could be drawn as same as the case 2.1 that it could be according to the formation effect creating higher or lower walk range than usual. In addition, there is an attempt to verify currently available data if each model parameter complies with the theory described in the past studies. This is conducted by inventing some test dataset and input them into the ANN model to see how much the prediction is varied according to the change of each parameter. The model number 8 which gives a better performance as shown in table 4.22 is used for this matter. As a result, a relationship between each parameter and walk rate (in range) can be generally summarized in table 4.23. The result confirms that following parameters, inclination, weight on bit (WOB) and rotational speed exhibit an inverse relationship, while torque demonstrates a direct relationship with walk rate. These summaries are in line with the past papers.

Table 4.23: Change in walk according to each parameter

Inclination (deg)	WOB (Klbs)	Rotational Speed (RPM)	Torque (Klbs*ft)	Walk range (deg/30m)	Input Observation	Output Observation
42.20	10.57	220.48	7491.50	0.3-0.7	WOB increase	Walk decrease
42.20	14.50	220.48	7491.50	0.1-0.3		
18.24	12.91	219.52	9444.04	0.3-0.7	RPM decrease	Walk increase
18.24	12.91	150.50	9444.04	0.7-1.3		
27.09	11.86	228.31	13793.10	0.7-1.3	Inclination increase	Walk decrease
50.50	11.86	228.31	13793.10	0.3-0.7		
42.25	13.22	217.16	8441.72	0.1-0.3	Torque increase	Walk increase
42.25	13.22	217.16	13650.00	0.3-0.7		

Moreover, the model number 8 could be further utilized to generate a general guideline on how much bit walk is varied according to the changes of the drilling parameters, namely weight on bit and rotational speed, as they are frequently adjusted during the drilling operation. The guideline is designed to cover three ranges of inclination which is normally kept unchanged during the design phase or minimally changed during the drilling operation. The entire range of inclination, namely 18-56 deg, is divided into low range covering 18-35 deg, medium range covering 35-45 deg, and high range covering 45-56 deg. In each inclination range, drilling parameters are set and input into the model to generate the bit walk range. Weight on bit covers the range of 9-16 Klbs, while rotational speed covers the range of 140-230 RPM. These are according to the range taken from the actual field data indicating the optimum ranges used in the drilling operation. Torque which is another input of the model is constantly set as 11000 Klbs*ft to represent a moderate formation hardness. This value is a median from the range of actual torque taken from field data. The bit walk ranges generated by the model are illustrated in the figure 4.48 to 4.50 as walk prediction plots.

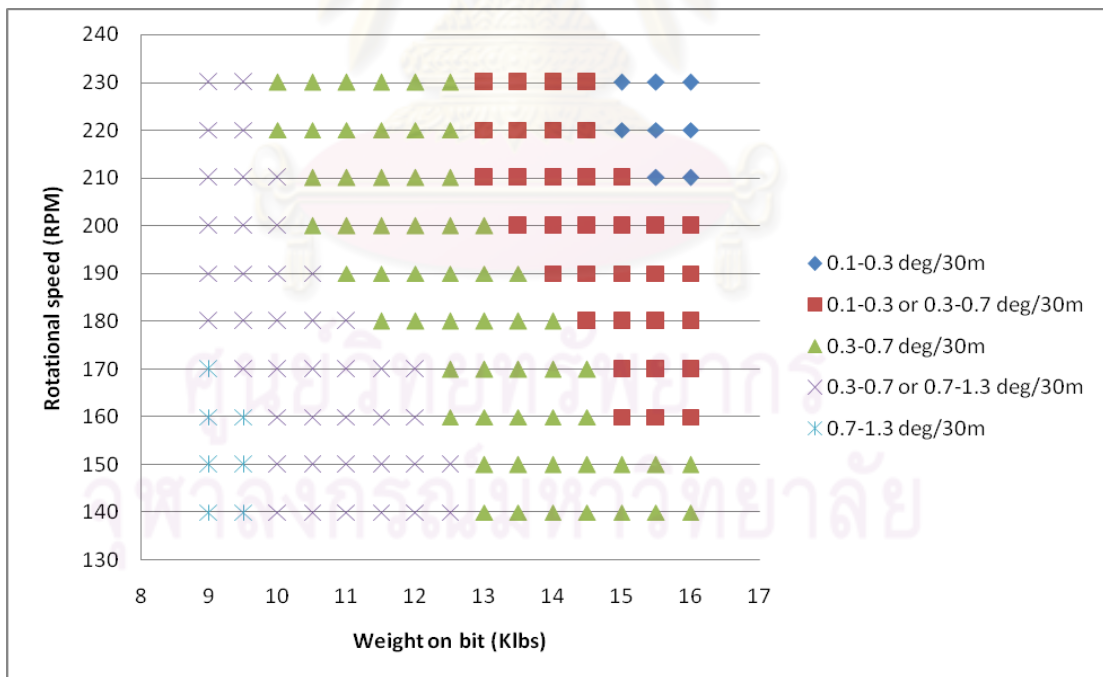


Figure 4.48: Bit walk range under low inclination range (18-35 deg)

The drilling parameters regime could be summarized to give a guideline on a proper scenario of varying the parameters namely weight on bit and rotational speed. As a result, the bit walk range is resulted in an expected and acceptable range. From figure 4.48, at low inclination range (18-35 deg), it can be summarized that WOB from 9 to 9.5 Klbs and rotational speed from 140 to 170 RPM make the bit walk to be in the range of 0.7 to 1.3 deg/30m at any inclination degree from 18 to 35 deg. WOB as 10 to 12.5 Klbs and rotational speed as 140 to 230 RPM yield bit walk either in the range of 0.3-0.7 or 0.7-1.3 deg/30m considering the range of inclination from 18 to 35 deg. If the exact inclination angle is input into the model, the model will yield the exact bit walk range. WOB as 13 to 16 Klbs and rotational speed as 140 to 230 RPM yield bit walk in the range of 0.3 to 0.7 deg/30m; eventhough the inclination angle is changed from 18 to 35 deg, it does not affect the bit walk range given these ranges of WOB and rotational speed. WOB as 15 to 16 Klbs and rotational speed as 160 to 230 RPM give bit walk in the range of either 0.1-0.3 or 0.3-0.7 deg/30m considering the range of inclination from 18-35 deg. WOB as 15 to 16 Klbs and rotational speed as 210 to 230 RPM could yield bit walk range from 0.1 to 0.3 deg/30m.

There are two points to be noted. Firstly, the described WOB and rotational speed might not be exactly matched with the walk prediction plots since the range of bit walk as displayed generally is not in a rectangular shape. Therefore, the ranges described here are considered as an approximation, the exact details could be viewed directly from the plots. Secondly, an uncertainty could be implied to the answer from the model that the predicted might be different from the actual walk range in some cases especially the case where there is a formation anistropies effect as seen in the case 2.1 and 2.2 discussed earlier.

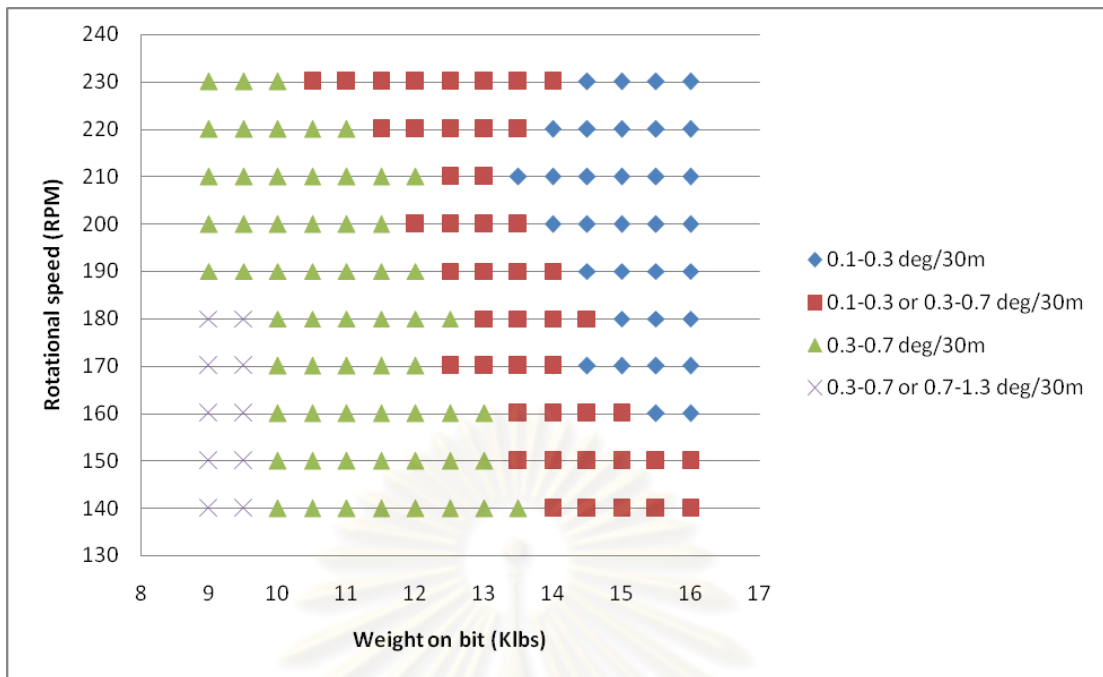


Figure 4.49: Bit walk range under medium inclination range (35-45 deg)

From the figure 4.49, at medium inclination range (35-45 deg), it can be summarized that WOB from 9 to 9.5 Klbs and rotational speed from 140 to 180 RPM could make the bit walk to be either in the range of 0.3 to 0.7 or 0.7 to 1.3 deg/30m depending on the exact inclination degree ranging from 35 to 45 deg. WOB as 9 to 10 Klbs and rotational speed as 190 to 230 RPM as well as WOB as 10 to 13.5 Klbs and rotational speed as 140 to 230 RPM yield bit walk in the range of 0.3-0.7 deg/30m at any inclination from 35 to 45 deg. WOB as 14 to 16 Klbs and rotational speed as 140 to 230 RPM yield bit walk either in the range of 0.1 to 0.3 or 0.3 to 0.7 deg/30m depending on the exact inclination degree from 35 to 45 deg. WOB as 15 to 16 Klbs and rotational speed as 160 to 230 RPM give bit walk in the range of 0.1-0.3 deg/30m at any inclination in the range of 35-45 deg. There are two cautions noted as same as the low inclination case above.

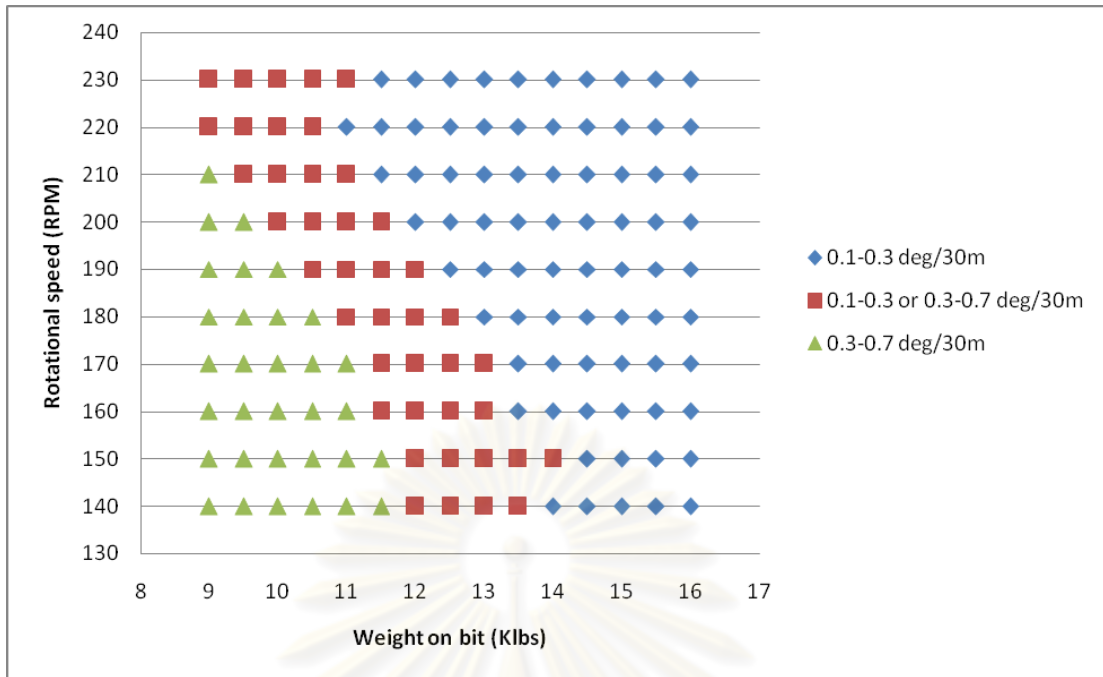


Figure 4.50: Bit walk range under high inclination range (45-56 deg)

From the figure 4.50, at high inclination range (45-56 deg), it can be summarized that WOB from 9 to 11.5 Klbs and rotational speed from 140 to 210 RPM could make the bit walk in the range of 0.3 to 0.7 deg/30m at any inclination angle ranging from 45 to 56 deg. WOB as 11 to 14 Klbs and rotational speed as 140 to 180 RPM as well as WOB as 9 to 12 Klbs and rotational speed as 180 to 230 RPM yield bit walk in either the range of 0.1-0.3 or 0.3-0.7 deg/30m depending on the exact inclination angle from 45 to 56 deg. WOB as 14 to 16 Klbs and rotational speed as 140 to 230 RPM yield bit walk in the range of 0.1 to 0.3 deg/30m at any inclination angle from 45 to 56 deg. There are two cautions noted as same as the low inclination case above.

In conclusion, from the generated walk prediction plots, it can be applied to the drilling operation as follows. The inclination is normally predefined at the drilling design phase. Therefore, the range of the inclination is initially determined that one of the three plots is chosen. The formation hardness is generally considered as a moderate hardness. The drilling parameters, namely weight on bit and rotational speed as the most frequently adjustable parameters, can be varied and their effect to the bit walk range can be viewed through the change of the bit walk range shown in the walk prediction plots.

CHAPTER V

CONCLUSIONS AND RECOMMENDATIONS

5.1 Conclusions

This thesis utilized an artificial neural network to create a model to predict the bit walk rate for the drilling operation in the Gulf of Thailand, particularly in the 6-1/8" drilling section. The model is trained with the actual field data obtained from several drilled wells. To develop the neural network model, four main steps are conducted as follows. Firstly, identify inputs and outputs of the neural network model through the reviewing and summarizing of the past studies to determine the factors and their effects to the bit walk. Secondly, screen and filter the data before training the network to ensure the qualified distribution of the data as well as the quality of the model training and prediction. Thirdly, develop the model training with several configurations to locate the best model configuration. And lastly evaluate the performance of the models by testing with the actual field data.

The conclusions drawn from the study and model applications are summarized as follows.

1. The selected parameters affecting bit walk tendency cover the domains of wellbore geometry represented by inclination, drilling parameters represented by the two important operating parameters which are weight on bit and rotational speed, and formation hardness represented by torque.

2. The total dataset of 140 mostly represent bit walk left. 20 of which represents bit walk right. This is concluded that given the selected bit and BHA configuration, bit walk exhibits a left tendency. The right direction is minimal and implied by the effect from the formation anisotropies which are dip angle for interbedded formation and laminated characteristic for shale formation.

3. The model is used for predicting bit walk quantity in an absolute amount as well as in range. Predicting the bit walk in range yields more precise result than the absolute amount case. The error occurred in the absolute amount case could be due to

the formation anisotropies. The percentage of correct prediction for the bit walk range case is 72% when tested with testing dataset.

4. The model is also used for checking the alignment with the previous studies. The result shows that the neural network model gives the same result in terms of relationship (either direct or inverse) between each parameter and walk rate.

5. Drilling parameters adjustment can be previewed by the walk prediction plots generated by the model covering three ranges of inclination. The plots display the variation of drilling parameters, namely weight on bit and rotational speed, affecting the change of bit walk range given moderate formation hardness.

As seen from the model development and testing, the models exhibit some errors. The main factor could be from the formation anisotropies corresponding to dip angle for interbedded formation and laminated characteristic for shale formation. The conclusion drawn from both absolute walk rate and walk range prediction cases shows that laminated characteristic demonstrated in the continuous shale formation could account for a high walk rate. This could be found from the geological prognosis. However, this is considered as qualitative information that cannot be directly input into the model.

5.2 Recommendations

The recommendations for future work are summarized as follows.

1. The formation anisotropies are seen to be disregarded from the model development due to the insufficiency of the information as well as the difficulties in obtaining the anisotropy information in a quantitative manner. When the formation anisotropies could be quantitatively identified and incorporated as parameters of the model in conjunction with synchronized directional data, the model should be able to extend its capability to predict more precise bit walk rate as well as bit walk direction.

2. This study scopes down to focus on a certain bit, BHA configuration and formation type. Therefore, the model could be further extended to cover several types of bits, BHA configurations and formation types so that the model can be utilized with more general and various types of applications.

3. It is also worth to be aware that the number of training dataset required for training the neural network model is according to the number of network inputs and outputs. Once model parameters are increased, additional inputs are added to the model. Consequently, the number of training dataset has to be increased to ensure the sufficiency of training samples.



ศูนย์วิทยทรัพยากร
จุฬาลงกรณ์มหาวิทยาลัย

REFERENCES

- Bannerman J.S. Walk Rate Prediction on Alwyn North Field by Means of Data Analysis and 3D Computer Model. SPE 20933 presented at Europec 90, The Hague, Netherlands, October, 1990.
- Basheer I.A. and Hajmeer M. Artificial neural networks: fundamentals, computing, design, and application. Journal of Microbiological Methods (2000): 3-31
- Boualleg R., Sellami H. and Menand S. Effect of Formations Anistropy on Directional Tendencies of Drilling Systems. SPE 98865 presented at the IADC/SPE Drilling Conferences held in Miami, Florida, U.S.A., February, 2006.
- Bourgoyne Jr. A.T. et al. Applied Drilling Engineering. SPE Textbook Series Vol.2, 1984.
- Chen S., Collins G.J. and Thomas M.B. Reexamination of PDC Bit Walk in Directional and Horizontal Wells. SPE 112641 presented at the 2008 IADC/SPE Drilling Conferences held in Orlando, Florida, U.S.A., March, 2008.
- Ernst S., Pastusek P. and Lutes P. Effects of RPM and ROP on PDC Bit Steerability. SPE 105594 presented at the 2007 IADC/SPE Drilling Conference held in Amsterdam, The Netherlands, February, 2007.
- Hilchie W.D. Applied Openhole Log Interpretation. Colorado: Golden Colorado,1978.
- Ho H.S. Prediction of Drilling Trajectory in Directional Wells via a New Rock-Bit Interaction Model. SPE 16658 presented at the 62nd Annual Technical

Conference and Exhibition of the Society of Petroleum Engineers held in Dallas, Texas, September, 1987.

Jadid M.N. and Fairbairn D.R. Predicting moment-curvature parameters from experimental data. Eng. Appl. Artif. Intell. (1996): 309-319.

Maldia E.E. and Sampaio J.H.B. Field Verification of Lead Angle and Azimuth Rate of Change Predictions in Directional Wells Using a New Mathematical Model. SPE 19337 presented at the SPE Eastern Regional Meeting held in Morgantown, West Virginia, October, 1989.

Menand S. et al. How Bit Profile and Gauges Affect Well Trajectory. SPE 82412 presented at the 2002 IADC/SPE Drilling Conference, Dallas, February, 2002.

Millhiem K.K. and Warren T.M. Side cutting characteristics of rock bits and stabilizers while drilling. SPE 7518 presented at the 53rd Annual Fall Conference and Exhibition of the Society of Petroleum Engineers of AIME, held in Houston, Texas, October, 1978.

Perry C.J. Directional Drilling with PDC Bits in the Gulf of Thailand. SPE 15616 presented at the 61st Annual Technical Conference and Exhibition of the Society of Petroleum Engineers held in New Orleans, LA, October, 1986.

Swingler K. Applying Neural Networks: A Practical Guide. New York: Academic Press, 1996.

Walker B.H. Factors Controlling Hole Angle and Direction. SPE 15963 published in the Journal of Petroleum Technology, November, 1986.

Wilamowski B.M. An Algorithm for Fast Convergence in Training Neural Networks. IEEE. (2001): 1778-1782.

Williamson J.S. and Lubinski A. Predicting Bottomhole Assembly Performance. SPE 14764 presented at the 1986 IADC/SPE Drilling Conferences, Dallas, February, 1986.

Wolcott D.S. and Bordelon D.R. Lithology Determination using Downhole Bit Mechanics Data. SPE 26492 presented at the 68th Annual Technical Conference and Exhibition of the Society of Petroleum Engineers held in Houston, Texas, October, 1993.



ศูนย์วิทยทรัพยากร
จุฬาลงกรณ์มหาวิทยาลัย



APPENDICES

ศูนย์วิทยทรัพยากร
จุฬาลงกรณ์มหาวิทยาลัย

APPENDIX A

Details of 140 dataset from the drilling operation in the Gulf of Thailand

Dataset no.	Inclination (deg)	WOB (Klbs)	Rotational Speed (RPM)	Torque (Klbs*ft)	Walk rate (deg/30m)	Walk direction
1	15.33	3.67	214	6036	0.52	Right
2	18.24	12.91	220	9444	0.36	Left
3	18.72	12.03	222	9792	0.36	Right
4	19.04	11.28	214	6450	0.18	Left
5	19.34	13.90	223	9803	0.71	Left
6	19.92	14.79	218	9632	0.18	Left
7	20.09	11.88	179	9843	0.18	Left
8	20.33	14.59	208	10078	0.35	Left
9	20.64	14.03	209	9866	0.35	Left
10	21.11	13.31	217	10075	0.36	Left
11	21.24	11.48	210	6298	0.88	Left
12	21.43	12.57	130	13522	0.69	Left
13	21.76	12.41	124	13724	0.89	Left
14	21.98	12.38	220	9634	0.18	Right
15	21.98	14.14	222	9740	0.35	Left
16	22.33	12.90	154	14241	1.08	Left
17	22.38	14.48	220	9964	0.82	Left
18	22.65	11.34	220	9570	0.35	Left
19	22.78	14.03	221	9592	0.47	Right
20	23.04	12.83	222	10822	0.53	Left
21	23.07	13.45	146	13862	1.17	Left
22	23.13	13.10	222	9437	0.35	Left
23	23.35	12.76	142	8824	0.71	Right
24	23.44	12.29	222	9453	0.35	Right
25	23.60	13.03	163	13586	0.82	Left
26	23.61	15.38	222	10766	0.53	Left
27	23.79	14.10	223	9310	0.35	Left
28	23.91	11.04	174	13786	1.05	Left
29	24.19	13.54	126	8500	0.70	Right
30	24.19	13.66	222	9179	0.18	Left
31	24.29	12.00	160	13586	1.15	Left
32	24.54	15.45	221	10711	0.71	Left
33	24.59	11.90	221	8994	0.18	Left
34	24.98	12.10	221	9307	0.17	Left
35	25.09	12.10	180	13333	1.30	Left
36	25.18	11.21	198	13464	0.82	Left

Dataset no.	Inclination	WOB	Rotational Speed	Torque	Walk rate	Walk direction
	(deg)	(Klbs)	(RPM)	(Klbs*ft)	(deg/30m)	
37	25.20	13.07	119	8034	0.36	Right
38	25.33	12.24	222	10610	0.70	Left
39	25.33	12.21	221	8936	0.71	Left
40	25.48	11.00	206	13621	1.28	Left
41	25.92	11.90	208	14345	1.22	Left
42	26.21	14.17	223	10719	0.35	Left
43	26.30	10.93	138	7966	0.88	Right
44	26.57	11.62	214	13966	0.71	Left
45	26.87	12.88	219	12613	0.53	Right
46	27.00	14.18	223	10448	0.53	Left
47	27.01	11.71	222	12839	0.18	Left
48	27.07	12.55	221	12976	0.19	Left
49	27.09	11.86	228	13793	0.88	Left
50	27.10	11.53	222	12891	0.70	Left
51	27.36	13.84	221	12234	1.59	Right
52	27.49	14.93	215	10525	0.17	Right
53	27.97	14.97	222	10369	0.70	Left
54	28.15	13.86	221	12280	0.88	Right
55	28.46	13.97	222	10280	0.18	Right
56	29.03	13.97	222	10525	0.36	Left
57	29.34	12.72	215	12522	1.06	Right
58	30.13	11.56	220	12408	0.17	Right
59	30.35	13.39	223	10136	0.35	Left
60	30.66	12.45	223	10097	0.35	Left
61	30.88	11.97	223	10155	0.18	Left
62	31.32	13.10	223	9873	0.70	Left
63	31.77	13.25	223	9403	0.18	Right
64	31.81	13.10	223	9796	0.17	Right
65	36.42	14.47	140	12107	0.86	Left
66	37.45	13.67	142	11771	0.88	Left
67	37.53	11.37	105	14296	0.71	Left
68	37.71	10.84	209	11008	0.35	Left
69	37.76	12.12	217	10589	0.53	Left
70	38.02	11.37	217	10332	0.35	Left
71	38.33	12.76	212	10183	0.18	Left
72	38.50	11.41	213	10021	0.35	Left
73	38.68	10.00	214	9852	0.35	Left
74	38.77	12.66	164	12163	0.71	Left
75	38.94	9.71	215	9698	0.18	Left

Dataset no.	Inclination	WOB	Rotational Speed	Torque	Walk rate	Walk direction
	(deg)	(Klbs)	(RPM)	(Klbs*ft)	(deg/30m)	
76	39.03	10.14	214	9679	0.35	Left
77	39.12	8.54	214	9555	0.35	Left
78	39.34	10.64	214	9721	0.36	Left
79	39.43	11.38	162	14483	0.36	Left
80	39.78	11.34	214	9698	0.35	Left
81	39.83	11.53	177	12000	0.35	Left
82	40.31	11.33	213	9620	0.18	Left
83	40.58	10.55	214	9362	0.35	Left
84	40.71	12.72	185	11884	0.71	Left
85	40.84	12.53	216	9401	0.35	Left
86	41.19	11.79	217	8966	0.53	Left
87	41.50	12.67	217	8964	0.18	Left
88	41.63	13.60	192	11690	0.70	Left
89	41.68	9.97	223	13862	0.52	Left
90	41.81	13.40	217	8807	0.17	Left
91	42.03	12.84	218	8570	0.18	Left
92	42.16	12.84	218	8412	0.17	Left
93	42.16	10.90	195	13897	0.36	Left
94	42.20	10.57	220	7492	0.35	Left
95	42.25	13.22	217	8442	0.18	Left
96	42.25	11.19	218	7886	0.18	Left
97	42.38	14.16	190	11781	1.06	Left
98	43.00	13.64	188	11973	1.06	Left
99	43.30	11.29	222	14321	0.35	Left
100	43.74	11.43	220	13929	0.35	Left
101	45.20	8.31	180	13145	0.18	Left
102	45.29	12.52	223	11585	0.53	Left
103	45.37	9.81	178	13169	0.53	Left
104	45.46	10.60	179	12811	0.17	Left
105	45.73	11.21	179	12789	0.53	Left
106	45.90	12.68	179	12794	0.35	Left
107	45.99	13.41	209	12118	0.52	Left
108	46.08	14.34	179	12587	0.36	Left
109	46.43	12.67	223	11757	0.88	Left
110	46.52	12.91	214	12119	0.18	Left
111	46.52	13.19	179	12532	0.35	Left
112	46.87	11.81	214	12016	0.18	Left
113	46.96	13.97	179	12638	0.17	Left
114	47.14	11.77	214	12062	0.35	Left

Dataset no.	Inclination (deg)	WOB (Klbs)	Rotational Speed (RPM)	Torque (Klbs*ft)	Walk rate (deg/30m)	Walk direction
115	47.22	12.19	178	12451	0.18	Left
116	47.49	12.43	214	12183	0.18	Left
117	47.75	12.67	179	12448	0.53	Left
118	47.84	12.60	214	12147	0.17	Left
119	47.93	13.65	214	12086	0.18	Left
120	48.15	11.72	222	11660	1.23	Left
121	48.28	11.71	214	12062	0.17	Left
122	48.63	13.45	214	12027	0.36	Left
123	48.81	9.82	213	11969	0.35	Left
124	49.07	9.54	214	11725	0.18	Left
125	53.70	12.32	181	10532	0.18	Left
126	53.94	7.41	179	12324	0.23	Left
127	53.97	8.26	180	11939	0.19	Left
128	54.11	12.17	181	11911	0.15	Left
129	54.23	10.95	219	9876	0.18	Left
130	54.28	11.96	220	9998	0.17	Left
131	54.45	12.53	212	10263	0.18	Left
132	54.51	12.82	180	12308	0.18	Left
133	54.58	11.09	212	9888	0.18	Left
134	54.67	12.22	220	9891	0.18	Left
135	54.86	12.62	180	11836	0.10	Left
136	55.07	12.72	220	9816	0.18	Left
137	55.22	11.72	179	10782	0.55	Left
138	55.23	12.42	180	11434	0.15	Left
139	55.24	12.28	220	9097	0.18	Right
140	55.68	12.39	220	9436	0.18	Right

ศูนย์วิทยทรัพยากร
จุฬาลงกรณ์มหาวิทยาลัย

APPENDIX B

Results from testing model number 3 with entire dataset (Case 2.1)

Dataset no.	Data type	Inclination	WOB	Rotational Speed	Torque	Walk rate (Actual)	Walk rate (Predicted)
		(deg)	(Klbs)	(RPM)	(Klbs*ft)	(deg/30m)	(deg/30m)
1	Train	18.24	12.91	220	9444	0.36	0.40
2	Train	19.34	13.90	223	9803	0.71	0.47
3	Train	20.09	11.88	179	9843	0.18	0.12
4	Train	21.11	13.31	217	10075	0.36	0.45
5	Train	21.98	14.14	222	9740	0.35	0.47
6	Train	22.33	12.90	154	14241	1.08	1.04
7	Train	22.38	14.48	220	9964	0.82	0.52
8	Train	22.65	11.34	220	9570	0.35	0.36
9	Train	23.04	12.83	222	10822	0.53	0.43
10	Train	23.07	13.45	146	13862	1.17	1.10
11	Train	23.13	13.10	222	9437	0.35	0.39
12	Train	23.60	13.03	163	13586	0.82	1.13
13	Train	23.79	14.10	223	9310	0.35	0.44
14	Train	24.29	12.00	160	13586	1.15	0.93
15	Train	24.59	11.90	221	8994	0.18	0.34
16	Train	25.09	12.10	180	13333	1.29	1.18
17	Train	25.18	11.21	198	13464	0.82	0.90
18	Train	25.33	12.24	222	10610	0.70	0.41
19	Train	25.33	12.21	221	8936	0.71	0.34
20	Train	25.92	11.90	208	14345	1.22	0.97
21	Train	26.21	14.17	223	10719	0.35	0.49
22	Train	26.57	11.62	214	13966	0.71	0.86
23	Train	27.00	14.18	223	10448	0.53	0.48
24	Train	27.07	12.55	221	12976	0.19	0.63
25	Train	27.09	11.86	228	13793	0.88	0.59
26	Train	27.10	11.53	222	12891	0.70	0.66
27	Train	27.97	14.97	222	10369	0.70	0.54
28	Train	30.66	12.45	223	10097	0.35	0.40
29	Train	30.88	11.97	223	10155	0.18	0.40
30	Train	31.32	13.10	223	9873	0.70	0.39
31	Train	36.42	14.47	140	12107	0.86	0.94
32	Train	37.45	13.67	142	11771	0.88	0.80
33	Train	37.71	10.84	209	11008	0.35	0.49
34	Train	38.02	11.37	217	10332	0.35	0.46
35	Train	38.50	11.41	213	10021	0.35	0.41
36	Train	38.94	9.71	215	9698	0.18	0.15
37	Train	39.34	10.64	214	9721	0.36	0.31
38	Train	39.43	11.38	162	14483	0.36	0.48
39	Train	39.83	11.53	177	12000	0.35	0.57
40	Train	40.31	11.33	213	9620	0.18	0.34
41	Train	40.71	12.72	185	11884	0.71	0.78
42	Train	40.84	12.53	216	9401	0.35	0.33
43	Train	41.63	13.60	192	11690	0.70	0.96
44	Train	42.03	12.84	218	8570	0.18	0.23
45	Train	42.16	12.84	218	8412	0.17	0.21

Dataset no.	Data type	Inclination	WOB	Rotational Speed	Torque	Walk rate (Actual)	Walk rate (Predicted)
		(deg)	(Klbs)	(RPM)	(Klbs*ft)	(deg/30m)	(deg/30m)
46	Train	42.16	10.90	195	13897	0.36	0.38
47	Train	42.20	10.57	220	7492	0.35	0.13
48	Train	42.25	11.19	218	7886	0.18	0.16
49	Train	42.25	13.22	217	8442	0.18	0.20
50	Train	42.38	14.16	190	11781	1.06	0.93
51	Train	43.74	11.43	220	13929	0.35	0.26
52	Train	44.14	13.30	194	11851	1.30	0.84
53	Train	45.37	9.81	178	13169	0.53	0.36
54	Train	45.46	10.60	179	12811	0.17	0.42
55	Train	45.90	12.68	179	12794	0.35	0.43
56	Train	46.43	12.67	223	11757	0.88	0.44
57	Train	46.52	12.91	214	12119	0.18	0.52
58	Train	46.96	13.97	179	12638	0.17	0.34
59	Train	47.14	11.77	214	12062	0.35	0.48
60	Train	47.49	12.43	214	12183	0.18	0.48
61	Train	47.84	12.60	214	12147	0.17	0.46
62	Train	47.93	13.65	214	12086	0.18	0.29
63	Train	48.15	11.72	222	11660	1.23	0.47
64	Train	48.28	11.71	214	12062	0.17	0.40
65	Train	48.63	13.45	214	12027	0.36	0.32
66	Train	48.81	9.82	213	11969	0.35	0.25
67	Train	49.07	9.54	214	11725	0.18	0.24
68	Train	53.70	12.32	181	10532	0.18	0.24
69	Train	54.11	12.17	181	11911	0.15	0.18
70	Train	54.45	12.53	212	10263	0.18	0.28
71	Train	54.51	12.82	180	12308	0.18	0.08
72	Train	54.58	11.09	212	9888	0.18	0.17
73	Train	54.67	12.22	220	9891	0.18	0.24
74	Train	54.86	12.62	180	11836	0.10	0.07
75	Train	55.07	12.72	220	9816	0.18	0.15
76	Train	55.23	12.42	180	11434	0.15	0.17
77	Validate	20.33	14.59	208	10078	0.35	0.52
78	Validate	21.43	12.57	130	13522	0.69	1.12
79	Validate	24.19	13.66	222	9179	0.18	0.40
80	Validate	24.54	15.45	221	10711	0.71	0.63
81	Validate	24.98	12.10	221	9307	0.17	0.36
82	Validate	37.76	12.12	217	10589	0.53	0.49
83	Validate	38.68	10.00	214	9852	0.35	0.22
84	Validate	39.03	10.14	214	9679	0.35	0.23
85	Validate	39.78	11.34	214	9698	0.35	0.36
86	Validate	40.58	10.55	214	9362	0.35	0.24
87	Validate	41.19	11.79	217	8966	0.53	0.27
88	Validate	41.68	9.97	223	13862	0.52	0.29
89	Validate	43.00	13.64	188	11973	1.06	0.92
90	Validate	45.73	11.21	179	12789	0.53	0.44
91	Validate	45.99	13.41	209	12118	0.52	0.57
92	Validate	46.87	11.81	214	12016	0.18	0.51
93	Validate	47.22	12.19	178	12451	0.18	0.43
94	Validate	54.23	10.95	219	9876	0.18	0.18

Dataset no.	Data type	Inclination	WOB	Rotational Speed	Torque	Walk rate (Actual)	Walk rate (Predicted)
		(deg)	(Klbs)	(RPM)	(Klbs*ft)	(deg/30m)	(deg/30m)
95	Test	19.92	14.79	218	9632	0.18	0.54
96	Test	20.64	14.03	209	9866	0.35	0.48
97	Test	21.76	12.41	124	13724	0.89	1.12
98	Test	23.61	15.38	222	10766	0.53	0.64
99	Test	23.91	11.04	174	13786	1.05	0.95
100	Test	27.01	11.71	222	12839	0.18	0.64
101	Test	30.35	13.39	223	10136	0.35	0.41
102	Test	38.33	12.76	212	10183	0.18	0.45
103	Test	38.77	12.66	164	12163	0.71	0.51
104	Test	41.50	12.67	217	8964	0.18	0.27
105	Test	41.81	13.40	217	8807	0.17	0.25
106	Test	43.30	11.29	222	14321	0.35	0.19
107	Test	45.29	12.52	223	11585	0.53	0.50
108	Test	46.08	14.34	179	12587	0.36	0.43
109	Test	46.52	13.19	179	12532	0.35	0.43
110	Test	47.75	12.67	179	12448	0.53	0.38
111	Test	54.28	11.96	220	9998	0.17	0.27
112	Test	55.22	11.72	179	10782	0.55	0.33

ศูนย์วิทยทรัพยากร
จุฬาลงกรณ์มหาวิทยาลัย

APPENDIX C

Results from testing model number 8 with entire dataset (Case 2.2)

Dataset no.	Data type	Inclination	WOB	Rotational Speed	Torque	Model Outputs (Actual walk range)			Model outputs (Predicted walk range)		
		(deg)	(Klbs)	(RPM)	(Klbs*ft)	Node 1	Node 2	Node 3	Node 1	Node 2	Node 3
1	Train	18.24	12.91	220	9444	0	1	0	0.210	0.642	0.139
2	Train	19.34	13.90	223	9803	0	1	0	0.189	0.648	0.154
3	Train	20.09	11.88	179	9843	1	0	0	0.451	0.359	0.183
4	Train	21.11	13.31	217	10075	0	1	0	0.186	0.612	0.192
5	Train	21.98	14.14	222	9740	0	1	0	0.282	0.563	0.149
6	Train	22.33	12.90	154	14241	0	0	1	-0.008	0.118	0.868
7	Train	22.38	14.48	220	9964	0	0	1	0.326	0.485	0.183
8	Train	22.65	11.34	220	9570	0	1	0	0.409	0.414	0.175
9	Train	23.04	12.83	222	10822	0	1	0	0.347	0.489	0.150
10	Train	23.07	13.45	146	13862	0	0	1	0.154	0.163	0.960
11	Train	23.13	13.10	222	9437	0	1	0	0.364	0.489	0.139
12	Train	23.60	13.03	163	13586	0	0	1	-0.033	0.123	0.883
13	Train	23.79	14.10	223	9310	0	1	0	0.370	0.533	0.093
14	Train	24.29	12.00	160	13586	0	0	1	-0.025	0.246	0.760
15	Train	24.59	11.90	221	8994	1	0	0	0.668	0.161	0.165
16	Train	25.09	12.10	180	13333	0	0	1	0.123	0.131	0.720
17	Train	25.18	11.21	198	13464	0	0	1	-0.014	0.470	0.661
18	Train	25.33	12.21	221	8936	0	1	0	0.704	0.140	0.150
19	Train	25.33	12.24	222	10610	0	1	0	0.414	0.491	0.084

Dataset no.	Data type	Inclination	WOB	Rotational Speed	Torque	Model Outputs (Actual walk range)			Model outputs (Predicted walk range)		
		(deg)	(Klbs)	(RPM)	(Klbs*ft)	Node 1	Node 2	Node 3	Node 1	Node 2	Node 3
20	Train	25.92	11.90	208	14345	0	0	1	0.266	0.209	0.518
21	Train	26.21	14.17	223	10719	0	1	0	0.405	0.516	0.080
22	Train	26.57	11.62	214	13966	0	1	0	0.150	0.340	0.508
23	Train	27.00	14.18	223	10448	0	1	0	0.396	0.603	0.004
24	Train	27.07	12.55	221	12976	1	0	0	0.528	0.241	0.222
25	Train	27.09	11.86	228	13793	0	0	1	0.252	0.463	0.290
26	Train	27.10	11.53	222	12891	0	1	0	0.084	0.545	0.371
27	Train	27.97	14.97	222	10369	0	1	0	0.191	0.687	0.113
28	Train	30.66	12.45	223	10097	0	1	0	0.505	0.626	0.133
29	Train	30.88	11.97	223	10155	1	0	0	0.612	0.542	0.151
30	Train	31.32	13.10	223	9873	0	1	0	0.245	0.803	-0.062
31	Train	36.42	14.47	140	12107	0	0	1	-0.069	0.084	0.939
32	Train	37.45	13.67	142	11771	0	0	1	0.181	-0.045	0.821
33	Train	37.71	10.84	209	11008	0	1	0	0.085	0.859	0.041
34	Train	38.02	11.37	217	10332	0	1	0	0.291	0.709	-0.021
35	Train	38.50	11.41	213	10021	0	1	0	0.359	0.618	0.002
36	Train	38.94	9.71	215	9698	1	0	0	0.444	0.463	0.079
37	Train	39.34	10.64	214	9721	0	1	0	0.350	0.589	0.049
38	Train	39.43	11.38	162	14483	0	1	0	0.116	0.970	0.000
39	Train	39.83	11.53	177	12000	0	1	0	0.116	0.658	0.215
40	Train	40.31	11.33	213	9620	1	0	0	0.457	0.520	0.005
41	Train	40.71	12.72	185	11884	0	1	0	0.093	0.435	0.443
42	Train	40.84	12.53	216	9401	0	1	0	0.555	0.424	-0.006
43	Train	41.63	13.60	192	11690	0	1	0	0.128	0.357	0.481

Dataset no.	Data type	Inclination	WOB	Rotational Speed	Torque	Model Outputs (Actual walk range)			Model outputs (Predicted walk range)		
		(deg)	(Klbs)	(RPM)	(Klbs*ft)	Node 1	Node 2	Node 3	Node 1	Node 2	Node 3
44	Train	42.03	12.84	218	8570	1	0	0	0.692	0.302	-0.020
45	Train	42.16	12.84	218	8412	1	0	0	0.712	0.284	-0.024
46	Train	42.16	10.90	195	13897	0	1	0	0.149	1.042	0.156
47	Train	42.20	10.57	220	7492	0	1	0	0.454	0.439	0.097
48	Train	42.25	13.22	217	8442	1	0	0	0.698	0.285	-0.011
49	Train	42.25	11.19	218	7886	1	0	0	0.629	0.326	0.026
50	Train	42.38	14.16	190	11781	0	0	1	0.200	0.354	0.417
51	Train	43.74	11.43	220	13929	0	1	0	-0.066	1.000	0.088
52	Train	44.14	13.30	194	11851	0	0	1	0.265	0.257	0.452
53	Train	45.37	9.81	178	13169	0	1	0	0.382	0.628	-0.095
54	Train	45.46	10.60	179	12811	1	0	0	0.353	0.587	0.029
55	Train	45.90	12.68	179	12794	0	1	0	0.418	0.364	0.243
56	Train	46.43	12.67	223	11757	0	0	1	0.653	0.114	0.201
57	Train	46.52	12.91	214	12119	1	0	0	0.592	0.163	0.220
58	Train	46.96	13.97	179	12638	1	0	0	0.486	0.364	0.168
59	Train	47.14	11.77	214	12062	0	1	0	0.481	0.253	0.252
60	Train	47.49	12.43	214	12183	1	0	0	0.651	0.114	0.215
61	Train	47.84	12.60	214	12147	1	0	0	0.688	0.084	0.208
62	Train	47.93	13.65	214	12086	1	0	0	0.546	0.189	0.244
63	Train	48.15	11.72	222	11660	0	0	1	0.563	0.213	0.205
64	Train	48.28	11.71	214	12062	1	0	0	0.544	0.207	0.240
65	Train	48.63	13.45	214	12027	0	1	0	0.638	0.107	0.236
66	Train	48.81	9.82	213	11969	0	1	0	0.501	0.665	0.143
67	Train	49.07	9.54	214	11725	1	0	0	0.541	0.604	0.140

Dataset no.	Data type	Inclination	WOB	Rotational Speed	Torque	Model Outputs (Actual walk range)			Model outputs (Predicted walk range)		
		(deg)	(Klbs)	(RPM)	(Klbs*ft)	Node 1	Node 2	Node 3	Node 1	Node 2	Node 3
68	Train	53.70	12.32	181	10532	1	0	0	0.965	0.034	-0.008
69	Train	54.11	12.17	181	11911	1	0	0	1.137	-0.037	-0.045
70	Train	54.45	12.53	212	10263	1	0	0	0.853	-0.034	0.165
71	Train	54.51	12.82	180	12308	1	0	0	1.206	-0.018	-0.094
72	Train	54.58	11.09	212	9888	1	0	0	0.704	0.341	-0.045
73	Train	54.67	12.22	220	9891	1	0	0	0.863	0.065	0.055
74	Train	54.86	12.62	180	11836	1	0	0	1.175	-0.107	-0.001
75	Train	55.07	12.72	220	9816	1	0	0	0.856	-0.023	0.146
76	Train	55.23	12.42	180	11434	1	0	0	1.148	-0.108	-0.002
77	Validate	20.33	14.59	208	10078	0	1	0	0.200	0.457	0.330
78	Validate	21.43	12.57	130	13522	0	1	0	-0.054	0.258	0.777
79	Validate	24.19	13.66	222	9179	1	0	0	0.417	0.460	0.118
80	Validate	24.54	15.45	221	10711	0	1	0	0.309	0.431	0.257
81	Validate	24.98	12.10	221	9307	1	0	0	0.599	0.255	0.140
82	Validate	37.76	12.12	217	10589	0	1	0	0.261	0.699	0.009
83	Validate	38.68	10.00	214	9852	0	1	0	0.390	0.529	0.068
84	Validate	39.03	10.14	214	9679	0	1	0	0.388	0.528	0.071
85	Validate	39.78	11.34	214	9698	0	1	0	0.435	0.543	0.004
86	Validate	40.58	10.55	214	9362	0	1	0	0.386	0.542	0.061
87	Validate	41.19	11.79	217	8966	0	1	0	0.631	0.366	-0.021
88	Validate	41.68	9.97	223	13862	0	1	0	-0.037	1.206	0.180
89	Validate	43.00	13.64	188	11973	0	0	1	0.185	0.333	0.457
90	Validate	45.73	11.21	179	12789	0	1	0	0.457	0.549	0.032
91	Validate	45.99	13.41	209	12118	0	1	0	0.455	0.257	0.264

Dataset no.	Data type	Inclination	WOB	Rotational Speed	Torque	Model Outputs (Actual walk range)			Model outputs (Predicted walk range)		
		(deg)	(Klbs)	(RPM)	(Klbs*ft)	Node 1	Node 2	Node 3	Node 1	Node 2	Node 3
92	Validate	46.87	11.81	214	12016	1	0	0	0.481	0.249	0.252
93	Validate	47.22	12.19	178	12451	1	0	0	0.610	0.237	0.184
94	Validate	54.23	10.95	219	9876	1	0	0	0.705	0.337	-0.041
95	Test	19.92	14.79	218	9632	1	0	0	0.285	0.520	0.188
96	Test	20.64	14.03	209	9866	0	1	0	0.175	0.556	0.258
97	Test	21.76	12.41	124	13724	0	0	1	-0.057	0.277	0.763
98	Test	23.61	15.38	222	10766	0	1	0	0.316	0.362	0.316
99	Test	23.91	11.04	174	13786	0	0	1	-0.016	0.507	0.649
100	Test	25.48	11.00	206	13621	0	0	1	-0.017	0.508	0.656
101	Test	27.01	11.71	222	12839	1	0	0	0.176	0.484	0.338
102	Test	30.35	13.39	223	10136	0	1	0	0.241	0.806	-0.055
103	Test	38.33	12.76	212	10183	1	0	0	0.274	0.616	0.080
104	Test	38.77	12.66	164	12163	0	1	0	0.078	0.516	0.380
105	Test	41.50	12.67	217	8964	1	0	0	0.636	0.353	-0.016
106	Test	41.81	13.40	217	8807	1	0	0	0.627	0.327	0.018
107	Test	43.30	11.29	222	14321	0	1	0	-0.013	1.129	0.035
108	Test	45.29	12.52	223	11585	0	1	0	0.591	0.178	0.196
109	Test	46.52	13.19	179	12532	0	1	0	0.275	0.433	0.306
110	Test	47.75	12.67	179	12448	0	1	0	0.188	0.591	0.249
111	Test	54.28	11.96	220	9998	1	0	0	0.863	0.100	0.021
112	Test	55.22	11.72	179	10782	0	1	0	0.895	-0.053	0.048

APPENDIX D

MATLAB source code

```

clear;
%--- Section 1 - definition ---%
% No. of neuron

hidden1 = 10;
hidden2 = 20;

% Learning rate and momentum
lr = 0.1;
mc = 0.1;

% Dataset (train, validate, test)
% input directly
% (examples)
input = [26.57 11.62 214.41 13965.52 ; 39.83 11.53 177.46 12000.32 ;
24.98 12.1 220.52 9307.34 ]';
output = [0 0 1 ; 0 1 0 ; 1 0 0 ]';
testing = [47.84 12.6 214.14 12146.55 ; 48.81 9.82 213.42 11969.09 ;
54.11 12.17 180.83 11911.14]';

% or via excel read function
% (example)
input = xlsread('input.xls',1);

%--- Section 2 - Network building ---%
net = newff(input, output, [hidden1,hidden2], {'logsig'});

% Weight initialization
net = init(net);

% Training function
net.trainFcn = 'trainlm';

% Configuration
net.trainParam.lr = lr;
net.trainParam.mc = mc;
net.trainParam.goal = 1e-5;
net.trainParam.epochs = 100000;
net.trainParam.show = 50;

% Dataset partitioning

net.divideFcn = 'divideblock';
[trainP,valP,testV,trainInd,valInd,testInd] = divideblock(input,
0.75, 0.25, 0);
[trainT,valT,testT] = divideind(output,trainInd,valInd,testInd);

```

```
%--- Section 3 - Training, Validating and testing process ---%  
net = train(net,input,output);  
y = sim(net, testing);  
  
% Result outputs  
  
y = y';  
x = sim(net, input);  
x = x';  
  
trainP = trainP';  
valP = valP';  
testV = testV';  
trainT = trainT';  
valT = valT';  
testT = testT';  
input = input';  
output = output';  
testing = testing';
```



ศูนย์วิทยทรัพยากร
จุฬาลงกรณ์มหาวิทยาลัย

VITAE

Phornlerd Sudhikiat was born on June 16, 1984 in Bangkok, Thailand. He received his B.Eng in Computer Engineering from the Faculty of Engineering, Chulalongkorn University in 2005. He has been a graduate student in the Master's Degree Program in Petroleum Engineering of the Department of Mining and Petroleum Engineering, Chulalongkorn University since 2010.



ศูนย์วิทยทรัพยากร
จุฬาลงกรณ์มหาวิทยาลัย